University of Calgary

PRISM Repository **https://prism.ucalgary.ca**

The Vault Open Theses and Dissertations

2014-01-30

Functional Neocortical Movement Encoding in the Rat

Brown, Andrew

Brown, A. (2014). Functional Neocortical Movement Encoding in the Rat (Doctoral thesis, University of Calgary, Calgary, Canada). Retrieved from https://prism.ucalgary.ca. doi:10.11575/PRISM/26247 http://hdl.handle.net/11023/1355

Downloaded from PRISM Repository, University of Calgary

UNIVERSITY OF CALGARY

Functional Neocortical Movement Encoding in the Rat

by

Andrew R. Brown

A THESIS

SUBMITTED TO THE FACULTY OF GRADUATE STUDIES

IN PARTIAL FULFILMENT OF THE REQUIREMENTS FOR THE

DEGREE OF DOCTOR OF PHILOSOPHY

DEPARTMENT OF NEUROSCIENCE

CALGARY, ALBERTA

JANUARY, 2014

© Andrew R. Brown 2014

Abstract

The motor cortex has long been known to play a central role in the generation and control of volitional movement, yet its intrinsic functional organization is not fully understood. Two alternate views on the functional organization of motor cortex have been proposed. Short-duration (>50 ms) intracortical stimulation (SD-ICMS) reveals a somatotopic representation of body musculature, whereas long-duration (~500 ms) ICMS (LD-ICMS) reveals a topographic representation of coordinated movement endpoint postures. The functional organization of motor cortex in the rat was probed using combined approaches of *in vivo* microstimulation, behavioural analysis of forelimb motor performance, and acute cortical cooling deactivation. The first study, using a rodent model of Parkinson's disease and therapeutic deep brain stimulation of the subthalamic nucleus, determined that acute changes (<60 s) in cortical output function and motor performance are reflected in reversible alterations in movement thresholds and representation sizes. A second study characterized forelimb movement representations under SD-ICMS revealing a dual-representation (digit, wrist, elbow, shoulder) within rostral (RFA) and caudal (CFA) forelimb motor areas. LD-ICMS elicited forelimb reach-to-grasp behaviour (elevate, advance, grasp, retract) with a functional segregation between RFA (grasp) and CFA (elevate, advance, retract) representations. Behaviourally distinct functional roles between these two areas was confirmed through behavioural assessment during selective cortical cooling deactivation. A final study demonstrated increased movement representation overlap assessed with LD-ICMS following repeated kindled-seizures that was not attributed to changes in intracortical inhibition. Current experimentation provides the first causal evidence for movement-based rather than muscle-based functional organization of motor cortex and functional neocortical movement encoding in the rat.

Acknowledgements

I wish to thank Dr. G. Campbell Teskey for invaluable guidance and support throughout my graduate program. Thanks to Dr. Bin Hu for spurring the development of Chapter 2. Thanks to Dr. Richard Dyck for use of the sliding microtome and imaging equipment. Thanks to Dr. Michael Antle for providing the TH^+ primary antibody, DAB reaction reagents, and visualization equipment in addition to technical support for the immunohistochemical analyses. Many thanks to Dr. Stephen Lomber for technical support and assistance in adapting cooling deactivation techniques for present use. Thanks to Gerard Coughlin for assistance with kindling and experimentation in Chapter 4. Thanks to Bonita Gunning for assistance and technical support. Appreciation to AI-HS, NSERC, Department of Neuroscience and University of Calgary for funding support.

Table of Contents

Abstract ii
Acknowledgements iii
Table of Contents iv
List of Tables vii
List of Figures and Illustrations viii
List of Abbreviations x

CHAPTER ONE: INTRODUCTION 1
1.1 Motor cortex organization as a somatotopic representation of body musculature 4
1.2 Short-duration intracortical microstimulation reveals somatic muscle encoding in motor cortex 7
1.3 Long-duration intracortical microstimulation reveals movement encoding in motor cortex 8
1.4 Sensorimotor neocortex and corticospinal projections in the rat 14
1.5 Lesion techniques to investigate neural function 22
1.6 Behavioural assessment of forelimb motor ability 25
1.7 Motor map plasticity and behaviour 30
1.8 Thesis objectives and hypothesis 32

CHAPTER TWO: 35

HIGH FREQUENCY STIMULATION OF THE SUBTHALAMIC NUCLEUS ACUTELY RESCUES MOTOR DEFICITS AND NEOCORTICAL MOVEMENT REPRESENTATIONS FOLLOWING 6-HYDROXYDOPAMINE ADMINISTRATION IN RATS 35
2.1 Abstract 36
2.2 Introduction 37
2.3 Materials and Methods 38
2.3.1 Rats 38
2.3.2 Experimental procedures 39
2.3.3 Behavioural testing 39
2.3.3.1 Cylinder Test 39
2.3.3.2 Open field 40
2.3.4 Lesion and chronic electrode implantation procedures 41
2.3.5 Deep brain stimulation 42
2.3.6 Intracortical microstimulation 42
2.3.7 Lesion assessment and verification of DBS electrode placement 45
2.3.8 Statistical analyses 47
2.4 Results 47
2.4.1 Lesion quantification 47
2.4.2 DBS electrode placement and stimulation intensity 48
2.4.3 STN DBS improves behavioural impairments in 6-OHDA lesion rats 48
2.4.3.1 Forelimb Placements 55
2.4.3.2 Line crossings 55
2.4.3.3 Rears 55

2.4.4 6-OHDA lesion decreases forelimb map area and increases movement thresholds 56
2.4.5 STN DBS acutely increases forelimb map area and reduces movement thresholds following 6-OHDA lesion....61
2.5 Discussion....65

CHAPTER THREE: 69

FUNCTIONALLY SEGREGATED MOVEMENT ENCODING IN RAT NEOCORTICAL FORELIMB MOTOR AREAS....69
3.1 Abstract....70
3.2 Introduction....71
3.3 Materials and Methods....73
3.3.1 Rats....73
3.3.2 Groups and experimental design....74
3.3.3 Single-pellet reach training....75
3.3.4 Cryoloop construction, implantation, and validation....76
3.3.5 Cooling deactivation....80
3.3.6 Single-pellet reach testing....81
3.3.7 Sunflower seed eating....82
3.3.8 Vermicelli pasta handling....82
3.3.9 Grip Strength....83
3.3.10 Intracortical microstimulation....84
3.3.11 Movement classification and motor map topography....84
3.3.12 Statistical analyses....85
3.4 Results....86
3.4.1 Characterization of forelimb movements and cortical movement topography derived with long-duration intracortical microstimulation.....86
3.4.2 Forelimb movement representation topography following skilled motor learning 94
3.4.3 Behavioural assessment during selective deactivation of the CFA and RFA .98
3.4.3.1 Single-pellet reaching....98
3.4.3.2 Vermicelli handling....104
3.4.3.3 Sunflower Seed eating....107
3.4.3.4 Grip strength....110
3.4.4 Cryoloop placement verification and movement representation integrity 110
3.5 Discussion....113

CHAPTER FOUR:....119

IMPAIRED SELECTION SPECIFICITY IN COMPLEX MOVEMENT REPRESENTATIONS FOLLOWING REPEATED SEIZURES 119
4.1 Abstract....120
4.2 Introduction....121
4.3 Materials and Methods....123
4.3.1 Rats and experimental groups....123
4.3.2 Intracortical microstimulation....124

4.3.3 Bicuculline application 125
4.3.4 Chronic electrode implantation 125
4.3.5 Kindling 126
4.3.6 Statistical analyses 127
4.4 Results 127
4.4.1 Kindling 128
4.4.1.1 Forelimb movement representation topography following callosal kindling 128
4.4.2 Forelimb movement representation topography under bicuculline administration 137
4.5 Discussion 143

CHAPTER FIVE: GENERAL DISCUSSION 148
5.1.1 Summary of findings 148
5.1.2 Major findings and limitations 151
5.1.2.1 Evidence for a movement-based functional organization of motor cortex 151
5.1.2.2 Threshold microstimulation remains a valuable tool to assess corticospinal activity 155
5.1.2.3 Evoked responses with LD-ICMS are not likely a result of excessive current spread 155
5.1.3 Future directions 157
5.1.3.1 Engram for motor learning? 157
5.1.3.2 Connectional properties of complex movement representations 157

REFERENCES 158

List of Tables

Table 3-1. Forelimb motor map topography 95

Table 4-1. Forelimb motor map topography 135

List of Figures and Illustrations

Figure 1-1: Penfield's motor homunculus 3

Figure 1-2. Complex movements elicited with LD-ICMS 11

Figure 1-3. Topography of hand and arm movement postures evoked with LD-ICMS 13

Figure 1-4: Forelimb motor map in the rat elicited with SD-ICMS 17

Figure 1-5: Corticospinal tract in the rat 20

Figure 2-1: SNc TH+ immunoreactivity and cell counts 50

Figure 2-2: STN electrode placements 52

Figure 2-3: DBS behavioural assessment 54

Figure 2-4: Forelimb motor map area and movement thresholds 58

Figure 2-5: Representative forelimb motor maps 60

Figure 3-1: Cryoloop cooling deactivation 78

Figure 3-2: Forelimb movements evoked with LD-ICMS 88

Figure 3-3. Representative forelimb motor maps elicited under SD-ICMS or LD-ICMS 91

Figure 3-4: Forelimb motor map area and stimulation parameter assay 93

Figure 3-5: Cumulative distribution of simple and complex movement topography 97

Figure 3-6. Motor map following skilled reach training 100

Figure 3-7. End-point success in skilled reaching ability during cooling 103

Figure 3-8. Qualitative assessment of reaching performance during cooling 106

Figure 3-9. Behavioural assessment during cooling 109

Figure 3-10: Cryoloop post-implantation assay 112

Figure 4-1: Kindling afterdischarge duration and seizure stage scores 130

Figure 4-2: Representative motor maps in kindle and sham-kindle groups 132

Figure 4-3: Motor map areas and overlap 134

Figure 4-4: Motor map topography 139

Figure 4-5: Motor map areas observed under saline and bicuculline 141

List of Abbreviations

Symbol	Definition
6-OHDA	6-hydroxydopamine
AD	Afterdischarge
ADT	Afterdischarge threshold
AMPA	α-Amino-3-hydroxy-5-methyl-4-isoxazolepropionic acid
ANOVA	Analysis of variance
AP	Anterior/Posterior
BOLD	Blood-oxygen-level-dependent
CFA	Caudal forelimb area
CST	Corticospinal tract
DAB	3,3'diaminobenzidine tetrahydrochloride
DBS	Deep brain stimulation
DV	Dorsal/Ventral
GABA	γ-Aminobutyric acid
ICMS	Intracortical microstimulation
LD-ICMS	Long-duration intracortical microstimulation
ML	Medial/Lateral
NMDA	*N*-Methyl-D-aspartic acid or *N*-Methyl-D-aspartate
PBS	Phosphate buffered saline
PD	Parkinson's disease

PFA	Posterior forelimb area
RFA	Rostral forelimb area
SD-ICMS	Short-duration intracortical microstimulation
SEM	Standard error of the mean
SNc	Substantia nigra pars compacta
STN	Subthalamic nucleus
TH	Tyrosine hydroxylase
VTA	Ventral tegmental area

Chapter One: Introduction

A fundamental function of the motor cortex is the execution and control of voluntary movement. Current understanding of motor cortical organization stems from early animal (Fritsch and Hitzig, 1870) and human (Penfield and Rasmussen, 1950) electrical stimulation studies to determine output function. A somatotopically-ordered representational map for movements (motor map) was found to exist across the cortical surface, whereby stimulation of discrete cortical areas elicited the movement of discrete joints (Fig. 1-1). Refined stimulation mapping techniques were later developed (Asanuma and Sakata, 1967) that were able to provide a much higher degree of spatial resolution by using brief focal stimulation of cortical neurons with a microelectrode positioned within the motor cortex (short-duration intracortical microstimulation; SD-ICMS). Results from microstimulation studies also revealed somatotopic maps of body musculature, but stimulation sites for particular body parts were found to be much more distributed, and overlapping, than expected (Kwan et al., 1987; Donoghue et al., 1992; Nudo et al., 1992).

The functional organization of the motor cortex, as revealed by SD-ICMS, was one of discrete muscle representations organized into narrow columns controlling individual muscles (Asanuma, 1975). However, this interpretation on motor cortex organization has been challenged. Spike-triggered averaging studies demonstrate that individual neurons in the motor cortex influence activity of multiple proximal and distal limb muscles (Fetz et al., 1989; McKiernan et al., 1998). Moreover, behavioural investigation using local deactivation of discrete portions of the finger representations in primates was not found to induce specific finger

Figure 1-1. The motor homunculus of the human brain as viewed in a coronal section of the left hemisphere through primary motor neocortex portraying somatotopic arrangement of contralateral muscle innervation. Modified from Penfield and Rasmussen (1950).

Figure 1-1: Penfield's motor homunculus

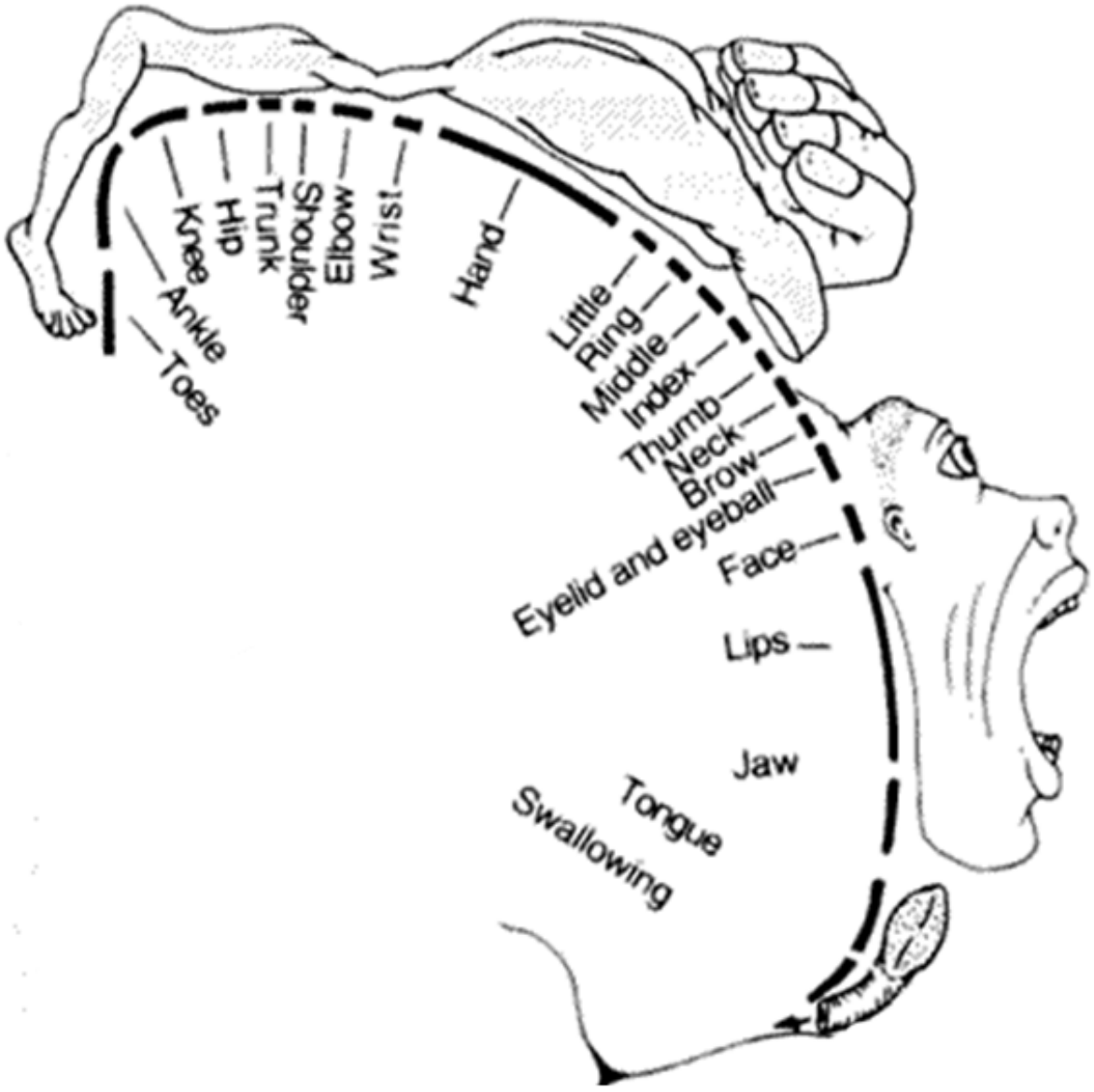

impairments corresponding to the site of inactivation, but rather led to a more diffuse deficit in forelimb motor ability (Schieber and Poliakov, 1998) Additionally, microstimulation of motor cortex using long-duration pulse trains (LD-ICMS) on a behaviourally relevant time scale has recently been shown to evoke complex (multi-joint) coordinated movements of one or more body parts towards a specific posture in both primates (Graziano et al., 2002, 2005; Haiss and Schwarz, 2005; Gharbawie et al., 2011) and rodents (Ramanathan et al., 2006; Harrison et al., 2012; Bonazzi et al., 2013). A variety of different classes of movements can be elicited with LD-ICMS from different cortical areas that bear resemblance to the behavioural repertoire of the species and have been purported to be ethologically relevant (Graziano et al., 2002).

This thesis primarily investigates the functional organization of the motor cortex in the rat in an attempt to help reconcile these two views: one of a map of muscles and the other a map of movements. These questions are addressed at the neural network level in the neocortex by investigating the organization of motor maps and their relation behaviour in three following experimental chapters. I begin with a brief historical overview of our understanding of the cortical motor system obtained from stimulation studies.

1.1 Motor cortex organization as a somatotopic representation of body musculature

Fritsch and Hitzig (1870) demonstrated, for the first time, that not only was cortex "excitable" in that stimulation lead to overt behaviour, but also that different regions of the cortex elicited different behaviours, suggesting specificity in cortical function. Brief galvanic discharges of direct current from a battery applied to anterior regions of frontal cortex of dogs were found to evoke muscle twitches in contralateral body regions. Furthermore, different

movements were found to be elicited from different cortical centers eliciting movement of the foreleg, hindleg, face, or neck. Note that a somatotopic view of motor cortex function was not advanced from these experiments for two reasons; 1) the movement centers were found to be discontinuous, surrounded by zones of unexcitable cortex, 2) no clear topography was reported within each centre and they were believed to represente undifferentiated collections of many muscles.

The first description of a somatotopic mapping of body muscular was proposed by Ferrier (1874), replicating the findings of Fritsch and Hitzig, localizing motor cortex in primates to the precentral gyrus. Although Fritsch and Hitzig and Ferrier revealed that surface stimulation of anterior frontal cortex evokes movement, differences in their stimulation methodologies yielded two possible interpretations for the organization of motor cortex (Graziano, 2009). Fritsch and Hitzig used brief direct current pulses to stimulate the brain, evoking short muscle twitches, whereas Ferrier used alternating current (faradaic), which can be maintained for several seconds without tissue damage, evoking the generation of complex, multi-joint movements (Gross, 2007; Taylor & Gross, 2003). Subsequent extension of Ferrier's work by Beevor and Horsley (1887) revealed that stimulation of different regions of the arm representation in non-human primates could elicit "purposeful" movements. Ventral stimulation elicited movements resembling feeding behaviour, consisting of hand movement towards the mouth, concurrent with suppination of the hand and flexing of the digits. Dorsal stimulation, however, tended to evoke advancing movements of the forearm and opening of the hand that was characterized as "reaching". Later work by Beevor and Horsley (1890) was confined to investigations of the primary components of these movements using short pulses of stimulation to derive an approximate plan of body representation across the cortical surface. Focus was shifted away from a cortical representation

of movements and towards a representation of muscles when it was found that following dissection of overlaying cortex, stimulation of remaining severed axonal ends produced a motor map matching that created by short duration stimulation of the cortex itself (Beevor and Horsley, 1890). From this finding, the corticomotor system was viewed as a series of parallel cables running down to the spinal cortex and topographically arranged according to the muscles they innervate. In this interpretation, motor cortex served no intrinsic processing functionality as the same muscle map was elicited with short duration stimulation of either the cortex or the axons forming the origin of the cables. This viewpoint persisted throughout the 20th century and informed the primary methodological approaches in this field until the early 2000s.

Sherrington later provided meticulous descriptions of primate motor representations and was the first to suggest that the organization of cortical movement representations mirrored patterns of spinal root innervations of somatic musculature (summarized in Sherrington, 1939). Although Sherrington revealed the organizational relationship between cortical movement representations and muscle innervations patterns, he did not reduce cortical function to a fixed mapping of muscles. Rather, a role for intrinsic cortical processing was also stressed in reports on the "functional instability of cortical motor points**"** (Leyton and Sherrington, 1917). Prior stimulation of one cortical site was shown to be able to influence movemen t evoked from a subsequent site. Depending on prior stimulation history, movement elicited by stimulation of a single cortical site could be modified to elicit either different muscle activation patterns in the same body part (i.e., forearm flexion could be changed into forearm extension), or could even be changed to elicit movement of a different body part. Sherrington was first to suggest the notion of a malleable, or plastic, activity-dependent role for motor cortex in the modulation of behavioural output.

Traditional views on the somatotopic organization of motor cortex are highlighted by the iconic human motor homunculus of Penfield and Boldrey (1937), obtained from surface stimulation in patients undergoing cortical resections for the management of epilepsy, that shows the relative size of cortical representations devoted to different body parts (Fig. 1-1). Although the motor homunculus has proved very influential, it has been argued to depict an idealized oversimplification of motor somatotopy (Graziano, 2009). While extensive overlap between adjacent body parts was noted by Penfield, the homunculus presents a clear segregation in body representations.

1.2 Short-duration intracortical microstimulation reveals somatic muscle encoding in motor cortex

Investigation of motor cortex output by Fritsch and Hitzig, Ferrier, Beevor, Horsley, Sherrington and Penfield relied on electrical currents being applied to the surface of the cortex. From these studies, motor cortex was thought to orderly decompose movement into discrete muscle actions across individual joints. Derived movement representations, however, were found to be blurred and demonstrated extensive somatotopic overlap between adjacent body parts (Gross, 2007). Asanuma and Sakata (1967) attributed movement representation overlap to be an artifact caused by indiscriminate spread of the high intensity electrical current used in surface stimulation. SD-ICMS (Asanuma and Sakate 1967; Stoney et al., 1968) was subsequently developed as a technique to probe motor cortex organization using the minimal possible stimulation intensity (μA vs mA) and train duration (μS vs ms) to efficiently stimulate cortical neurons with a high degree of spatial resolution (μM vs mm). SD-ICMS revealed a strict

somatotopic representation of body muscular organized as discrete cortical micro columns eliciting extensions or flexions of musculature around a single joint (Asanuma and Ward, 1971; Asanuma & Rosén, 1972). Although cases of overlapping representations were observed, they were attributed to noxious effects of current spread (Asanuma, 1975).

Assumptions of a strict somatotopic mapping of body musculature were later challenged by findings that individual corticospinal neurons can influence activity in multiple muscle groups (Shinoda et al., 1981; Fetz and Cheney; 1980; Cheney and Fetz, 1985) and that disparate corticospinal neurons can innervate the same spinal motorneuron (Jankowska et al., 1975). In addition to a role in mapping body musculature, recordings from motor cortex neurons revealed a neuronal encoding movement direction (Georgeopoulos et al., 1982; Kakei et al., 1999), velocity (Moran and Schwartz, 1999), force (Evarts, 1968), and preparatory set (Sanes and Donoghue, 1993).

1.3 Long-duration intracortical microstimulation reveals movement encoding in motor cortex

Graziano et al. (2002) proposed a novel theory on the motor cortex organization based on the following argument: muscle activity during volitional movement is not necessarily equivalent, with certain muscle groups being activated more strongly, or for a greater duration than others. Accordingly, if the motor cortex is organized into complex movement representations involving many muscles, minimal threshold stimulation of a given cortical site may only elicit the component of that movement that is most strongly activated (Graziano, 2009). In this interpretation of motor cortex function, muscle somatotopy revealed by SD-IMCS

is an artifact of the threshold stimulation protocol revealing only the strongest muscle component of a cortically-encoded movement. SD-ICMS by its very nature, then, only exposes the tip-of-the-iceberg of motor encoding (Graziano, 2009). While SD-ICMS minimizes current spread in attempt to restrict cortical activation to discrete cortical columns, hypothesized to reflect individual representations of somatotopic musculature, Graziano argues that motor cortex organization is better reflected by promoting cortical activation using longer duration stimulation trains in order to recapitulate activity patterns generated in naturalistic behaviour.

Using stimulation train durations that roughly match the duration of a monkey's natural reach (500 ms), as well as the timescale of motor cortex neuron firing activity during reaching (Georgopoulos et al., 1986), Graziano et al. (2002; 2005) elicited reproducible complex, multi-joint movements in unanaesthetized primates. This is in stark contrast to individual joint flexions and extensions of the digits, wrist, elbow and shoulder evoked with SD-ICMS. Movements elicited with LD-ICMS were found to cluster on the cortical surface according to behavioural class in discrete action zones (Fig. 1-3). A variety of different classes of movement deemed "ethologically relevant" can be evoked from distinct action zones represented on the cortical surface including reaching-to-grasp, climbing and leaping, defensive reactions and hand to mouth manipulations to name a few (Graziano, 2009; Fig. 1-2). Within a given action zone, movement direction and final posture is topographically organized. For example, a representational map of hand positions in peripersonal space is revealed with LD-ICMS of forelimb motor regions, with stimulation of different cortical areas driving the forelimb and hand to different locations (Fig. 1-3).

Figure 1-2. Complex movement action zones evoked from long-duration microstimulation of the precentral gyrus in the monkey. Within each action zone in the motor cortex, movement of similar behavioural category were elicited. Modified from Graziano and Aflalo (2007).

Figure 1-2. Complex movements elicited with LD-ICMS

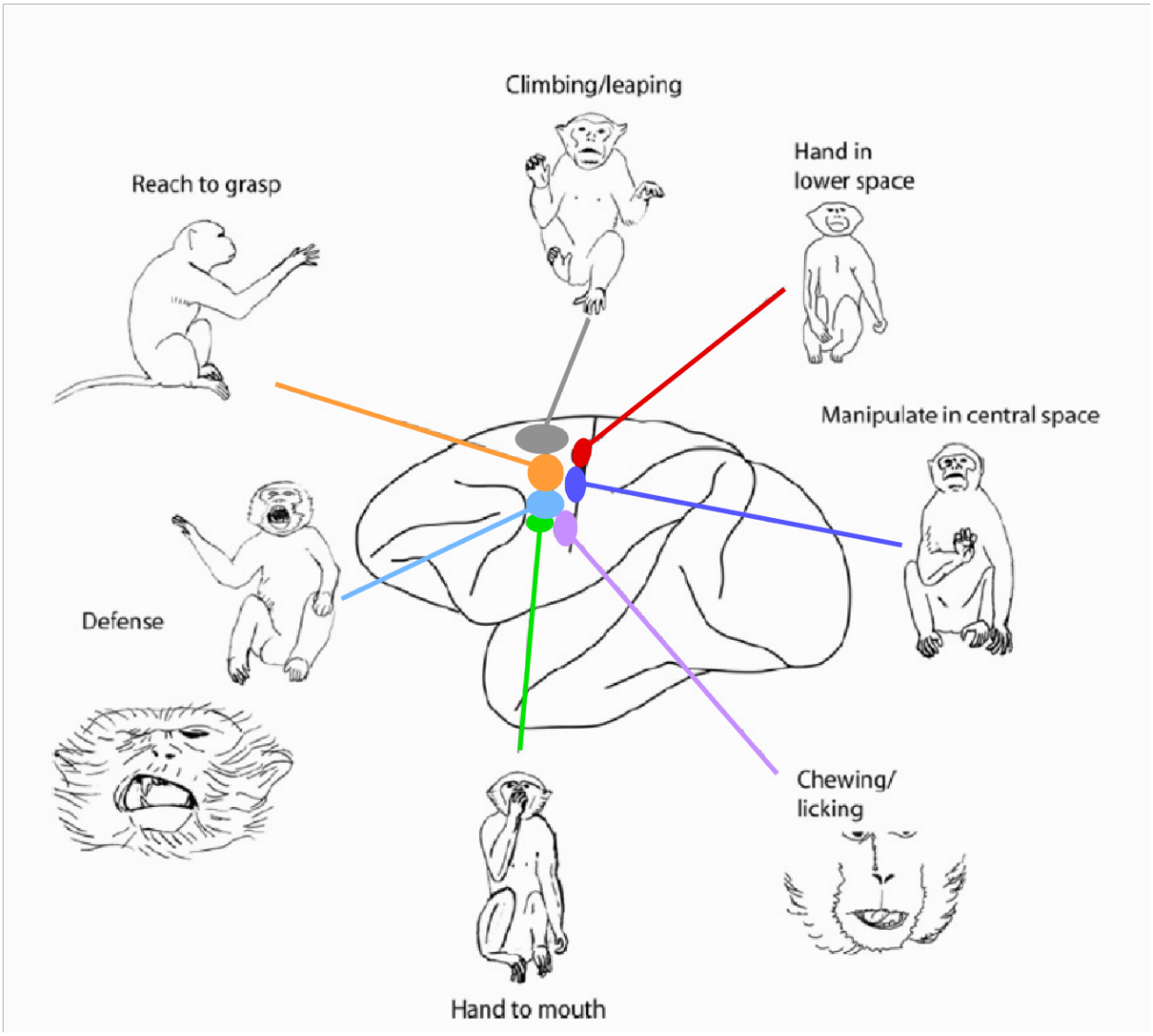

Figure 1-3. Distribution of hand positions along the vertical axis (top) and horizontal axis (bottom) elicited with long-duration intracortical microstimulation (LD-ICMS). Modified from Graziano et al. (2002).

Figure 1-3. Topography of hand and arm movement postures evoked with LD-ICMS

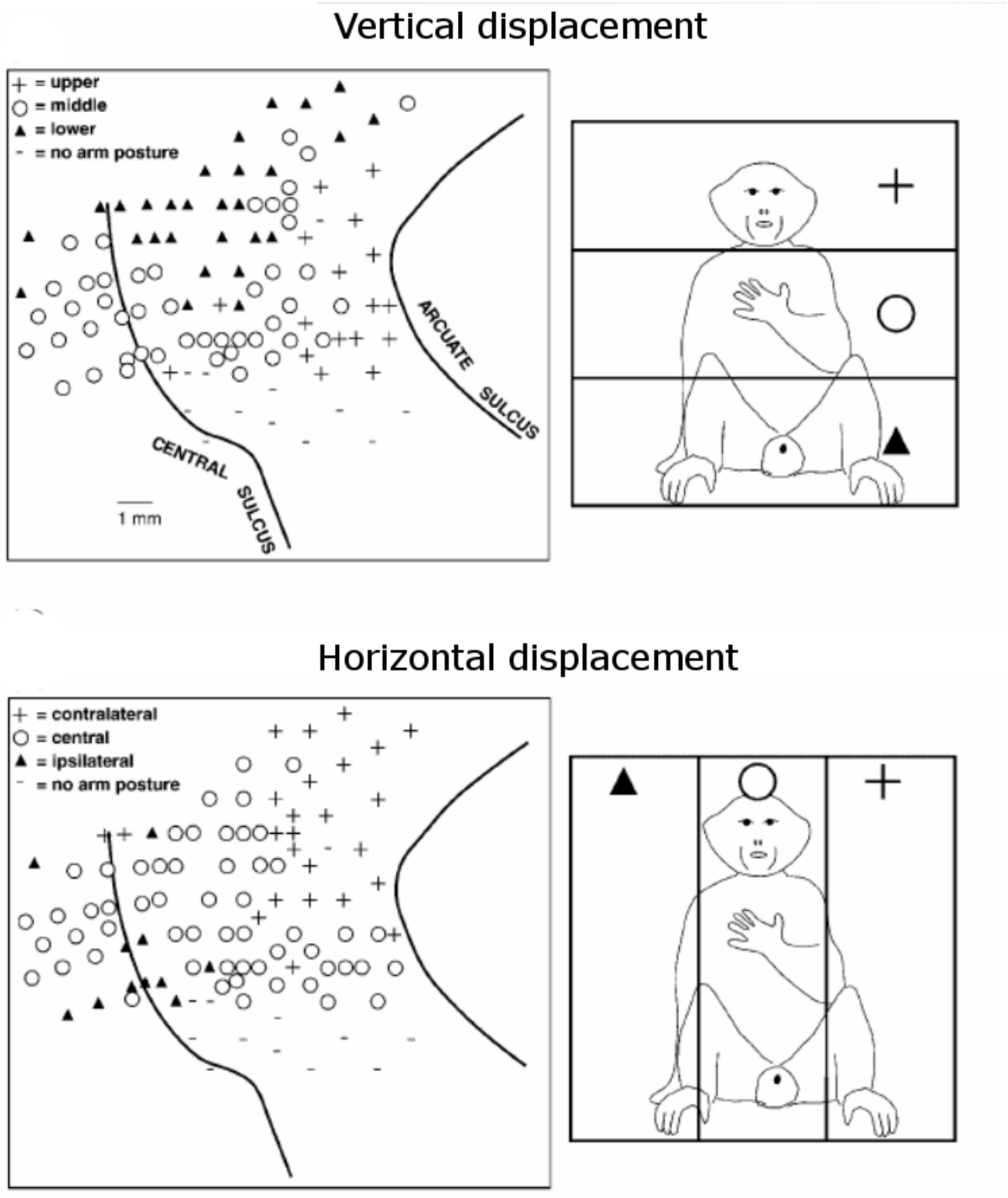

Complex movement representations have also been documented in the rat in which forelimb reaching, grasping, and retraction is evoked with LD-ICMS of forelimb sensorimotor cortex (Ramanathan et al., 2006; Bonazzi et al., 2013). LD-ICMS findings suggest that motor cortex comprises a map of motor repertoire encoding coordinate movement direction of the limbs across multiple muscle groups rather than a somatotopic map of muscles (Graziano et al., 2002; 2005; Aflalo and Graziano 2006). This hypothesis is derived from electrical stimulus-driven activity, however, and does not necessarily speak to functional motor output encoding in naturalistic behaviour. A causal test of functional movement encoding in motor cortex was conducted in this thesis. I conclude with a brief review on the organization of the corticomotor system in the rat and current understanding of its organization and potential for reorganization prior to a description of the research objectives of this thesis.

1.4 Sensorimotor neocortex and corticospinal projections in the rat

A six layer neocortex is ubiquitous in placental mammals and is differentiated according to cytoarchitecture and connectivity (Douglas & Martin, 1990; Braak, 1984). Each layer is numbered sequentially from cortical surface to subcortical white matter: Layer I (molecular layer) is the most superficial layer and predominantly acellular, consisting mainly of axons and dendrites; Layer II (external granular layer) contains densely packed granule cells projecting locally to adjacent cortical layers; Layer III (external pyramidal layer) contains a dense packing of pyramidal cells projecting intracortically; Layer IV (internal granular layer) consists mainly of of granule cells receiving thalamocortical afferents; Layer V (internal pyramidal layer) contains mainly medium to large pyramidal cells (named Betz cells in motor cortex) forming the major

output layer from the cortex and the origin of the corticospinal tract; and layer VI (multiform layer) consisting of a heterogeneous mixture of cell types projecting corticofugally. A non-uniform distribution of layers is observed between cortical regions in which motor cortex is characterized by a prominent layer V and is often referred to as agranular cortex, lacking or with a greatly reduced layer IV. Conversely, somatosensory areas are characterized by a prominent layer IV and are often referred to as granular cortex with a reduced layer V.

Motor and somatosensory cortices are partially overlapping in the rat and are often collectively referred to as sensorimotor neocortex, consisting of both granular and agranular regions (Donoghue and Wise, 1982). Agranular zones are found most rostral in the frontal cortex and are classified into medial (AgM) and lateral zones (AgL). AgM is found is found most rostral and characterized by dense layers II and III. AgL is found more caudally, consisting of a thick layer V. Primary somatosensory cortex is found caudal to AgL exhibiting a prominent granular layer IV, and contains cells that are activated by light tactile stimuli under barbiturate anesthesia (Welker, 1971). Motor cortex in the rat comprises AgL and the rostrolateral portions of granular SI containing corticospinal projections and eliciting stimulation evoked movement. Craniofacial, forelimb, hindlimb, and trunk movement representations are found within AgL and partially extend into rostral SI (Wise et al., 1979; Donoghue and Wise, 1982; Neafsey and Sievert, 1986). The rat sensorimotor cortex contains two separate motor representations of the forelimb within AgL, known as the rostral forelimb area (RFA) and the caudal forelimb area (CFA) (Neafsey et al., 1986; Neafsey & Seivert, 1982; Fig. 1.4). The CFA, extending caudally from bregma in the coronal plane, is the larger of the two areas and has purported to be analogous to the primary motor cortex in primates (Rouiller et al., 1993; Nudo and Frost, 1996). A strip of craniofacial representation separates the two forelimb motor areas.

Figure 1-4. Forelimb and craniofacial motor map derived with SD-ICMS in Long-Evans Rat. Forelimb movement representations area outlined in bolded borders demonstrating rostral (RFA, filed in red) and caudal (CFA, filled in blue) forelimb representations bounded by craniofacial representation. Dashed lines indicate cytoarchitectonic borders between medial (AgM) and lateral (AgL) agranular cortex(medial line) and between AgL and granular primary somatosenroy cortex (Gr(SI)) (lateral line). Df, digit flexion; Ee, elbow extension; Ef, elbow flexion; We:, wrist extension; Nk, neck; VI, vibrissae; Ja, Jaw. Modified from Neafsey and Sievert et al. (1986).

Figure 1-4: Forelimb motor map in the rat elicited with SD-ICMS

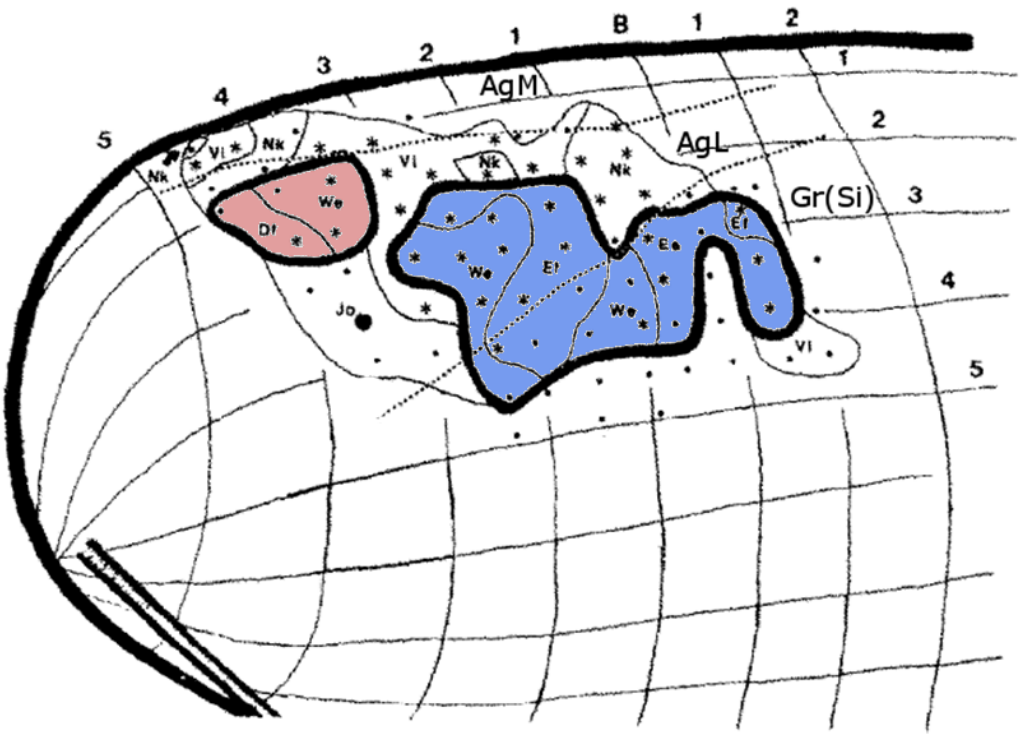

SD-ICMS elicits twitches of proximal (shoulder, elbow) and distal (digit, wrist) forelimb musculature from both motor regions without clear topographic distribution (Donoghue and Wise, 1982; Neafsey and Sievert, 1986). The corticospinal tract (CST) is the major descending pathway for the control of volitional movement ubiquitous in all mammals and prominently developed in primates (Nudo and Frost, 2006). In primates, CST fibers originate from layer V pyramidal neurons in frontal and anterior parietal lobes and terminate in spinal grey matter. In non-human primates, the primary, premotor, and supplementary motor cortices give rise to roughly 60% of CST axons. In humans, these cortical regions account for about 80% of CST fibers. The remainder of CST innervation arises from the cingulate motor and parietal somatosensory regions (Towe, 1973; Kuypers, 1981; Dum & Strick 2005). In rodents, the corticospinal tract arises from large pyramidal neurons situated in layer V of the sensorimotor neocortex (Miller, 1987). Although there may be large functional overlap in the distribution of CST neuron origins and terminations, projections for motor cortical regions are primarily involved in the control of volitional movement parameters, while those from somatosensory parietal areas have been associated with mediating descending control of afferent sensory input. (Porter and Lemon, 1993).

CST fibers course through the internal capsule, run along the ventral medullary pyramids, decussate in the caudal medulla, and continue down the contralateral dorsolateral funiculi in primates (Porter and Lemon, 1993) and in the base of the dorsomedial funiculi in rats (Armand, 1982)(Fig. 1-5). A small number (~5-10 %) of corticospinal projections do not cross at the

Figure 1-5. The corticospinal tract (cst) in the rat originates in layer V of the cerebral cortex and project to spinal grey matter via the medullary pyramids. Corticospinal fibers from the RFA and CFA terminate in the cervical enlargement (C) After decussating, it continues within the ventral dorsal funiculus. Modified from Joosten and Bär (1999).

Figure 1-5: Corticospinal tract in the rat

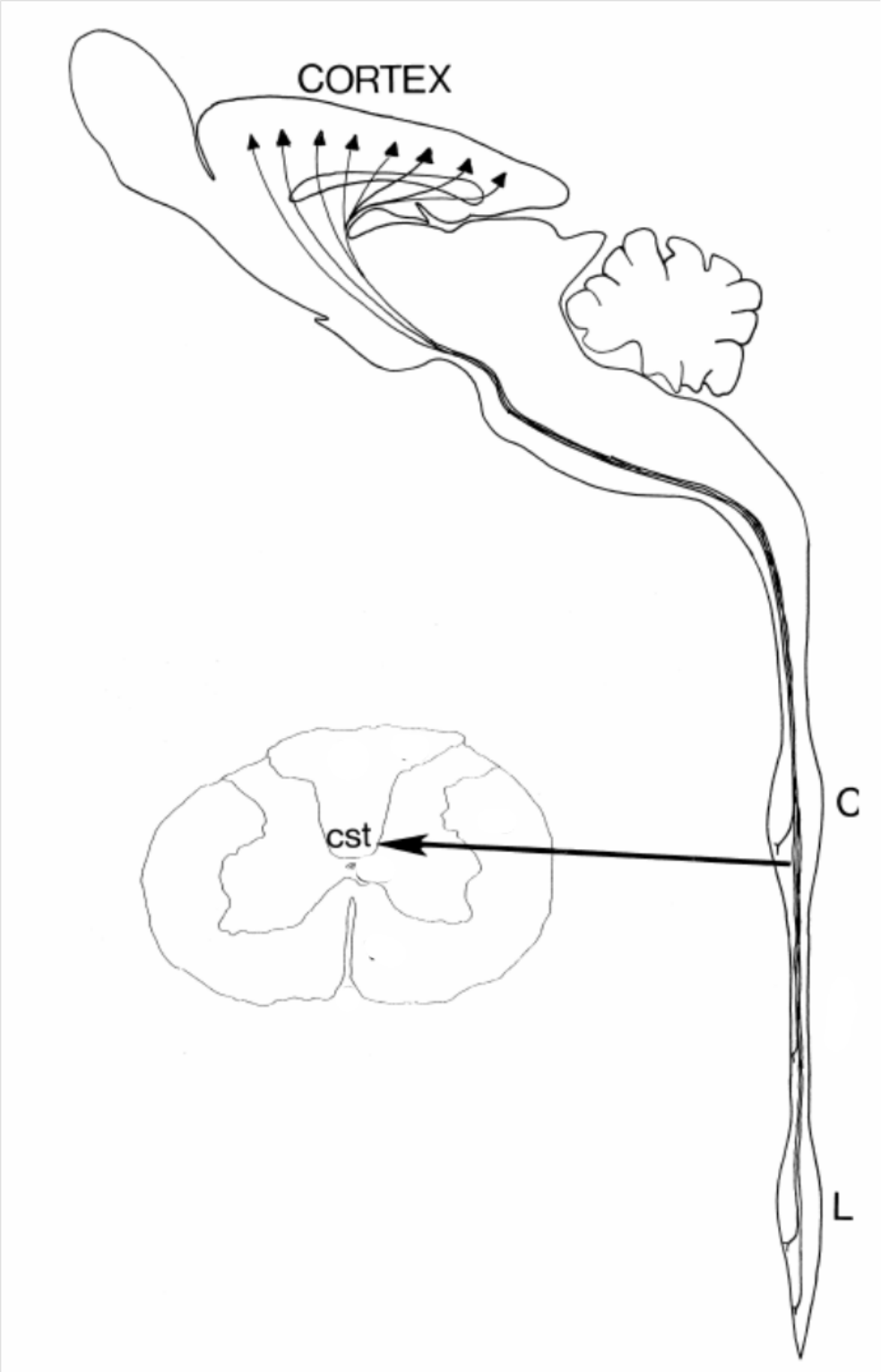

pyramidal decussation, however, and form the ventral CST (Terashima, 1995; Martin, 2005). Within the spinal cord, motor neurons and interneurons that project to common targets are often grouped together, leading to a high amount of spatial organization (Rothwell, 2012). CST fibers innervate the entire length of the spinal cord and terminate in all spinal laminae in primates and rats (Heffner and Masterton, 1975; Tracey 2004). CST terminals synapse in all mammals indirectly with lower motoneurons via spinal interneurons, while in primates there is also evidence for a small number of terminals forming direct cortico-motorneuron connections (Isa et al., 2007; Lemon, 2008). In addition to primary spinal terminations, CST neurons also sends widespread collateral fibers to the neocortex, the rubrospinal, tectospinal, vestibulospinal and reticulospinal descending motor systems, striatum, thalamus, and dorsal column sensory nuclei (see Canedo, 1997 for an excellent review; Lévesque et al., 1996). There is a functional segregation in the caudal extent of CST termination at the spinal cord level with fibers innervating upper limb motoneurons terminating in the cervical enlargement and. those for lower limb projecting to the lumbosascral enlargement (Li et al., 1990; Kiernan, 2009).

The motor cortex and CST has been widely implicated in a variety of motor functions and parameters including flexor activity, muscle tonus, digit dexterity, force, velocity, direction, and timing (Beck and Chambers, 1970; Cheney and Fetz, 1980; Evarts, 1986; Georgopoulos, 1988; Hepp-Reymond and Wiesendanger, 1972; Lamarre et al, 1980; Martin and Ghez, 1988; Lawrence and Kuypers, 1968). The role for the CST is exceptionally highlighted in skilled motor behaviour involving distal limb musculature (Passingham et al., 1983; Colebatch and Gandevia, 1989; Whishaw et al., 1991; Freund et al., 2006). In addition to its role in motor function, the CST is also involved in the descending control of afferent proprioceptive inputs (Wolpert et al., 2001) and primary sensory afferent fibers (Canedo, 1997). Accordingly, CST lesions lead not

only to motor impairment, but also to deficits in fine sensorimotor control (Lemon & Griffiths, 2005).

1.5 Lesion techniques to investigate neural function

Lesion techniques involve the removal, destruction or deactivation of neural tissue. Lesions have been widely used to localize and infer the function of discrete brain regions by examining the behavioural effects resulting from their absence. There are two primary types of lesion techniques involving either irreversible or reversible loss of the affected tissue. Irreversible lesions cause permanent alterations to neural function through the removal or destruction of tissue whereas reversible lesions cause temporary changes to neural function through the inhibition of synaptic transmission or the conduction of action potentials.

Conventional irreversible lesion techniques involve the surgical removal of tissue through ablation (Lashley, 1950) or aspiration (Weiskrantz, 1956). Destruction of tissue is typically induced by electrolytic (Horsley and Clarke, 1908), radiofrequency (Aggleton and Passingham, 1981), or freezing (Dvorák, 1977) lesions. Irreversible lesions have proved invaluable in the localization of function in the brain, but suffer two primary limitations. The first is that while behavioural deficits occurring immediately following the lesion procedure are inferred to reflect loss of function from the affected tissue; after time, new adaptive functions from remaining structures can exert a large role in behavioural compensation. Partial recovery of function following irreversible lesions are common (Hicks & D'Amato, 1970; Newsome and Paré, 1988; Nudo et al., 1996) and can make it difficult to interpret findings by indicating either that the damaged area is not essential to the lost function, or that other areas can take over its functional

role. A second limitation to permanent lesion techniques is that they involve indiscriminate injury to both local cell bodies as well of fibers of passage originating outside of the lesion area. It can therefore be difficult to ensure that the loss of function is directly related to the loss of circuitry intrinsic to the lesion area, rather than being influenced by the destruction of fibers of passage coursing through the lesion area. In effort to avoid damage to fibers of passage, excitotoxic chemical ablations can be performed with ibotenic (Sullivan and Gratton, 2002) or kainic acid (Hiraba and Sato, 2005) to selectively destroy cell bodies while sparing fibers of passage but these techniques have their own set of disadvantages and can induce seizure activity (see Malpeli, 1999).

Cell-type selective permanent lesions can also be made with certain neurotoxins. Chapter 2 utilizes an irreversible cytotoxic lesion of dopamine neurons in the substantia nigra pars compacta with 6-hydroxydopamine (6-OHDA) in a rodent model of Parkinson's disease. 6-OHDA was the first chemical known to exert a specific neurotoxic effect on catecholamine neurons (Ungerstedt, 1968). 6-OHDA is a hydroxylated analogue of dopamine and is selective taken up by catecholamine transporters. It induces cell death via oxidative stress from the generation of hydrogen peroxide and hydroxyl radials (Cohen and Werner, 1994). 6-OHDA does not cross the blood-brain barrier and must be stereotaxically infused. Application of 6-OHDA into the lateral ventricles produces widespread central catecholamine depletion (Ungerstedt, 1968; Bloom et al., 1969) and noradrenergic cell loss can be prevented by pretreatment with norepinephrine transporter inhibitors. Nigrostriatal degeneration can be induced by local 6-OHDA infusion into substantia nigra pars compacta (Carman et al., 1991), the striatum (Kirik et al., 1998), or the medial forebrain bundle (Ungerstedt, 1968). Partial recovery of function is observed at protracted time points following 6-OHDA administration (Deumens et al., 2002);

however, it was used in Chapter 2 to model nigrostriatal dopamine pathway degeneration observed in Parkinson's disease at a time point in which maximal cell loss and behavioural impact is observed (Ben et al., 1999).

Reversible lesions can be performed using pharmacologic agents or cryogenic techniques to temporarily deactivate neural tissue. A benefit of reversible lesions is the ability localize functions in the brain without resorting to irreversible damage or alteration of neural functioning. Reversible lesions allow for direct investigation of a structure's function during the time of deactivation without the influence of compensatory recovery of function observed with irreversible lesions. Pharmacologic deactivation agents can be broadly classed into four categories (Malpeli, 1999): 1) Local anesthetics (e.g., lidocaine hydrochloride) can provide complete reversible inactivation in both cell bodies and fibers of passage (Malpeli et al., 1981). 2) Sodium channel blocks such as tetrodotoxin cause complete synaptic and conduction block (Narahanshi, 1972) with a slower and longer lasting time course compared to lidocaine (Zhuravin and Bures, 1991). 3) Divalent cations (cobalt, magnesium, manganese) are all able to block synaptic transmission by preventing calcium uptake in presynaptic terminals (Hagiwara and Byerly, 1981). Repeated administration of divalent cations, however, has been associated with cell death (Malpeli, 1999). 4) Inhibitory transmitters and their analogues such as GABA (Maunsell et al., 1990) and the $GABA_A$ agonist muscimol (Hikosaka and Wurtz, 1985) provide effective neuronal inhibition by promoting somatic hyperpolarization while sparing conduction in fibers of passage. Pharmacological agents excel at providing temporary deactivation of small volumes of cortical and subcortical tissues. Limitations of pharmacological inactivation (reviewed in Lomber, 1999) are that 1) repeated infusions have been shown to lead to permanent damage, 2) it is difficult to replicate the extent of inactivation between both repeated infusions

and animals, and 3) larger (> 2 mm^3) deactivation areas necessitate the use of multiple infusion penetrations which can lead to mechanical damage of overlaying tissue.

Reversible Cryogenic lesion techniques involve the cooling of neural tissue below 20° C to achieve a synaptic block of neural transmission (Horel, 1984; Lomber et al., 1999). Strengths of cryogenic deactivation are that limited regions of tissue can be selectively, rapidly (minutes), reversibly, and repeatedly deactivated while sparing activity in fibers of passage. Surface structures are commonly deactivated with thermoelectric-type devices (Fuster and Alexander, 1970; Schiller and Malpeli, 1977) requiring fixed-head restraint, or chronically cryoloop devices permitting physiological or behavioural assessment in freely-moving animals (Horel, 1991; Lomber et al., 1999). Cryoloops are constructed with stainless steel hypodermic tubing that can be conformed to the cortical area desired to be deactivated. Cryoloop deactivation is achieved by pumping chilled methanol through the tubes, and temperatures held stable to desired values by varying flow rate. Deep structures can be effectively deactivated with the use of penetrating cryoprobes (Zhang et al., 1986; Campeau and Davis, 1990). The surgical procedure to implant cryoloops, their presence in contact with the cortex, and their operation has been shown not to disrupt either the structural or functional integrity of the cerebrum (Lomber and Payne, 1994; Lomber et al., 1999; Yang et al., 2006). In Chapter 3 chronic cryoloop deactivation is adapted for use in the rat to provide a causal test for a functional dissociation between the RFA and CFA forelimb motor areas revealed by long-duration ICMS.

1.6 Behavioural assessment of forelimb motor ability

Rats exhibit dexterous forelimb motor abilities sharing homologies with primates (Iwaniuk and Whishaw, 2000; Cenci et al., 2002). The main focus of this thesis is to address the functional organization of motor cortex. Behavioural assessment of forelimb motor performance, along with microstimulation and lesion techniques, is a key component of the methods used in the following experimental chapters. In this section I provide an overview the various behavioural tasks used and their rational.

The open field test involves placement of a rat inside a square, rectangular, or circular arena cordoned off by walls allowing for naturalistic behaviour to occur unperturbed for a set amount of time. A number of dependent variables can be recorded reflecting measure of locomotor activity, exploratory behaviour, emotionality and autonomic activity (Walsh and Cummins, 1976). Originally developed for use as an index of timidity, in which the amount of defecation occurring during testing was assessed (Hall, 1934), the open field test has also shown to be a sensitive assay of locomotor activity. When used to assess locomotor activity, both rearing behaviour (Invinskis, 1968) and ambulation (Walsh and Cummins, 1976) have proved to be reliable measures. These measures have also proved to be sensitive alterations in motor cortical function resulting from degeneration of nigrostriatal dopamine projections (Rauch et al., 2010; Abedi et al., 2013). In Chapter 2, rearing behaviour (total frequency) and ambulation (measured as the number of entries to equal-seized partitioned sectors on the floor) were recorded prior to and following a bilateral Parkinson's disease lesion model incorporating subthalamic deep brain stimulation in effort to assess both lesion-induced deficits and stimulation-induced improvements in locomotor activity.

The cylinder test (Tillerson et al., 1998) involves placement of a rat within a transparent acrylic cylinder and recording coordinated forelimb use, assessed as the frequency of hand

placements made on the cylinder walls during exploratory activity when rearing. The test has been shown to be highly sensitive to deficits in contralateral hand use ability observed following nigrostriatal degeneration, injury to forelimb motor neocortex, and cervical spinal damage (Schallert et al., 2000). In particular, a significant negative correlation between forelimb use and the amount of dopamine depletion following 6-OHDA nigrostriatal lesions is observed (Tillerson et al., 1998; Schallert and Tillerson, 1999). Moreover, the test has also shown to be sensitive to therapeutic intervention following nigrostriatal dopamine depletion (Choi-Lundberg et al., 1998). In Chapter 2, forelimb use (scored as total number of left, right, and simultaneous forelimb placements) prior to and following a bilateral Parkinson's disease lesion model incorporating subthalamic deep brain stimulation in effort to assess both lesion-induced deficits and stimulation-induced improvements on limb-use function.

Skilled forelimb reach-to-grasp shaping in the rat can be learned with repeated training in the single pellet reaching task (Whishaw and Pellis, 1990). Rats are tasked to reach through a horizontal slit at the front of the testing apparatus to grasp a food pellet reward and bring in back to the mouth for consumption. Reaching success is initially low during initial stages training, but improves to asymptotic levels during task acquisition with repeated training. Motor learning in this task is also reflected in cortical synaptogenesis and the reorganization of cortical forelimb movement representations (Kleim et al., 1998, 2004). In addition to endpoint reaching success, each reach movement can be broken down into ten discrete subcomponents for qualitatative kinematic assessment according to an ordinal rating scale (Whishaw et al., 2003). Analysis of limb movements made by rats in this task have been shown to be remarkably similar to upper limb movements performance by humans during reaching (Whishaw et al., 2002), with the exception that rats rely on olfactory rather than visual cues (Whishaw and Tomie, 1989).

Lesions of the sensorimotor cortex (Whishaw et al., 1991) and corticospinal tract (Peicharka et al., 2005) are associated with impairments in reaching ability and the abolishment of forelimb responses evoked with ICMS. In Chapter 3, reaching success and kinematic assessment of reaching subcomponent scores were used to assess deficits in skilled reaching performance in RFA-cooled and CFA-cooled rats under baseline, cortical cooling, and rewarm conditions.

The vermicelli handling test provides a quantitative test of dextrous pasta handling in rats sensitive to lateralized impairments in hand grasping ability (Allred et al., 2008). Central nervous system damage has been known to influence the way in which rats grasp and handle food (Peterson, 1951). Rats use both forelimbs during spontaneous feeding, and forelimb use asymmetries are observed following frontal neocortical damage resulting in disuse of the affected limb (Whishaw et al., 1992). The vermicelli handling test capitalizes on asymmetric hand grasping deficits, sensitive to lateralized impairment following unilateral lesions of sensorimotor cortex, by assessing the number of forepaw adjustments made by each hand during grasping and consumption of short strands of uncooked vermicelli pasta strands. Adjustments are defined as releases and re-grasping of the pasta or reformations of the hand hold exhibited as extension-flexion or abduction-adduction of the digits. Following forelimb sensorimotor cortical lesions, the number of adjustments made by the affected (contralateral) limb are reduced and can be reflected by a reduction in the vermicelli asymmetry ratio (proportion of contralateral to ipsilateral hand adjustments made during a trial; Allred et al., 2008). The test provides a simple method by which to quantify bilateral coordinated hand use that not only is sensitive to lateralized impairment, but tests both forelimbs at the same time. The test is primarily sensitive to distal forelimb function unlike skilled reaching tasks which involved both proximal and distal function. In Chapter 3, the forelimb adjustment asymmetry ratio is used to assess deficit in distal

hand use in RFA-cooled and CFA-cooled rats under baseline, cortical cooling, and rewarm condition. The total time required to consume each strand was also recorded to assess for a deficit in cranial (tongue and jaw) motor function between cooling conditions.

Forelimb and digit use during sunflower seed consumption among rodents has been reported in which rats manipulate the seeds into a preferred position, before shelling with the fat end of the seed oriented into the mouth (Whishaw et al., 1998). The seed is first picked up bilaterally with a hand grip then transferred to the mouth. A portion of the seed is chewed away and subsequently shelled longitudinally, being manipulated numerous times, involving bilateral and unilateral forelimb movements. The task represents a mixed assessment cranial (tongue and jaw) and forelimb (proximal and distal) motor function (Prine et al., 20132). The total amount of time spent manipulating, opening, and consuming a preset number seeds was recorded in addition to the number of shell fragments the rat needed to break to gain access to the seed are recorded. Both measures have shown to be sensitive to sensorimotor cortical injury (Gonzalez and Kolb, 2003). In Chapter 3, seed manipulation times and number of shell fragments produced were used to assess forelimb motor deficits in RFA-cooled and CFA-cooled rats under baseline, cortical cooling, and rewarm condition.

Forelimb grip performance can be used to measure subtle changes in forelimb muscle strength (Maurissen et al., 2003) and has been introduced into the functional observation battery to screen for neurobehavioural toxicity (Tilson et al., 1979). Grip strength measurements are taken by allowing a rat to grasp a bar attached to a tension meter and recording the peak force exerted by the forelimbs (g) as the rat is pulled away until the its grip is broken. In Chapter 3, forelimb grip performance was used to assess deficits in muscle strength in RFA-cooled and CFA-cooled rats under baseline, cortical cooling, and rewarm condition.

1.7 Motor map plasticity and behaviour

The functional organization of motor cortex can be revealed by investigating the relationship between cortical organization and behaviour. An important process in motor learning and behavioural recovery following injury is the reorganization, or plasticity, of sensory and motor cortices (Nudo et al., 1996; Kaas, 1997; Xerri et al., 1998 Kleim et al., 2002; Adkins et al., 2006). Motor maps have been shown to be highly plastic. Skilled motor learning (Kleim et al., 2004), repeated seizures (Teskey et al., 2002), and disease and injury affecting the motor system (Kleim et al., 2003; Thickbroom et al., 2006; Brown et al., 2009) have all been demonstrated to induce map reorganization. Importantly, map plasticity appears to be a conserved trait among mammals: reorganization has been observed following the acquisition of skilled motor learning in humans (Tyc et al., 2005) non-human primates (Nudo et al., 1996) and rats (Kleim et al., 2004). Following skilled motor learning, the cortical representations corresponding to movements used in the learning tasks are found to be selectively magnified in size. Cortical reorganization has been shown to be supported by changes in protein synthesis (Kleim et al., 2003), synapse formation (Kleim et al., 2002) and synaptic efficacy (Monfils and Teskey, 2004). These results indicate that motor cortex function is alterable in adult animals in a use-dependent manner.

Improvements in motor function with rehabilitation training following cortical injury has been well documented in primates and rats (Friel et al., 2000; Nudo et al., 2006a; Nudo et al., 2006b) and forms the basis for constraint induced movement therapy used in stroke rehabilitation (Blanton et al., 2008). In rats, both rehabilitation training (Moon et al., 2009) and cortical

stimulation (Zhou et al., 2010) improve behavioural recovery following cortical injury. Loss of cortical movement representations are known to lead to deficits in skilled behaviour (Kleim et al., 2003) and are restored along with behavioural proficiency after skilled motor training. Additionally, manipulations that prevent map reorganization impair skilled motor learning (Conner et al., 2003). Concomitant with behavioural improvement, rehabilitation therapy is associated with cortical synaptogenesis (Kleim et al., 2004) and synaptic changes have shown to be localized to areas of motor cortex undergoing map reorganization (Kleim et al., 2002). Motor map plasticity is observed in association with behavioural recovery following brain injury in both non-human primates (Rouiller et al, 1998; Frost et al., 2003) and rats (Castro-Alamancos and Borrel, 1995; Castro-Alamancos et al., 1995; Sanes and Donoghue, 2000; Kleim et al., 2003). After focal injury to the motor cortex, impairments of the contralateral forelimb are observed. Following rehabilitative training, motor performance improves in association with the appearance of new cortical representations adjacent to the lesion area. When cortical reorganization is disrupted (Kleim et al., 2003), induced by repeated seizures (Teskey et al., 2008; Henry et al., 2008), or newly responsive cortical sites following recovery after injury are inactivated (Rouiller et al., 1998; Castro-Alamancos and Borrel, 1995), deficits in skilled motor learning and reinstatement of injury-related impairments are observed. These results demonstrate a relationship between motor map and behavioural plasticity.

While there is ample evidence of a link between motor map and behavioural plasticity, the nature of how changes in map organization relate to specific changes in behaviour is not well understood. As SD-ICMS elicits movement about individual joints, it is difficult to associate map changes to alterations in specific behaviours requiring the coordinate involvement of across multiple muscle groups. LD-ICMS may provide a valuable technique towards this endeavour.

SD-ICMS remains an invaluable technique to assess cortical excitability and the strength of synaptic link between cortical neurons and spinal motoneurons.

1.8 Thesis objectives and hypothesis

This thesis addresses the general question of relating the functional organization of motor cortex with behaviour across three empirical chapters. In chapter 2, I demonstrate that acute (< 60 s) changes in motor ability can be reflected with alterations in cortical movement representations. In chapter 3, I investigate and provide evidence for a movement vs. muscle based organization to motor cortex. In chapter 4, I indicate that a movement-based organization to motor cortex can be useful in explaining behavioural sequelae following alterations in functional cortical organization. The three chapters share a united theme of explaining motor cortical organization with behavioural ability and answer three, related specific hypotheses:

1) Loss of frontal neocortical activation is one of the main neurophysiological abnormalities of Parkinson's disease (PD) and can be observed in rodent models of nigrostriatal degeneration. High-frequency deep brain stimulation (DBS) of the subthalamic nucleus improves motor deficits in PD. However, it is unknown whether this general therapeutic effect is associated with a restoration of frontal output function. **The objective of Chapter 2 was to determine whether acute changes in motor ability would be reflected in neocortical movement representations.** To address this question, chronic stimulating electrodes were implanted bilaterally into the subthalamic nuclei of adult rats that received either bilateral intrastriatal 6-

hydroxydopamine (6-OHDA) or vehicle infusion to induce nigrostriatal degeneration. Forelimb use and locomotor activity was assessed based in the cylinder and open field tests in intact, post-lesion+sham DBS, and post-lesion+DBS conditions. SD-ICMS was then used to probe frontal output function by assessing forelimb movement thresholds as a measure of cortical excitability (Brown et al., 2009; Viaro et al., 2013). **It was hypothesized that effective STN DBS would improve behavioural deficits following 6-OHDA administration and would be associated with a rescue of forelimb movement representation size and movement thresholds assessed under SD-ICMS**

2) Motor cortex has been proposed to be functionally organized as either a somatotopic representation of body musculature or a topographically arranged encoding of species-typical movements. **The objective of chapter 3 was to investigate distinct and conflicting predictions that can be made depending on whether motor cortex is functionally organized as a map of muscles (as suggested by SD-ICMS) or a map of complex movements (as suggested by LD-ICMS).** LD-ICMS has been shown to evoke reach-to-grasp behaviour in the rat with distal forelimb hand closing and grasping representations localized in the RFA and proximal forelimb advance and retraction representations elicited from the CFA (Ramanathan et al., 2006; Bonazzi et al., 2013). Selective and reversible functional deactivation of the RFA and CFA was conducted using chronic cryoloop cooling deactivation (Lomber et al., 1999) during a behavioural test battery assessing forelimb motor function. **According to the muscle somatotopy hypothesis, acute selective deactivation of the RFA would not be predicted to induce a specific deficit in forelimb motor ability relative to CFA deactivation as both regions contain a representation of forelimb**

musculature as indicated by SD-ICMS. On the other hand, if the motor cortex is organized as a map of complex movement representations, acute deactivation of the RFA, selectively removing grasping representations as indicated by LD-ICMS, would be be hypothesized to result in specific deficits in forelimb grasping ability relative to CFA deactivation.

3) Repeated frontal lobe seizures are associated with larger neocortical movement representations (motor maps) in addition to concomitant interictal motor deficits in both clinical populations with epilepsy and in experimental models of epilepsy. However a functional relationship between motor map reorganization and specific behavioural impairment has yet to be established. **The objective of chapter four was to determine whether repeated seizure activity would be associated with alterations in evoked motor responses and complex movement representation topography assessed with LD-ICMS.** To investigate the functional mechanisms underlying seizure-induced cortical plasticity, LD-ICMS was used to derive complex forelimb movement representations following chronic kindling of the corpus callosum. **It was hypothesized that repeated seizure activity would be associated with increased overlap between forelimb movement representations.**

Chapter Two:

High frequency stimulation of the subthalamic nucleus acutely rescues motor deficits and neocortical movement representations following 6-hydroxydopamine administration in rats

Andrew R. Brown[1,2], Michael C. Antle[1,3,4] , Bin Hu[1,5] & G. Campbell Teskey[1,3,6]

[1]*Hotchkiss Brain Institute*, [2]*Department of Neuroscience,* [3]*Department of Psychology,*

[4]*Department of Physiology and Pharmacology,* [5]*Department of Clinical Neurosciences,*

[6]*Department of Cell Biology and Anatomy, University of Calgary, Alberta, Canada*

Published in *Experimental Neurology* 231: 82-90, 2011.

First author contributions: experimental design, lesion and electrophysiological mapping surgery, behavioural testing, immunocytochemistry, data analysis, manuscript preparation.

2.1 Abstract

Loss of frontal neocortical activation is one of the main neurophysiological abnormalities of Parkinson's disease (PD) and can be observed in rodent models of nigrostriatal degeneration. High-frequency deep brain stimulation (DBS) of the subthalamic nucleus improves motor deficits in PD. However, it is unknown whether this general therapeutic effect is associated with a restoration of frontal output function. To address this question, chronic stimulating electrodes were implanted bilaterally into the subthalamic nuclei of adult rats that received either bilateral intrastriatal 6-hydroxydopamine (6-OHDA) or vehicle infusion to induce nigrostriatal degeneration. Forelimb use and locomotor activity was assessed based on the cylinder and open field tests in intact, post-lesion+sham DBS, and post-lesion+DBS conditions. Intracortical microstimulation was then used to probe frontal output function of forelimb motor areas. DBS was found to improve motor deficits arising from 6-OHDA lesions, increase forelimb map area, and decrease movement thresholds relative to baseline. These effects were significantly greater in 6-OHDA lesion rats compared to vehicle controls. Results indicate that a large scale reorganization of motor cortex can take place during subthalamic DBS following dopamine depletion in a rodent model of PD.

2.2 Introduction

Degeneration of the nigrostriatal dopamine pathway is a hallmark of Parkinson's disease and impairs motor function. According to the basal ganglia-thalamocortical circuit model, nigrostriatal dopamine cell loss results in excessive activity in basal ganglia output nuclei. Increased basal ganglia output inhibits thalamocortical projections and, in turn, suppresses frontal neocortical activity leading to hypokinesia (Alexander et al., 1990; DeLong and Whichmann, 1993; Parent and Hazrati, 1995). Indeed, impaired movement-related activation in PD is observed in some, but not all, frontal motor areas (Jenkins et al., 1992; Playford et al., 1992; Rascol et al., 1992; Sabatini et al,. 2000; Haslinger et al., 2001; Buhmann et al., 2003). This cortical abnormality is at least partially reversed with dopaminergic therapy (Jenkins et al., 1992; Rascol et al., 1994; Haslinger et al., 2001; Buhmann et al, 2003).

Nigrostriatal degeneration following 6-hydroxydopamine (6-OHDA) administration in rats provides a valuable model for investigating the pathophysiology of substantia nigra dopamine cell loss and behavioural impairments in PD (Schwarting and Huston, 1996; Deumens et al., 2002). Following 6-OHDA administration reduced metabolic activity and immediate early gene expression in frontal cortical areas including the primary motor cortex has been observed (Rolland et al., 2007; Steiner and Kitai, 2000). The size of forelimb movement representations or motor maps is significantly reduced in 6-OHDA lesioned in rats (Brown et al., 2009; Prine et al., 2010) and this may reflect reduced functional cortical output (Young et al., 2011a) resulting in behavioural impairment.

Deep brain stimulation of the subthalamic nucleus (STN DBS) improves cardinal motor symptoms in PD (Limousin et al., 1995; Krack et al., 2003; Deuschl et al., 2006); however, the

therapeutic mechanisms involved are not fully understood (McIntyre et al., 2004). Recent evidence suggests that DBS activates motor cortex (Dejean et al., 2009; Gradinaru et al., 2009; Li fet al., 2007). As dopamine loss has been shown to decrease motor map size, reflective of reduced cortical excitability, we hypothesize that DBS can reverse this effect and lead to improved motor performance following nigrostriatal degeneration. Intracortical microstimulation (ICMS) techniques were used to probe changes in forelimb motor map size and movement thresholds under conditions of sham or STN DBS in rats receiving either bilateral 6-OHDA or vehicle control infusion. Therapeutic effectiveness of STN DBS was assessed by analysis of forelimb use and locomotor activity.

2.3 Materials and Methods

2.3.1 Rats

Twenty five adult male Long-Evans rats weighing 278-417 g at the time of electrophysiological mapping were used in this experiment. Rats were obtained from Charles River (Saint-Constant, QC) and housed individually in clear plastic cages in a colony room maintained on a 12h light/dark cycle (lights on at 07:00) at 21°C. Upon arrival, rats were gently handled once per day for five days to minimize stress during testing. All experimentation was conducted between 08:00 and 19:00h. Rats were provided free access to food and water throughout the duration of their housing except for an overnight food restriction prior to electrophysiological mapping. Additionally, free access to a liquid diet (AIN-76, Bioserve, Frenchtown, NJ) was provided for three days following 6-OHDA infusion surgery. All rats were able to resume a solid diet by this time point.

All procedures involving rats used in this study strictly adhered to the guidelines of the Canadian Council on Animal Care and were approved by the Health Sciences Animal Care Committee of the University of Calgary. All efforts were made to adhere to the principles of reduction, refinement, and replacement in experimental design (Russell & Burch, 1959), with every attempt made to limit the number of subjects and minimize animal suffering.

2.3.2 Experimental procedures

Rats were assigned into two groups: those receiving either bilateral intrastriatal 6-OHDA (n=14, DA lesion group) or vehicle (n=11, sham lesion control) infusion. Pre-lesion behavioural testing was conducted in one session in the cylinder and open field tests as a baseline control to compare with sessions following dopamine depletion and under DBS conditions. After baseline behavioral testing, rats underwent surgical procedures for 6-OHDA infusion and chronic electrode implantation. Behaviour was tested again 13-18 days later in two sessions, first under sham DBS conditions and then under DBS stimulation in following testing sessions. Testing sessions were separated by at least 24 hours. Intracortical microstimulation was performed 21-25 days following 6-OHDA infusion and electrode implantation.

2.3.3 Behavioural testing

2.3.3.1 Cylinder Test

Forelimb use was assessed in the cylinder test (Schallert et al., 2000). Rats were placed in a transparent acrylic cylinder (20 cm diameter and 30 cm height) for 7-minute sessions. All sessions were video recorded for later analysis. The cylinder rested on a glass shelf with a mirror

placed beneath at a 90° angle to permit simultaneous views facing and underneath the cylinder in order to record forelimb use when the rat was turned away from the camera. Testing occurred under red-light illumination to promote vertical exploration (Schallert and Woodley, 2005). Forelimb use was scored as the total number forelimb placements (left, right, and both) made on the walls of the cylinder during rearing and for lateral movements along the wall. The first forelimb to make a wall contract during rearing was scored as an independent placement for the limb. Subsequent wall contact of the other forelimb while the initial placement was maintained was scored as an additional use of both forelimbs. Simultaneous placement of both forelimbs was scored as a single placement. In order for additional contacts to be scored following a placement, both forelimbs must have been removed from the walls. Stepping behaviour, in which alternating limb placements were made during lateral exploration of the cylinder in a single rear, was counted as a single "both" for each pair of forelimb placements.

2.3.3.2 Open field

Locomotor and vertical exploratory activity was assessed in an open field apparatus. The open field consisted of a 60 x 45 cm rectangular Plexiglas arena with walls 62 cm high. The arena was divided into 12 squares (4x3 grid) of equal dimension. Sessions were 5 minutes long and recorded from above for later behavioural scoring. Locomotor activity was scored as the number of squares entered by the rat during a session. Entries were defined as when all four paws were placed within a square. Vertical exploration was assessed as the number of rears.

2.3.4 Lesion and chronic electrode implantation procedures

Rats were anaesthetized with isoflurane (4% induction, 1.5% maintenance; VIP-3000 Vaporizer, Matrix, Orchard Park, NY) and placed in a stereotaxic instrument (Kopf, Tujunga, CA) with the incisor bar set to skull flat. Rats were monitored continuously throughout the surgery and levels adjusted as needed to maintain a surgical level of anaesthesia. The local anaesthetic Lidocaine (2%) was administered subcutaneously at the incision sites.

The lesion protocol used was adapted from Ben et al. (1999) and reported previously (Brown et al., 2009). Lesions were made by double intrastriatal infusions, per hemisphere, of 8 μg (free base) of 6-OHDA hydrochloride (Sigma, Oakville, ON) in 2 μl of physiological saline containing 1% ascorbic acid per site (4 sites in total) at a rate of 0.5 μl/min via 32-gauge microsyringe (Hamilton, Reno, NV) fixed to a manual microdrive manipulator (Kopf, Tujunga, CA). The microsyringe was then left in place for an additional minute to aid infusate diffusion. Coordinates relative to bregma were: AP +1.7, ML ± 2.8, DV -5.6 mm & AP – 0.92, ML ± 4.0, DV -5.5 mm. Vehicle control rats received infusions of 2 μl of physiological saline containing 1% ascorbic acid at the same coordinates.

Chronic twisted bipolar stimulating electrodes were implanted bilaterally targeting the dorsal limit of the STN (AP -3.5, ML ± 2.5, DV -7.8 mm) according to the stereotaxic co-ordinates of Paxinos and Watson (2005). Electrodes were constructed from Teflon-coated stainless steel wire 178 μm in diameter (A-M Systems, Everett, WA) with a tip separation of 0.5 mm. Electrode terminals were connected to gold-plated male amphenol pins which were inserted into a nine-pin McIntyre connector plug (Molino & McIntyre, 1972; Ginder Science, Ottawa, ON) that was adhered to the skull with dental cement and anchored with five stainless steel screws. An area of the skull on the left hemisphere extending between 6 mm anterior to and

2 mm posterior to bregma was left free of dental cement to aid the latter craniotomy. The scalp was then sutured around the headcap comprising the dental cement and plug, and rats were given a topical application of Xylocaine jelly (2%) analgesic around the incision.

2.3.5 Deep brain stimulation

High-frequency stimulation of the subthalamic nucleus consisted of 60 μs biphasic square-waves at frequency of 120 Hz delivered through isolated stimulators (A-M Systems model 2100). Stimulation intensity was independently assigned for each hemisphere for each rat based on the threshold level that induced stimulation bound side effects. In home cage testing, current intensity was slowly increased from 0 to a maximum of 150 μA until noticeable orofacial and forelimb contractions or contraversive turning was apparent. Stimulation intensity was then lowered until these elicited behaviours ceased, and this value was used in subsequent experimentation. Cases where activational effects from stimulation were not apparent and electrode placements were found to miss the STN target were excluded from the experiment.

2.3.6 Intracortical microstimulation

Standard ICMS techniques were used to generate detailed threshold maps of forelimb regions of the motor cortex (Kleim et al., 1998; Nudo et al., 1990; Teskey et al., 2002). Rats were anaesthetized with ketamine hydrochloride (100 mg/kg i.p.) and xylazine (5 mg/kg i.p.) and secured in a stereotaxic frame with the incisor bar set to skull flat. Supplemental injections of either ketamine (25 mg/kg) or a mixture of ketamine (17 mg/kg) and xylazine (2 mg/kg) were given i.p. as required throughout surgery to maintain a constant level of anaesthesia as

determined by monitoring vibrissae whisking, breathing rate, and foot and tail reflex in response to a gentle pinch.

A 7 x 5 mm craniotomy was performed over the left sensorimotor cortex. The window roughly extended between 4 mm anterior to and 2 mm posterior to bregma and from midline to 5 mm lateral of midline. A small puncture was made in the cisterna magna to reduce cortical edema. Dura was removed and silicone fluid (Factor II, Inc. Lakeside, AZ) heated to body temperature was used to cover the cortical surface. A 42x image of the exposed portion of the brain was captured using digital camera (Canon Canada Inc., Mississauga, ON) coupled to a Stemi 2000-C stereomicroscope (Carl Zeiss, Thornwood, NY), and displayed on a personal computer. A grid of 500 μm squares was then overlaid on the digital image using Canvas imaging software (9.0.1, ACD systems Inc., Miami, FL). Penetrations were performed at the intersections of the grid lines and in the center of each square to give an interpenetration distance of 354 μm, except when located over a blood vessel in which case a penetration was not performed.

Microelectrodes were made from borosilicate glass capillary tubes (World Precision Instruments, Sarasota, FL) using a micropipette puller (Kopf, Tujunga, CA), filled with 3.5 M NaCl, and bevelled at 30 degrees to yield a 3 μm tip with impedance values ranging between 1.0 and 1.5 MΩ at 12.5 Hz. Electrodes were guided into the neocortex to a depth of 1,550 μm by a microdrive (Narishige, Tokyo), corresponding to the somatic region of neocortical layer V pyramidal neurons. We have observed that movements can be readily elicited within a large (1550 ± 150 μm depth from surface) profile of forelimb sensorimotor cortex with negligible effect on thresholds (Young et al., 2011a). A platinum filament inserted into the micropipette was used to deliver electrical current via isolated stimulator unit (A-M Systems, Carlsborg, WA).

A ground stimulation lead was placed in contact with exposed neck musculature from the incision to puncture the cisterna magna. Current output reliability was measured via the voltage drop across a 1 kΩ resistor connected in series with the return lead to the stimulator. Stimulation trains consisted of 13 monophasic cathodal pulses, each 200 μs in duration, delivered at a frequency of 333 Hz, with a train rate of 1 Hz referenced to the neck.

Rats were maintained in a prone position, with the right forelimb supported by placing one finger below the elbow joint and elevating the forelimb to allow visual inspection of all possible forelimb movements. To determine a movement threshold current intensity started at 0 μA, was rapidly increased until a movement was elicited, decreased until the movement was no longer present, and then slowly increased until the movement was evoked again. Any penetration site that failed to elicit a movement up to a maximum intensity of 60 μA was considered non-responsive. A maximum of 15 trains of pulses were delivered to any given penetration site.

Three microstimulation trials were conducted for each penetration site. The microelectrode was lowered into forelimb sensorimotor cortex and movement thresholds taken before (baseline), during (DBS), and after STN DBS (post-DBS). Once the threshold of a responsive site was determined (baseline condition), the micropipette was left in place and the STN was stimulated for 60 s. Following 45 seconds of STN DBS a second threshold was taken (DBS condition). This was done to ensure the movement threshold was obtained just prior to the end of the 60 s stimulation window. A third threshold was determined 45 s following DBS termination (post-DBS). This was done to ensure the movement threshold was obtained just prior to 60 s following DBS termination.

The border of the forelimb motor map was first defined consisting of either non-forelimb movements (neck, jaw, vibrissae, trunk, tail, hindlimb) or non-responsive points in a systematic fashion. Once the border of the maps was defined, the central, forelimb regions (Neafsey et al., 1986; Neafsey and Sievert, 1992) were then determined. Forelimb movements were classified as either distal (wrist/digit) or proximal (elbow/shoulder). This procedure was used to minimize the likelihood of the microstimulation session affecting the map boundaries (Stoney et al., 1968; Nudo et al., 1990). Throughout the surgery, anaesthetic levels were additionally monitored by verifying the thresholds for previously defined positive-response sites.

Canvas imaging software was used to calculate the size of the caudal (CFA) and rostral (RFA) forelimb regions, which can be distinguished physiologically by a separating strip of intervening non-forelimb or non-responsive sites (Neafsey and Sievert, 1992). Each responsive site was taken to represent 0.125 mm^2 of cortical surface (354 x 354 μm). Map size and movement thresholds during baseline trials were compared between groups to determine a lesion effect on movement representations. Map size and movement thresholds during baseline, DBS, and post-DBS trials were compared within groups to determine a DBS effect on movement representations. As movement representations have been shown to be dependent upon the level of ketamine-xylazine anaesthesia (Tandon et al., 2008), group differences in anaesthetic levels were assessed by calculating the total amount of each drug given as a ratio of each rat's weight and the total duration of the ICMS surgery.

2.3.7 Lesion assessment and verification of DBS electrode placement

Immediately following electrophysiological mapping, rats were deeply anaesthetized with sodium pentobarbital and perfused through the heart with cold 0.1 M phosphate buffer

saline (PBS) followed with cold 4% paraformaldehyde in PBS. Brains were extracted and postfixed in 4% paraformaldehyde in PBS. The tissue was then cryoprotected in 30% sucrose for two days. The tissue was cut in 40μm coronal sections on a cryostat and collected into 0.1 M phosphate buffer containing 0.02% sodium azide. Free-floating sections collected through the striatum and substantia nigra were then processed for tyrosine hydroxylase (TH) immunohistochemistry, while tissue collected through the STN were nissl stained with cresyl violet. Sections were rinsed in 0.5% hydrogen peroxide in PBS-Triton X (0.3% Triton X-100 in 0.1M PBS) for 15 minutes to inactivate endogenous peroxidases. Three subsequent 5-minute PBS-Triton X rinses were conducted. The tissue was blocked in 1% normal goat serum in PBS-Triton X for 90 minutes and then incubated in a rabbit anti-TH primary antibody (Chemicon, diluted 1:8000) for 48 hours at 4ºC. Sections were given 3 5-minute PBS-Triton X rinses and then incubated in biotinylated goat anti-rabbit IgG for 90 minutes. Following 3 more 5-minute PBS-Triton X rinses, the tissue was incubated in ABC complex (Vector, Burlingame, CA) for 60 minutes and was developed in a solution containing 25 ml tris buffer, 12.5 mg 3,3'diaminobenzidine tetrahydrochloride (DAB), 60 μl of 8% NiCl, and 80 μl of 30% H_20_2. After 110 s, the DAB reaction was rapidly quenched in a series of PBS rinses. The tissue was mounted on gelatine-coated slides, air dried, dehydrated in an alcohol series (70, 95, 100% EtOH) and cover slipped with permount.

Mesencephalic sections were viewed with an Olympus BX51 microscope using a QImaging QICAM 1394 camera and were captured using ImagePro Plus software (Media Cybernetics). Quantification of SNc dopaminergic cell loss was adapted from Metz et al. (2004). Three separate sections through the mesencephalon between 4.8 and 5.8 mm posterior from bregma were used for analysis for each rat. Care was taken to utilize sections in which a clear

boundary between the SNc and ventral tegmental area was formed by the medial terminal nucleus. Where this was not possible, SNc boundaries were established according to the stereotaxic atlas of Paxinos and Watson (2005). TH+ SNc cell counts from each of the three sections for each rat, performed manually with the aid of the cell counter plugin to ImageJ (NIH), were separately averaged for each hemisphere and used for statistical analysis. TH+ neurons were identified and defined as densely stained cell bodies visible on the sections. STN sections were stained with cresyl violet, dehydrated, and mounted for histological assessment of electrode placements.

2.3.8 Statistical analyses

Repeated measures analysis of variance (ANOVA) with post hoc pairwise Tukey HSD tests were used to assess within group differences in behavioural and microstimulation data. Planned independent *t*-tests were used to assess between group differences in TH+ cell counts, DBS stimulation intensity, and microstimulation data. All analysis were two-tailed unless otherwise noted. An *a priori* alpha level of .05 was used. Statistical analyses were conducted using Graphpad Prism. Data are presented as mean ± SEM.

2.4 Results

2.4.1 Lesion quantification

Striatal 6-OHDA infusions resulted in sub-total significant loss of TH+ cell bodies in the SNc (Fig. 2-1). Mean SNc TH+ cell counts in the left hemisphere were 93.7 ± 4.1 in 6-OHDA treated rats and 197.7 ± 5.3 in vehicle controls (t_{12} = 15.2, p < .001). Mean SNc TH+ cell counts

in the right hemisphere were 94.1 ± 4.8 in 6-OHDA treated rats and 201.3 ± 5.2 in vehicle controls (t_{12} = 14.2, p < .001). No differences in mean total SNc TH+ cell counts were detected between left and right hemispheres in either 6-OHDA treated rats (p = 0.95) or vehicle controls(p = 0.64).

2.4.2 DBS electrode placement and stimulation intensity

Electrode placements within 500μm of the STN and excluding localization in the cerebral peduncle in addition to the presence of activational effects from DBS were requisite for inclusion in the study and were observed in 9 6-OHDA lesion rats and 6 vehicle controls. Only data from these rats were included in analyses. Histological verification of stimulating electrode sites relative to the STN are depicted in Figure 2-2. Mean stimulation intensity was 136 ± 5 μA in lesion rats and 140 ± 7 μA in vehicle controls and did not significantly differ between groups (p = 0.68).

2.4.3 STN DBS improves behavioural impairments in 6-OHDA lesion rats

Behavioural effects of 6-OHDA infusion and STN DBS was assessed through analysis of spontaneous forelimb use in the cylinder test and exploratory activity and rearing in the open field (Fig. 2-3) Rats first underwent testing prior to 6-OHDA infusion, with follow-up testing sessions occurring after 6-OHDA infusion under conditions of sham DBS and DBS. Significant behavioural changes were noted between testing sessions in 6-OHDA rats in the number of forelimb placements in the cylinder test ($F_{2,16}$ = 7.29, p < .01), and lines crossings ($F_{2,16}$ = 6.20, p < .05) and rearing in the open field ($F_{2,16}$ = 16.29, p < .001). Post-hoc Tukey comparisons

Figure 2-1: Effects of intrastriatal 6-hydroxydopamine (6-OHDA) infusion on the density of tyrosine hydroxylase immunoreactive (TH+) staining in the striatum and the number of TH+ cell bodies in the substantia nigra pars compacta (SNc) and ventral tegmental area (VTA). Photomicrographs of coronal sections through the striatum of rats following a) vehicle and b) 6-OHDA infusion. Left hemisphere is shown on the left. Scale Bar = 5000 μm. Photomicrographs of coronal sections through the left mesencephalon of rats following c) vehicle and d) 6-OHDA infusion. A moderate reduction in SNc TH+ cell bodies is seen in 6-OHDA rats, with a sparing of VTA TH+ immunoreactivity. Scale Bar = 500 μm. e) Quantification of mean total SNc TH+ cell counts in the SNc. *$p < .05$. Modified from Brown et al. (2009).

Figure 2-1: SNc TH+ immunoreactivity and cell counts

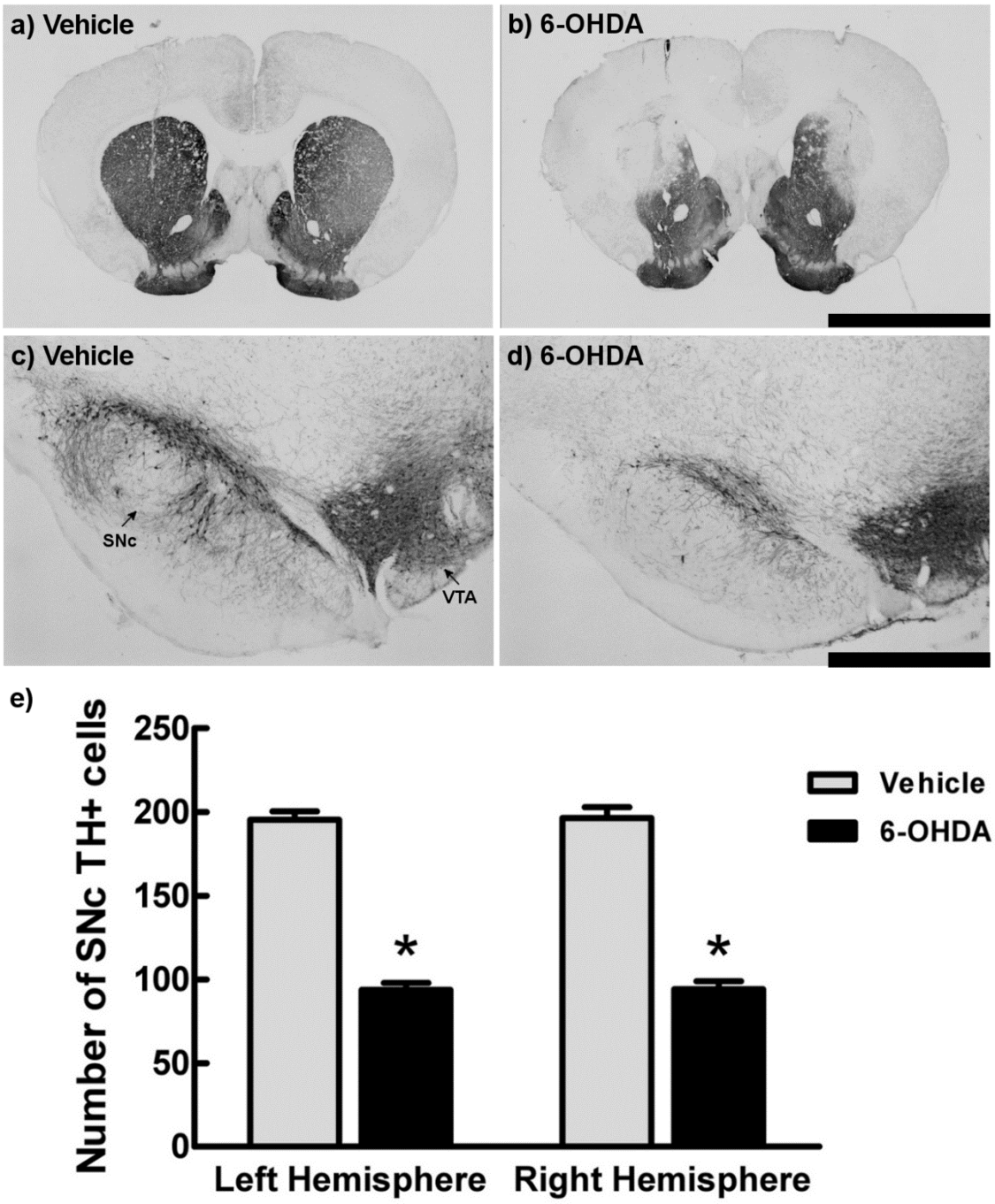

Figure 2-2: Histological verification of stimulating electrode loci targeted at the subthalamic nucleus (STN). Stimulation electrode loci targeted at the STN that elicited stimulation-bound side effects in 6-hydroxydopamine (6-OHDA, ●) and vehicle control (□) rats included in behavioural and electrophysiological mapping analyses. Plates are adapted from the atlas of Paxinos and Watson (2005). Modified from Brown et al. (2009).

Figure 2-2: STN electrode placements

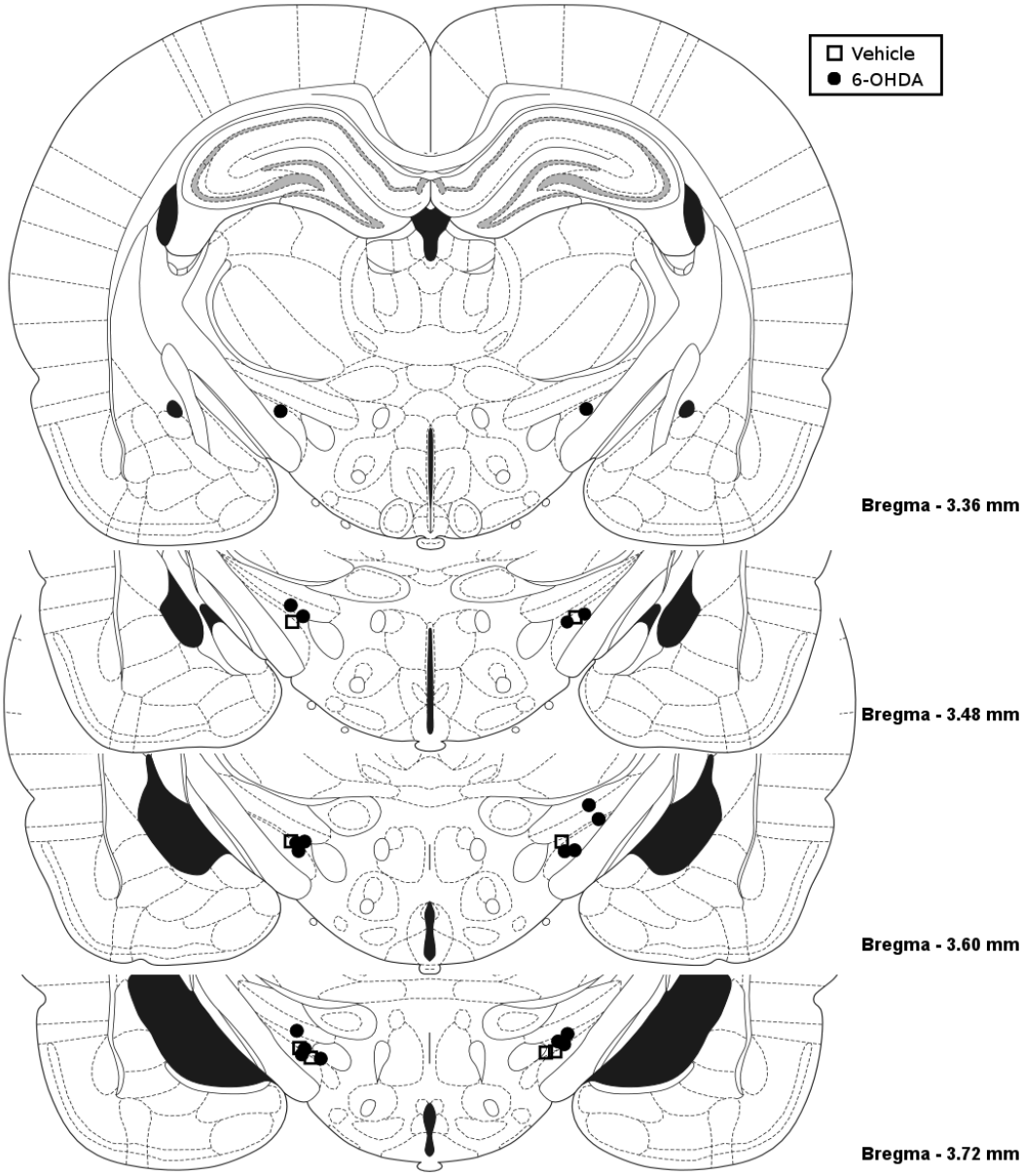

Figure 2-3: Behavioural assessment in the cylinder test and open field in rats before (baseline) and following 6-hydroxydopamine (6-OHDA) or vehicle infusion during sham (post-infusion) and subthalamic deep brain stimulation (STN DBS) conditions. a) Total forelimb placements in 7-minute cylinder testing sessions (mean + SEM). 6-OHDA infusion reduced forelimb placements compared to baseline testing and DBS increased forelimb placements compared to post-infusion testing. No differences were observed between testing sessions in vehicle control rats. b) Total line crossings in 5-minute open field testing sessions (mean + SEM). 6-OHDA infusion reduced the number of line crossings compared to baseline testing and DBS increased line crossings compared to post-infusion testing. No differences were observed between testing sessions in vehicle control rats. c) Total rears in 5-minute open field testing sessions (mean + SEM). 6-OHDA infusion reduced the number of rears compared to baseline testing and DBS increased line crossings compared to post-infusion testing. No differences were observed between testing sessions in vehicle control rats. *$p < .05$. Modified from Brown et al. (2009).

Figure 2-3: DBS behavioural assessment

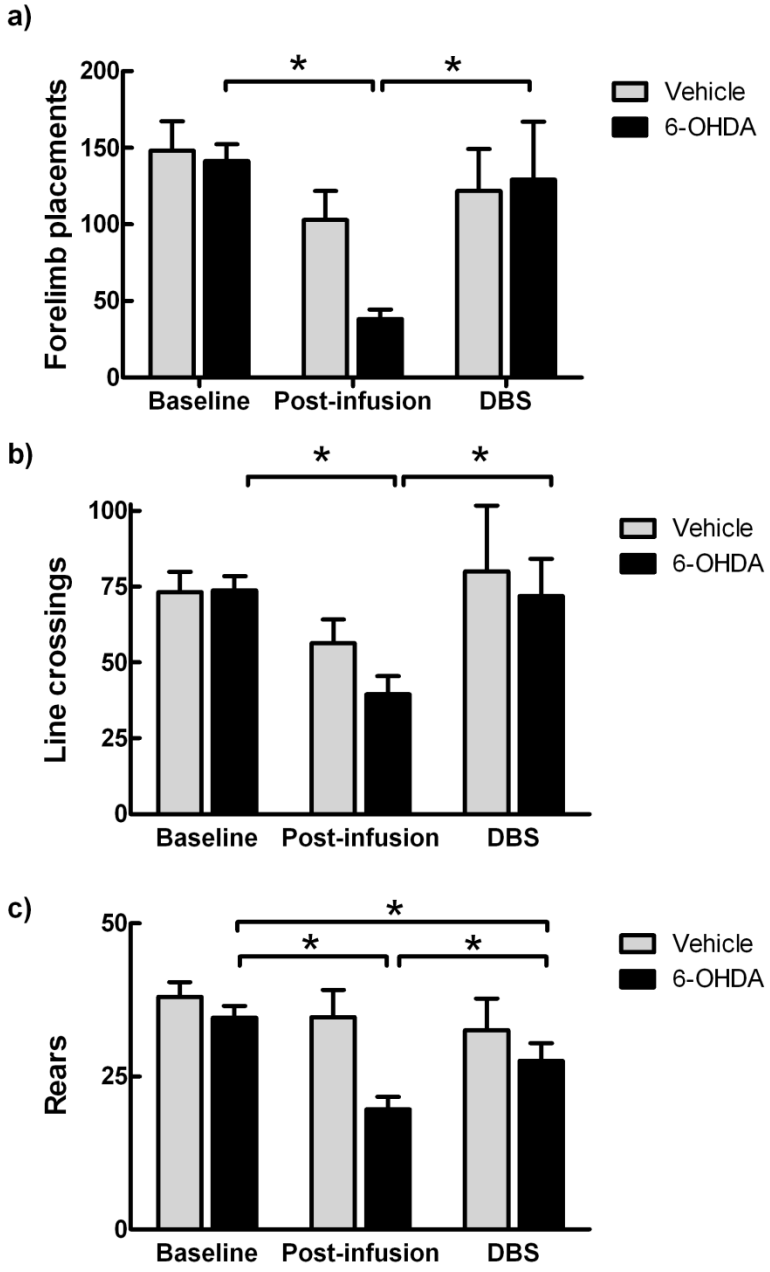

revealed that these differences were attributed to reduced performance in all measures following 6-OHDA infusion that was restored under DBS.

2.4.3.1 Forelimb Placements

Following 6-OHDA infusion rats made significantly ($p < .05$) fewer forelimb placements (38.0 ± 6.4) compared to pre-lesion baseline testing (141.2 ± 11.0). DBS increased forelimb placements (129.0 ± 37.9) compared to post-lesion testing (38.0 ± 6.4) in 6-OHDA lesion rats ($p < .05$). No differences were observed in the number of forelimb placements during cylinder test sessions between baseline and DBS conditions ($p > .05$). No differences in forelimb placements were observed in vehicle control rats between testing conditions ($F_{2,10} = 1.123$, $p = 0.36$).

2.4.3.2 Line crossings

Following 6-OHDA infusion rats made significantly ($p < .05$) fewer line crossing (41.2 ± 6.4) compared to pre-lesion baseline testing (72.3 ± 4.9). DBS increased line crossings (75.3 ± 13.12) compared to post-lesion testing (41.2 ± 6.4) in 6-OHDA lesion rats ($p < .05$). No differences in the number of line crossings between baseline and DBS conditions were observed in lesion rats ($p > .05$). No differences in the number of line crossings were observed between testing conditions in vehicle control rats ($F_{2,10} = 2.74$, $p = 0.33$).

2.4.3.3 Rears

Following 6-OHDA infusion rats made significantly ($p < .05$) fewer rears (19.4 ± 2.0) compared to pre-lesion baseline testing (35.6 ± 1.7). DBS increased rearing (27.33 ± 2.9) compared to post-lesion testing (19.4 ± 2.0) in 6-OHDA lesion rats ($p < .05$). While DBS

increased rearing in lesion rats, the number of rears was still significantly reduced compared to baseline testing ($p < .05$) No differences in the number of rears in the open field were observed in vehicle control rats between testing conditions ($F_{2,10} = 1.17$, $p = 0.35$).

2.4.4 6-OHDA lesion decreases forelimb map area and increases movement thresholds

Intracortical microstimulation was used to derive threshold forelimb motor maps in 6-OHDA (n=8) and sham (n=4) lesion rats. 6-OHDA lesions resulted in significant reductions in total forelimb map area ($t_{10} = 6.08$, $p < .001$) compared to vehicle controls (Figs. 2-4, 2-5). Total forelimb map area under sham DBS conditions were 2.27 ± 0.20 mm^2 in 6-OHDA lesion rats and 4.22 ± 0.29 mm^2 in vehicle controls. Reduced forelimb map area in 6-OHDA lesion rats was due to proportional reductions in both caudal and rostral forelimb areas as their distribution in terms of the total map area did not differ from vehicle controls ($t_{10} = 1.844$, $p= 0.10$). The caudal forelimb area comprised 90.0 ± 2.5% of total forelimb area in 6-OHDA lesion rats and 81.4 ± 4.3% in vehicle controls. Reduced forelimb map area in 6-OHDA lesion rats was associated with a significant map reorganization exhibited as a preferential loss of proximal (elbow, shoulder) over distal (wrist, digit) movement representations compared to vehicle controls. Proximal movement representations accounted for a significantly lower proportion of total forelimb map area ($t_{10} = 2.87$, $p > .05$) in 6-OHDA lesion rats (3.0 ± 1.3%) compared to vehicle controls (11.8 ± 3.6%). In addition to decreased forelimb map area, 6-OHDA lesions resulted in significant increases in total movement thresholds compared to vehicle controls ($t_{278} = 2.48$, $p < .05$; Fig. 2-4b). Movement thresholds under sham DBS conditions were 38.0 ± 1.0 μA in 6-OHDA lesion rats and 34.5 ± 1.0 μA in vehicle controls. Movement threshold increases following 6-OHDA lesion was attributed to a global increase at all responsive sites as no differences between groups

Figure 2-4. Forelimb map area (mm^2) and movement thresholds (μA) derived by intracortical microstimulation in 6-hydroxydopamine (6-OHDA) and vehicle control rats under conditions of sham DBS. 6-OHDA infusion reduced forelimb map area a) and increased movement thresholds b) compared to vehicle controls. *$p < .05$. Modified from Brown et al. (2009).

Figure 2-4: Forelimb motor map area and movement thresholds

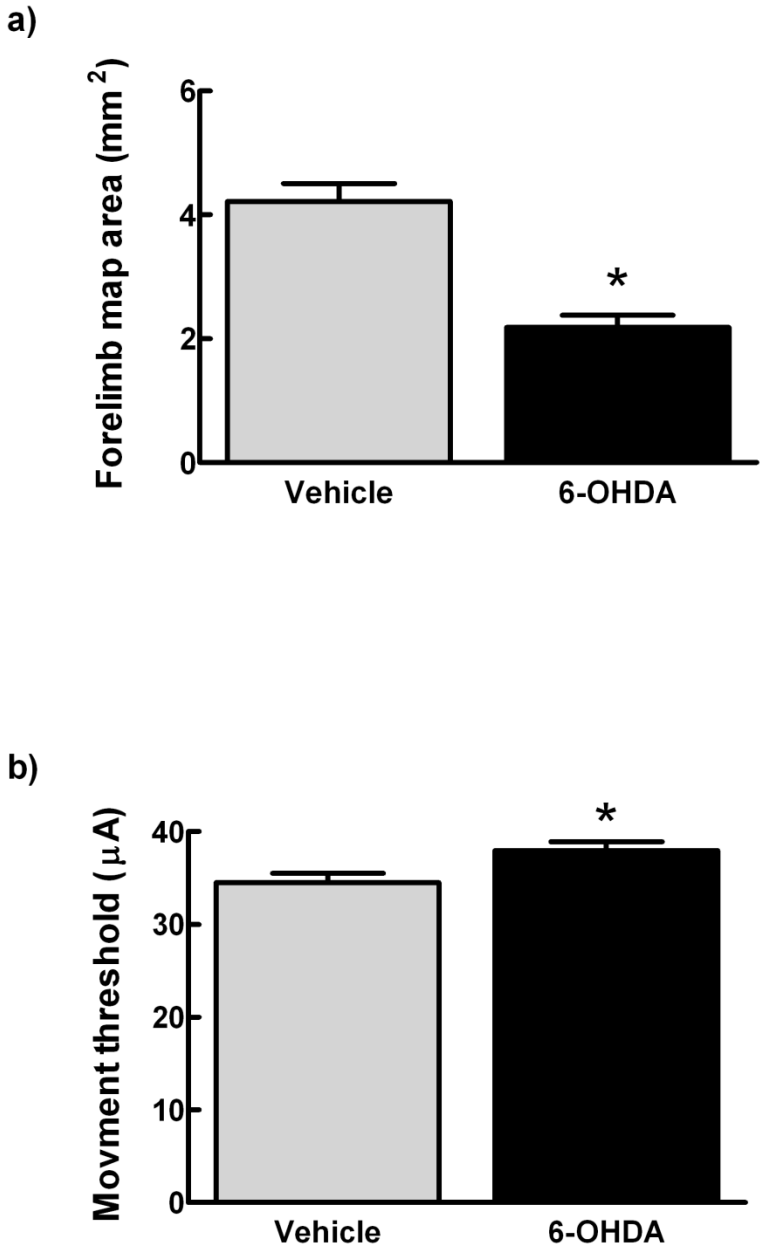

Figure 2-5. Coded forelimb motor representations of the left neocortex derived by intracortical microstimulation. Representative threshold maps from a 6-hydroxydopamine and vehicle control rat. Map boundaries are defined as electrode penetration stimulations ≤ 60 μA that failed to elicit movement or elicited non-forelimb movements. Each penetration site was tested three times: before, following 60 s of subthalamic deep brain stimulation (STN DBS) and 60 s following DBS termination. Solid black vertical line indicates location of bregma in the coronal plane. Modified from Brown et al. (2009).

Figure 2-5: Representative forelimb motor maps

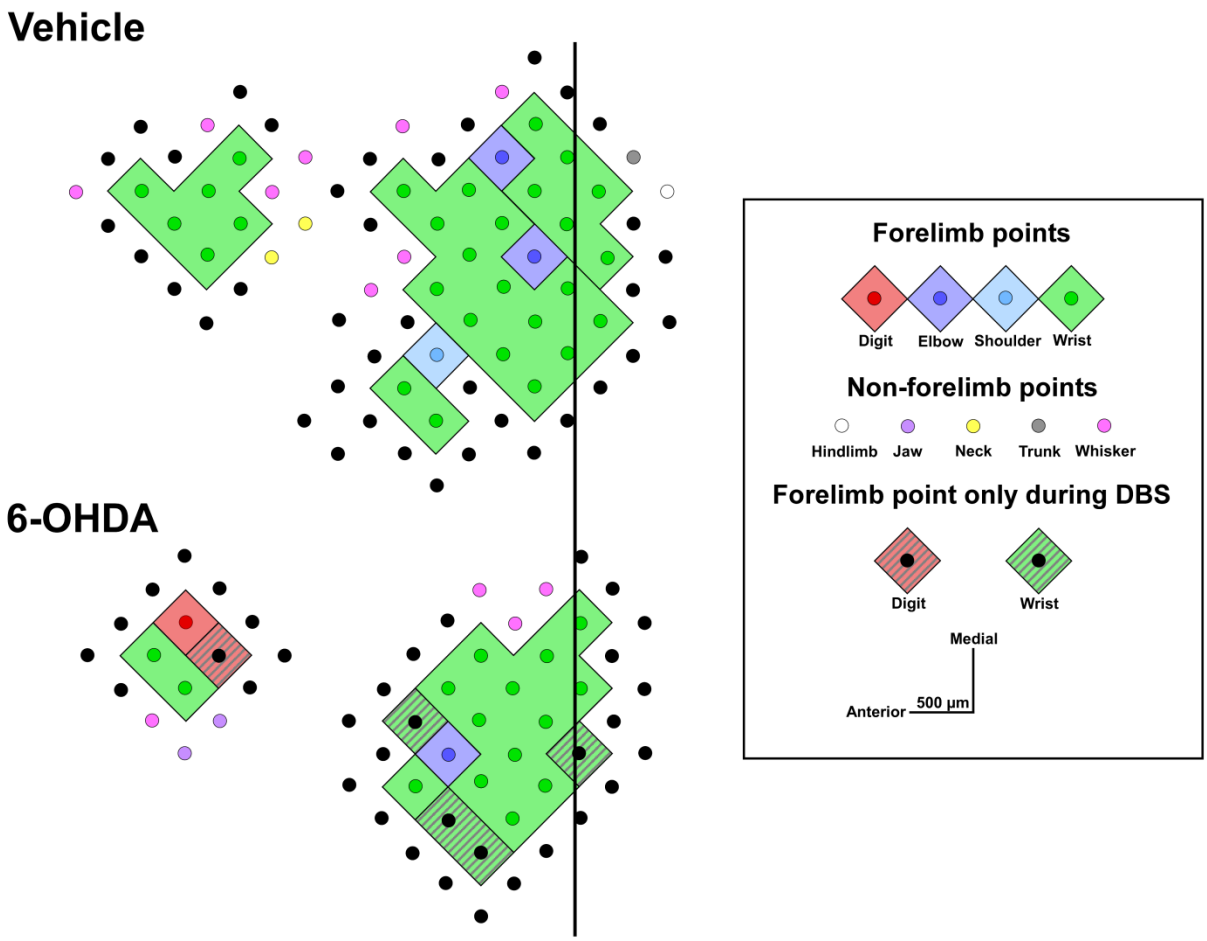

were observed when thresholds were assessed separately for proximal and distal movement, or for caudal and rostral forelimb regions.

Observed movement representation differences between groups are unlikely to be influenced by differences in anaesthetic levels as no differences in the amounts of either ketamine (t_{10} = 0.79, p = 0.45) or xylazine (t_{10} = 1.18 p = 0.26) administered for microstimulation procedures, as a function of body weight and duration of surgery, was observed between groups. Mean amounts of ketamine administered were 0.944 ± 0.056 mg/kg/min for 6-OHDA lesion rats and 0.879 ± 0.023 mg/kg/min for vehicle controls. Mean amounts of xylazine delivered were 0.041 ± 0.002 mg/kg/min for 6-OHDA lesion rats and 0.038 ± 0.002 mg/kg/min for vehicle controls.

2.4.5 STN DBS acutely increases forelimb map area and reduces movement thresholds following 6-OHDA lesion

During STN DBS, total forelimb map area was significantly ($p < .05$, tukey post-hoc comparisons) increased (2.55 ± 0.18 mm^2) compared to both baseline (2.27 ± 0.20 mm^2) and post-DBS conditions (2.27 ± 0.20 mm^2; $F_{2,14} = 13.19$, $p < .001$). No differences in map area were found between baseline and post-DBS conditions ($p > .05$). Increased map area during DBS was associated with equivalent increases in both caudal and rostral forelimb regions, as their proportion of the total map area did not differ between stimulation conditions ($p > .05$). Increased map area during DBS was also associated with equivalent increases in both distal and proximal movement representations, as their proportion of total map area did not differ between stimulation conditions ($p > .05$). Map area in vehicle control rats was 4.22 ± 0.29 mm^2

(baseline), 4.28 ± 0.28 mm^2 (DBS), and 4.22 ± 0.29 mm^2 (post-DBS) and did not significantly differ between stimulation conditions ($F_{2,6} = 3.00$, $p = .13$).

During STN DBS, thresholds were significantly ($p < .05$, Tukey post-hoc comparisons) decreased (32.4 ± 1.0 μA) compared to both baseline (38.0 ± 1.0 μA) and post-DBS values (37.4 ± 1 μA; $F_{2,286} = 156.3$, $p < .001$) in 6-OHDA lesion rats. No differences in movement thresholds were found between baseline and post-DBS conditions ($p > .05$). A significant main effect of stimulation condition on movement thresholds was also found in vehicle control rats ($F_{2,268} = 23.45$, $p < .001$). During STN DBS, thresholds were significantly ($p < .05$) decreased (32.9 ± 1.0 μA) compared to both baseline (34.5 ± 1.0 μA) and post-DBS values (34.6 ± 1.0 μA).

Although DBS acutely decreased movement thresholds in both 6-OHDA lesion and vehicle control rats, the effect in 6-OHDA treated rats was more pronounced (Fig. 2-6). 6-OHDA lesion rats exhibited a significantly ($t_{274} = 6.33$ $p < .05$, one-tailed) larger percent decrease in movement thresholds during DBS (21.7 ± 2.0%) compared to baseline than vehicle controls (6.0 ± 1.3%). Similarly, 6-OHDA lesion rats exhibited a significantly ($t_{10} = 2.16$ $p < .05$, one-tailed) larger percent increase in map area during DBS (11.7 ± 3.2%) compared to baseline than vehicle controls (1.5 ± 0.9%). DBS decreased movement thresholds proportionately between both caudal and rostral forelimb regions as well as proximal and distal movements. No differences in the magnitude of thresholds decreases during DBS were seen between either caudal and rostral forelimb map regions or proximal and distal forelimb movements in either 6-OHDA or vehicle controls (all *p's* > .05).

Figure 2-6. Percent change in a) forelimb map area and b) movement thresholds in 6-hydroxydopamine (6-OHDA) and vehicle control rats during 60 s of subthalamic deep brain stimulation (STN DBS) compared to baseline, pre-stimulation values. Lesion rats displayed greater map area increases and threshold reductions during STN DBS compared to vehicle controls. *$p < .05$. Modified from Brown et al. (2009).

Figure 2-6: DBS-induced changes in motor map area and movement thresholds

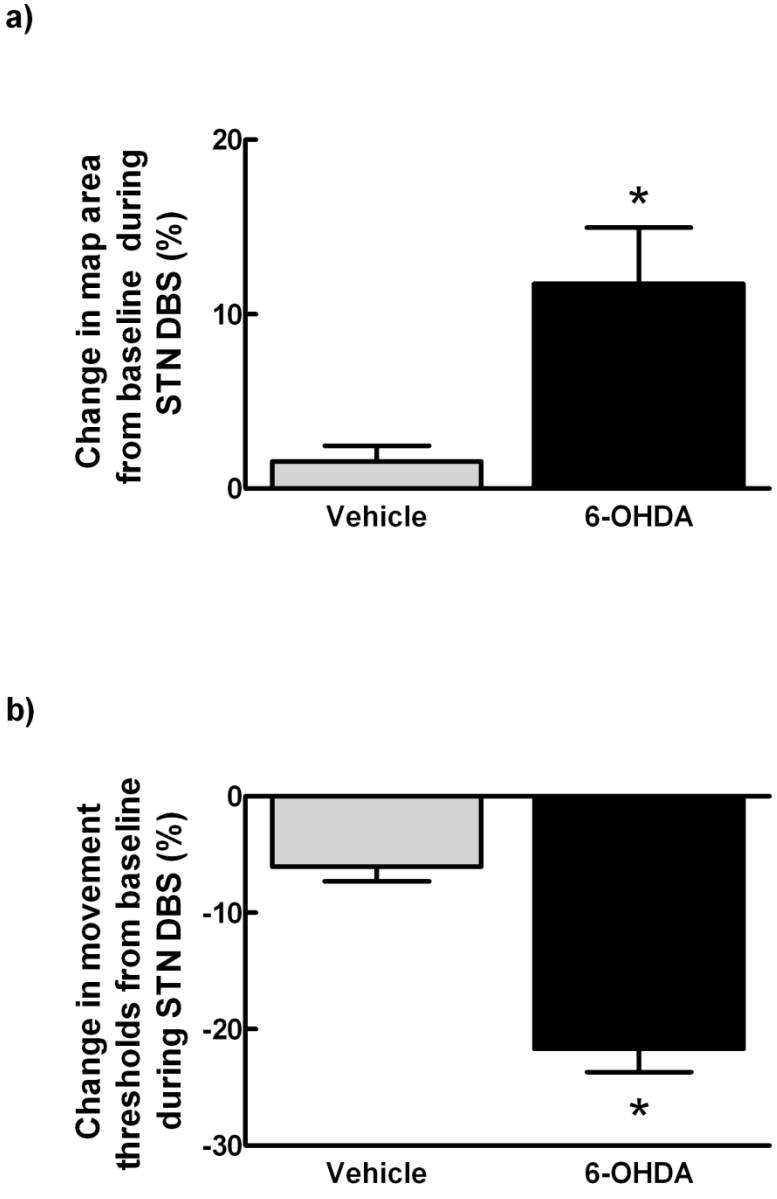

2.5 Discussion

Bilateral nigrostriatal degeneration following 6-OHDA administration resulted in behavioural deficits in forelimb use and locomotor activity in association with reduced size and increased thresholds of forelimb movement representations (motor maps) as assessed by ICMS. STN DBS resulted in significant amelioration of lesioned-induced behavioural deficits, and was associated with acute, stimulation-bound, increases in forelimb map area and decreases in movement thresholds in 6-OHDA lesion rats. Motor map expression is sensitive to the influence of both brain injury and experience and map changes are associated with changes in motor ability (Piecharka et al., 1995; Nudo et al., 1997; Kleim et al., 1998; Friel et al., 2000; Kleim et al., 2003; Kleim et al., 2004; Teskey et al., 2008; Flynn et al., 2010; Boychuk et al., 2011). Presented here is evidence that map integrity is 1) impacted by damage to nigrostriatal projections, 2) partially restored by STN DBS, and 3) associated with return of spontaneous motor activity to pre-lesion levels.

It has previously been reported that nigrostriatal degeneration in rats leads to a marked decrease in the size of cortical forelimb motor maps (Brown et al., 2009; Prine et al., 2010). Here, we extend those findings by testing whether STN DBS is associated with alterations forelimb motor map size and movement thresholds. To ensure that the 6-OHDA lesion procedures resulted in motor deficits and that STN DBS was therapeutically effective, motor behaviour was assessed following either striatal 6-OHDA or sham lesion procedures and under STN DBS. Marked akinesia in forelimb use in the cylinder test and locomotor activity in the open field was observed following striatal 6-OHDA but not sham lesions. Lesioned rats exhibited significant reductions in total forelimb placements in the cylinder test and line

crossings and rears in the open field. STN DBS significantly improved performance in these measures in lesion rats, but was without effect on performance in sham controls. These results are similar to previous findings of selective motor improvement in unilateral dopamine depleted/antagonised, but not intact, rats with STN DBS (Shi et a., 2004; Dejean et al., 2009; Gradinaru et al., 2009), and extended in the present case to a bilateral model. The motor deficits observed following 6-OHDA infusion likely reflect lesion-induced movement impairment rather than habituation to the behavioural apparatus with repeated testing as sham lesion rats did not exhibit significant changes in performance during testing sessions in the behavioural measures assessed.

Forelimb map area was significantly decreased, and movement thresholds increased in 6-OHDA, but not vehicle control rats. Given that maximal ICMS intensity in many cortical loci was unable to elicit movements in these rats, map hypotrophy may reflect reduced excitability in cortical motor neurons and/or enhanced intracortical inhibition as has been reported by (Young et al., 2011a). This would be consistent with previous findings of reduced cortical activation in 6-OHDA lesion rats as indicated by reduced metabolic activity (Orieux et al., 2002) and immediate early gene expression (Steiner and Kitai, 2000) in frontal cortical areas. Observed map changes were not likely influenced by anaesthetic level differences (Tandon et al., 2008) as the amounts of ketamine and xylazine administered between groups as a function of body weight and duration of surgery did not differ. Further, any influence of cortical damage from the infusion tracts or electrode implantations on map expression were accounted for in sham lesion controls. ICMS stimulation parameters in the present study gave rise to a similar map expression in the control condition as reported previously (Kleim et al., 1998; Teskey et al., 2002; Teskey et al., 2007; Brown et al., 2009).

STN DBS was associated with acute expansion of forelimb motor map size and reduction of movement thresholds following 6-OHDA lesion. These results are similar to reports of increased activation of prefrontal cortical motor regions with STN stimulation in PD (Limousin et al., 1997; Ceballos-Baumann et al., 1999). Increased sensorimotor cortical excitability, as assessed by multi-unit activity and BOLD activation is known to correspond with motor map expansion and movement threshold reduction in rats (Young et al., 2011b). In 6-OHDA, but not vehicle controls, DBS resulted in a significant expansion in map area. Similarly, movement thresholds were reduced during DBS, although this effect was observed in both 6-OHDA and vehicle controls. However, the magnitude of threshold changes during DBS (relative to baseline) were significantly greater in 6-OHDA treated rats. DBS effects on map changes appear to be stimulation-bound as no differences in map area or movement threshold were observed between baseline measures and those obtained following DBS termination, indicating that effects do not outlast the stimulation. Furthermore, DBS exerted a dramatic and rapid activating effect on behaviour that ended with stimulation termination as previously reported (Shi et al., 2004).

Although not fully understood, several hypotheses exist to explain the mechanisms of DBS therapeutic effects (reviewed in Perlmutter and Mink, 2006**)** including depolarization block (Beurrier et al, 2001), transmitter depletion (Anderson et al., 2006) synaptic inhibition and depression (Dostrovsky and Lozano, 2002), normalization of pathological network oscillations (Brown and Eusebio, 2008), and antidromic cortical activation of motor cortex (Ashby et al., 2001; Gradinaru et al, 2009). As STN stimulation has shown to activate motor cortex in rats, both freely-awake and under ketamine-xylazine anaesthesia (Dejean et al., 2009; Li et al., 2007), increased magnitude of STN DBS changes on forelimb motor maps in 6-OHDA lesion rats observed in this study may then be due to combined influence of downstream and antidromic

effects on cortical excitability (Chomiak and Hu, 2007) That vehicle control rats also displayed reduced movement thresholds, but no significant behavioural effects of DBS, could suggest that the magnitude of map changes were insufficient in modulating spontaneous motor activity, or that small changes in behaviour were present but not robust enough to be detected in the analyses. Alternatively, that the significantly higher movement thresholds in 6-OHDA lesion rats compared to sham controls were lowered under DBS to sham control values may indicate a maximal, floor, effect for the influence of STN DBS on cortical activation at the stimulation intensities used here.

In summary, bilateral depletion of striatal dopamine in the rat can induce a significant reduction in the size and sensitivity of forelimb neocortical movement representations in association with deficits in spontaneous motor activity. STN DBS that improves lesion-induced behavioural deficits is associated with acute partial rescue of motor map size and movement thresholds.

Chapter Three:

Functionally segregated movement encoding in rat neocortical forelimb motor areas

Andrew R. Brown[1,2], G. Campbell Teskey[1,3,4]

[1]Hotchkiss Brain Institute, [2]Department of Neuroscience, [3]Department of Psychology,

[4]Department of Cell Biology and Anatomy, University of Calgary, Alberta, Canada

First author contributions: experimental design, cryoloop implantation and electrophysiological mapping surgery,behavioural testing, immunocytochemistry, data analysis, manuscript preparation.

3.1 Abstract

Intracortical microstimulation (ICMS) studies have yielded two possible interpretations on the functional organization of motor cortex. Short-duration stimulation trains (<50ms, SD-ICMS) reveal a somatotopic representation of body musculature, whereas "behaviourally relevant" long-duration stimulation trains (~500 ms, LD-ICMS) indicate a topographic distribution of complex, multi-joint movement encoding. Using SD-ICMS a dual representation of the forelimb in the rat is found in rostral (RFA) and caudal (CFA) forelimb motor areas of the sensorimotor neocortex. Using LD-ICMS forelimb grasping was found to be localized to RFA, while forelimb advance and retraction was evoked with stimulation within CFA. To investigate a behavioural dissociation between the two forelimb motor areas, reversible cortical cooling deactivation was selectively targeted at either the CFA or RFA by pumping chilled methanol through chronically implanted cryoloops. Forelimb motor performance in the single-pellet reaching, vermicelli handling, sunflower seed eating, and grip strength tasks was assessed under baseline (sham-cooling), cortical deactivation (cooling), and rewarm (post cooling) conditions. Despite reductions in skilled reaching performance in both groups during cooling, a specific impairment in the grasp subcomponent of the reach was observed in RFA-cooled but not CFA-cooled rats. CFA-cooled rats demonstrated trends for impairment in elbow abduction and reach advance during cooling. Significant reductions in the ratio of contralateral forelimb adjustments in the vermicelli handling task was also observed in RFA-cooled, but not CFA-cooled rats. Grip strength was reduced during cooling in both groups. Results provide behavioural evidence for a functional dissociation between RFA and CFA motor areas suggested by LD-ICMS and support a movement-based, rather than muscle-based view of motor cortex organization.

3.2 Introduction

Motor cortex has long been known to be involved in the generation and execution of volitional movement (Fritsch and Hitzig, 1870), yet its intrinsic functional organization for encoding movement is not fully understood. Electrical stimulation of motor cortex has been widely used to investigate its functional organization by mapping behavioural output across its surface and two alternate views have been presented. Traditionally, stimulation of motor cortex using short-duration pulse trains (< 50 ms), with surface electrodes or intracortical microstimulation (SD-ICMS), elicits brief muscle twitches that reveal a somatotopic mapping of body musculature (muscle map) overlaid across the cortical surface in primates (Penfield and Boldrey, 1937; Woolsey et al., 1952; Asanuma and Rosén, 1972; Andersen et al., 1975; Donoghue et al., 1992) and rodents (Donoghue and Wise, 1992; Neafsey and Sievert, 1986; Henderson et al., 2011). Distinct body parts are represented in separate, but intermingled, representations of the limbs, trunk, and face. An internal somatotopic organization within these representation areas, however, is not readily observed: although forelimb representations can be delineated from hindlimb representations, individual muscle representations within the forelimb area are intermixed. In addition, multiple and overlapping representations of the same body part have been found (Neafsey and Sievert, 1992; Luppino et al., 1991; Schieber, 2001). In contrast, stimulation using long-duration pulse trains (~500 ms, LD-ICMS) on a behaviourally relevant time scale has recently been shown to evoke complex (multi-joint) coordinated movements of one or more body parts towards a specific posture in both primates (Graziano et al., 2002, 2005; Haiss and Schwarz, 2005; Gharbawie et al., 2011) and rodents (Ramanathan et al., 2006; Harrison et al., 2012; Bonazzi et al., 2013). A variety of different classes of movements can be

elicited from different subregions of cortex (movement map) that bear resemblance to the behavioural repertoire of the species and have been purported to be ethologically relevant (Graziano et al., 2002). These two stimulation paradigms implicate drastically different interpretations for the functional organization of motor cortex.

Forelimb movements evoked with SD-ICMS in the rat comprise twitches of distal (digits, wrist) and proximal (elbow, shoulder) forelimb musculature elicited from both representations without a clear topographical distinction between a smaller rostral forelimb area (RFA) and a larger caudal forelimb area (CFA), separated by an intervening strip of craniofacial representation (Neafsey and Sievert, 1982). LD-ICMS has been shown to evoke reach-to-grasp behaviour in the rat with distal forelimb hand closing and grasping representations localized in the RFA and proximal forelimb advance and retraction representations elicited from the CFA (Ramanathan et al., 2006; Bonazzi et al., 2013). The segregation of these two motor areas provides an ideal model in which to investigate distinct predictions that can be made depending on whether motor cortex is functionally organized as a map of muscles (SD-ICMS) or map of complex movements (LD-ICMS). According to the muscle somatotopy hypothesis, acute selective deactivation of the RFA would not be predicted to induce a specific deficit in forelimb motor ability relative to CFA deactivation as both regions contain a representation of forelimb musculature as indicated by SD-ICMS. On the other hand, if the motor cortex is organized as a map of complex movement representations, acute deactivation of the RFA, selectively removing grasping representations as indicated by LD-ICMS, would be expected to result in specific deficits in forelimb grasping ability relative to CFA deactivation.

The purpose of the current study was to test the hypothesis that reversible deactivation of the RFA, but not CFA, would be associated with specific deficits in forelimb grasping ability.

Complex forelimb movement representation topography under LD-ICMS was first characterized in the Long-Evans rat and was found to be consistent with reports in other strains exhibiting a selective representation of forelimb grasping localized to the RFA (Ramanathan et al., 2006; Bonazzi et al., 2013). As skilled motor learning has been previously associated with a reorganization of forelimb movement representations elicited under SD-ICMS (Kleim et al., 1998) but not LD-ICMS (Ramanathan et al., 2006), a second experiment was used to derive complex movement representations following acquisition of a skilled reaching task to ensure grasping representations remained exclusive to the RFA. Cortical cooling deactivation (Lomber et al., 1999) of the RFA or CFA via chronically implanted cryoloops was then used to investigate the consequence of selective, reversible deactivation of the RFA and CFA in a behavioural test battery assessing forelimb motor function.

3.3 Materials and Methods

3.3.1 Rats

39 male Long-Evans rats (250-478g at the time of electrophysiological mapping) were used in this experiment. Rats were obtained from Charles River (Saint-Constant, QC) and housed individually in clear plastic cages in a colony room maintained on a 12h light/dark cycle (lights on at 07:00) at 21°C. Upon arrival, rats were gently handled once per day (5 min) for five days to minimize stress during behavioural testing. Experimentation was conducted between 08:00 and 23:00h. Rats were provided free access to food and water (Prolab RMH 2500 lab diet, PMI Nutrition International, Brentwood, MO, USA) throughout the duration of their housing except for an overnight food restriction prior to electrophysiological mapping, and during behavioural

training on the single pellet reaching task. During reach training, rats were maintained to 90% free-feeding weight. All procedures involving rats used in this study strictly adhered to the guidelines of the Canadian Council on Animal Care and were approved by the Health Sciences Animal Care Committee of the University of Calgary. All efforts were made to adhere to the principles of reduction, refinement, and replacement in experimental design (Russell & Burch, 1959), with every attempt made to limit the number of subjects and minimize animal suffering.

3.3.2 Groups and experimental design

Rats were assigned one of four experimental groups consisting of unimplanted untrained (Naïve; n=10), unimplanted reach-trained (Reach-trained; n=9), CFA cryoloop implanted reach-trained (CFA-cooled; n=8), and RFA cryoloop implanted reach-trained (RFA-cooled; n=9) rats. Three additional rats were used to determine the time course and extent of cortical deactivation as well as to verify the efficacy of the deactivation in abolishing evoked forelimb responses to ICMS. Non-implanted behaviourally naive rats were used to assess forelimb movement representation expression with LD-ICMS. Non-implanted reach-trained rats were used to assess reorganization of complex forelimb movement representations following 14 daily sessions of skilled reach training. Cryoloop implanted groups were used to assess the behavioural impact of cooling deactivation in RFA-cooled and CFA-cooled groups. Implantation rats first underwent 14 days of pretraining in the single pellet reaching task to determine hand preference and to establish baseline reaching performance. Cryoloops were then chronically implanted contralateral to the preferred reaching limb. Following 7-12 days of recovery rats underwent ordered testing in a behavioural test battery of single-pellet reaching, vermicelli pasta handling, sunflower seed opening, and forelimb grip strength to access limb motor function. Behavioural

testing sessions consisted of three repeated cooling cycles under baseline (cooling off), cooling (cryoloop temperature maintained at 4°C), and rewarm (cooling off) conditions. Each cycle was separated by 5 minute intermissions to allow stable cortical temperatures to be reached. A single testing session was conducted per rat per day. Following behavioural testing, long-duration ICMS was used to confirm appropriate cryoloop placement and motor map integrity. Behavioural testing and ICMS sessions were video recorded (30 frames/s, 1/1000 s shutter) for offline analysis.

3.3.3 Single-pellet reach training

Rats were placed on a restricted died to maintain 90% of normal free-feeding body weight for the duration of training. Reach training was conducted in clear Plexiglas test boxes 45 X 14 X 35 cm. A 1 cm vertical aperture of Plexiglas was removed from the front wall, extending from 2 cm above the floor to a height of 15 cm. A 4 cm wide shelf was fixed to the outside front wall 3 cm from the floor. The shelf contained two indentations 2 cm from the front wall and aligned with the edges of the aperture.

During initial training, rats were placed in the apparatus for 10-minute daily sessions where sucrose food pellets (45 mg, Bioserv inc., Frenchtown, NJ, USA) were placed in the shelf indentations to promote rat reaching through the front wall aperture and to determine hand preference. Hand preference was established when at least 60% of a minimum of 10 reach attempts were made using either the left or right forelimb. Following hand preference determination, daily training sessions were performed for a total of 14 sessions. Over the course of training rats were shaped to reach with their preferred hand through the front wall aperture to successfully obtain a food pellet reward on the shelf. During each trial, the rat started at the rear

of the test box and approached the front to reach through the aperture to obtain a pellet placed in the shelf indentation contralateral to the preferred hand. Only one reach attempt was permitted per trial. The reach was considered successful if the rat was able to successfully grasp the pellet from the shelf transfer it to the mouth without being dropped. Following each reach attempt rats were shaped to return to the rear of the box for the next trial. During initial training sessions, rats were rewarded with a pellet placed in the back of the box after each trial to facilitate shaping. As training progressed, rats were only rewarded for successful reach attempts. Each session lasted 15 minutes during which time rats could perform as many trials as possible with the number of successful and unsuccessful reach attempts recorded. Performance in the task was measured using the percent success of reaching attempts calculated as [100 * (number of successful reaches) / (number of total reaches)] (Whishaw et al., 2003).

3.3.4 Cryoloop construction, implantation, and validation

Cryoloops were fashioned from 23 gauge (0.635 mm O.D x 0.33 mm I.D) hypodermic stainless steel tubing. A linear 2 mm portion of the loop was shaped to conform to the surface to the cortical surface (Fig. 3-1a). A microthermocouple made from 30 AWG gauge Teflon insulated copper and constantan wire was soldered to the union of the of the inlet and outlet tubes, which were led through a plastic, outside-threaded, cylinder pedestal (1.7 mm height, 3.5 mm diameter). The microthermocouple wire was attached to terminating connector pins (Omega Engineering, Laval, QC) and dental acrylic was used encase the cryoloop tubes, pedestal, and microthermocouple assembly. A detailed description of cryoloop manufacturing and operation is provided by Lomber et al. (1999).

Figure 3-1. Time course and spread of cortical cooling. (a) Cortical cryoloop assembly. (b) Cortical temperature time course from cooling onset recorded 1500 μm below the pial surface at varying distances from the cryoloop with a stable holding loop temperature of 4 °C. The threshold deactivation isotherm of 20 °C (Lomber et al., 1999), below which synaptic block occurs, is plotted as a stippled line and is achieved within 1 mm of the cryoloop configuration used in this study. A rapid onset/offset of cortical inactivation can be achieved within 120 s. (c) Cortical depth temperature readings obtained from a penetration site 500 μM away from the midpoint of the cryoloop with a holding loop temperature of 4 °C. Consistent temperatures were recorded across cortical laminae. (d) Schematic diagrams for cryoloop implantations and the extent of cortical deactivation (loop holding temperature of 4°C) for RFA-cooled and CFA-cooled groups. Deactivation area is plotted to 1 mm away from the cryoloop using thermocline isotherm data in (b). Scale bar = 10 mm.

Figure 3-1: Cryoloop cooling deactivation

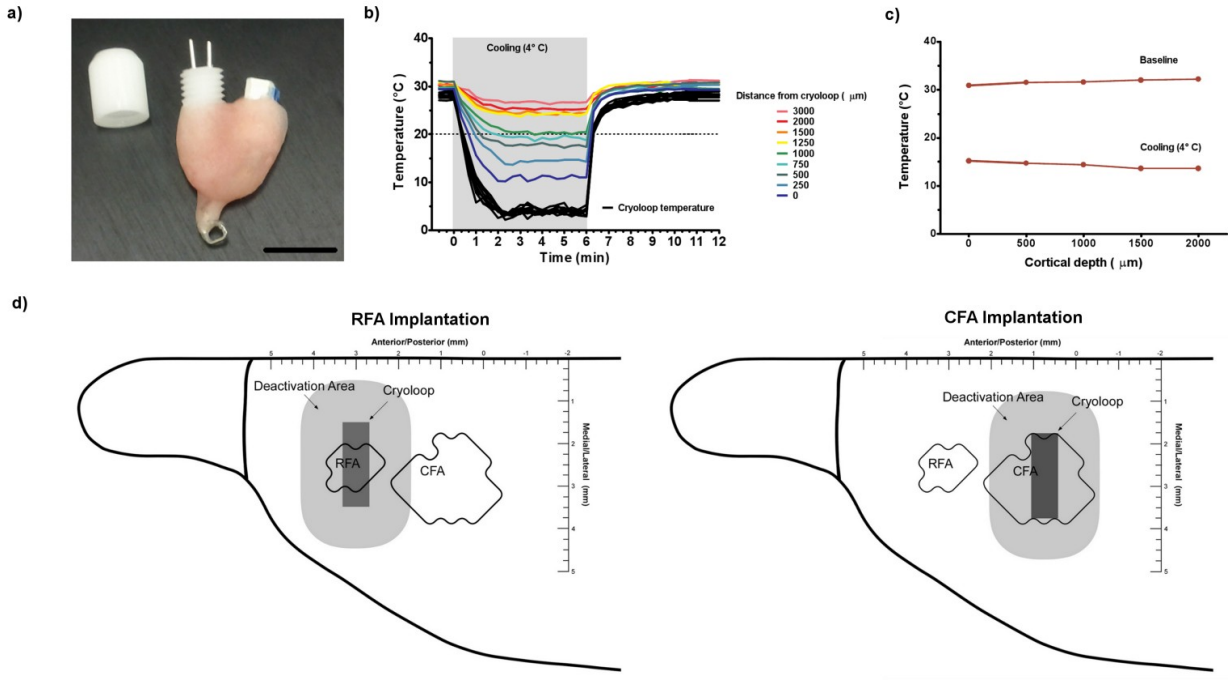

Rats were placed under general, surgical plane anesthesia with ketamine hydrochloride (100 mg/kg i.p.) and xylazine (5 mg/kg i.p.) and fixed in a stereotaxic instrument (Kopf, Tujunga, CA) with the incisor bar set to skull flat. Supplemental injections of either ketamine (25 mg/kg) or a mixture of ketamine (17 mg/kg) and xylazine (2 mg/kg) were given i.p. as required throughout surgery to maintain a constant level of anaesthesia as determined by monitoring vibrissae whisking, breathing rate, and foot and tail reflex in response to a gentle pinch. The local anaesthetic lidocaine (2%) was administered subcutaneously at the incision site in the scalp. The skull was exposed, a partial craniotomy of frontal bones was made over the sensorimotor neocortex, and dura reflected. Five stainless steel jeweler screws were placed in the skull adjacent to the craniotomy to permit firm anchoring of the cryoloop headcap assembly.

The cryoloop assembly was disinfected with 70% ethanol and positioned in place over the exposed neocortex, resting on the pial surface. Loops targeting the RFA were implanted 3.0 mm anterior to bregma and 1.5-3.5 mm lateral to midline. CFA loops were implanted 0.75 mm anterior to bregma and 1.75-3.75 mm lateral to midline (Fig. 3-1d). Dura was replaced and a silicone elastomer (Kwik-Sil, World Precision Instruments, Sarasota, Florida) was used to fill the cranial vault. Dental acrylic was used to secure the cryoloop assembly to the skull and screws. The scalp was sutured around the cryoloop and acrylic headcap and rats given a topical application of Xylocaine jelly (2%) analgesic around the incision. The surgical procedure to implant cryoloops, their presence in contact with the cortex, and their operation has been shown not to disrupt the structural or functional integrity of the cerebrum (Lomber and Payne, 1996; Lomber et al., 1999; Yang et al., 2006).

Loop dimensions, holding temperature, and implantation coordinates were chosen to provide effective deactivation of the CFA or RFA with minimal overlap. Acute cortical

temperature recordings revealed an effective isotherm for cortical deactivation (20°C, Lomber et al., 1999; Antunes & Malmiera, 2011; Coomber et al., 2001) in layer V at a distance of 1 mm from the cryoloop with a holding loop temperature of 4°C (Fig. 3-1b, 3-1c). ICMS-evoked forelimb motor responses were abolished during cooling deactivation within this isotherm. Implantation coordinates were obtained from unimplanted rats in which long-duration ICMS generated forelimb movement representations (n=10) were localized relative to bregma with a CFA mean of 0.88 mm, 2.71 mm (anterior/posterior, medial/lateral; range: 2.50 – (-0.75), 1.75-4.50 mm) and RFA mean of 3.11 mm, 2.30 mm (anterior/posterior, medial/lateral; range of 4.25 – 2.00; 1.5-2.5 mm). Cooling deactivation in this experiment would be expected to effectively block synaptic transmission completely in the RFA and near completely in the CFA (> 90%) with minimal overlap between the two.

3.3.5 Cooling deactivation

The cortex was cooled by pumping chilled methanol from a methanol/dry ice bath mixture through Teflon tubing connected to cryoloop inlet/outlet tubes with a reciprocating piston pump (QG150-Q1-CSC, Fluid Metering Inc., Oyster Bay, NY) to maintain a constant loop temperature of 4°C. Loop temperature was monitored (HH-25TC digital thermometer, Omega Engineering, Stamford, CT) and controlled to ± 1°C of the desired value by controlling the rate of methanol flow. Cooling deactivation was terminated by stopping methanol flow and allowing passive rewarming of the cortex.

3.3.6 Single-pellet reach testing

Following cryoloop implantation, five 15-minute reaching session were provided for reacclimation to the task under sham cooling with tubing-attached cryoloops. Three testing sessions were performed on separate days and the data pooled. Rats were given 5 minutes within each cooling cycle to perform as many trials as possible. In addition to endpoint measures of percent success and the number of reach attempts, the qualitative rating for each movement of the reach was assessed using frame-by-frame analysis of the video recordings according the criteria of Whishaw et al. (2003). Reaching behaviour was broken down into 10 discrete subcomponents that were assessed according to an ordinal rating scale. (1) Digits to the midline: the reaching limb is lifted from the floor so that the tips of the digits are aligned with the midline of the body; (2) Digits semi-flexed: As the limb is lifted, the digits are maintained in a semi-flexed position; (3) Elbow to midline: the elbow is adducted to the midline while the tips of the digits retain their alignment with the midline of the body; (4) Advance: The limb is advanced directly through the slot toward the food pellet; (5) Digits extend: the digits extend during the advance so that the digit tips are pointing toward the target; (6) Arpeggio: While the forelimb is over the target, the hand pronates from digit 5 (the outer digit) through to digit 2 while the hand simultaneously opens; (7) Grasp: The digits flex with the hand closing over the pellet, and the wrist is extends slightly; (8) Supination I: As the limb is withdrawn, the hand supinates by nearly 90 ° to allow withdrawal through the slot; (9) Supination II: Once withdrawn from the slot, the hand further supinates by nearly 45 ° to place the food in the mouth; (10) Release: The hand contacts the mouth and opens to release the food. Movements that appeared normal were given a score of 0, ambiguous movements a score of 0.5, impaired but recognizable movements a score of 1, and absent or unrecognizable movements a score of 2. The first five successful

reaches per rat per cooling condition were assessed. The mean (±SEM) percent success, number of reaches, and error score for each movement subcomponent across trials of each cooling cycle were used for analyses.

3.3.7 Sunflower seed eating

The sunflower seed task was used to assess object manipulation abilities. Forelimb and digit use during sunflower seed consumption among rodents has been reported in which rats manipulate the seeds into a preferred position before shelling (Whishaw et al., 1998). Rats were trained for five days in a transparent acrylic cylinder (20 cm diameter and 30 cm height) to consume an unlimited amount of sunflower seeds in 20 minute sessions. The cylinder rested on a glass shelf with a mirror placed beneath at a 90° angle to permit simultaneous views facing and underneath the cylinder in order to record forelimb use when the rat was turned away from the camera. Behaviour was assessed on the sixth session in which rats were given 5 seeds during each cooling cycle. The total amount of time spent manipulating, opening, and consuming the seeds was recorded in addition to the number of pieces of shell needed the rat needed to break to gain access to the seed. Timing started the moment the rat touched the first seed and would stop every time the rat was distracted. The mean time to eat and number of shell pieces (±SEM) across the five trials of each cooling cycle were used for analyses.

3.3.8 Vermicelli pasta handling

Rats were trained for five days in a transparent acrylic cylinder (20 cm diameter and 30 cm height) to consume an unlimited amount of uncooked vermicelli strands (7 cm length, 1.5 mm diameter, Primo Brand) in 20 minute sessions. The cylinder rested on a glass shelf with a mirror placed beneath at a 90° angle to permit simultaneous views facing and underneath the

cylinder in order to record forelimb use when the rat was turned away from the camera. To acclimate rats to pasta handling, five strands of vermicelli were provided in their home cages several days prior to testing. Testing occurred on the sixth day of training in which rats were presented with five vermicelli strands under each cooling cycle. The vermicelli asymmetry ratio (Allred et al., 20008) was used to quantify forelimb motor performance and was defined as [(number of contralateral adjustments/total number of contralateral and ipsilateral forelimb adjustments) × 100]. Forelimb adjustments consisted of either 1) hand release or re-contact of the strand, 2) reformation of hand hold, or 3) digit extension/flexion or abduction/adduction. Time to eat each strand (beginning when the pasta piece was first placed in the mouth and ending when the piece was released by the hands and disappeared into the mouth) was also recorded. The audible sounds made when rats are eating pasta were used to determine eating onset/offset. The mean (±SEM) across the five trials of each cooling cycle were used for analyses.

3.3.9 Grip Strength

A grip strength meter (Columbus Instruments; Columbus, OH) with T-bar attachment was used for recording contralateral forelimb grip strength during each cooling cycle. The animal's contralateral hand was placed on the grip bar, with the rat being held by the examiner at the base of the neck and tail, and the rat steadily pulled away horizontally from the bar the hand was released. Maximum grip strength was defined as the value of the peak force (g) recorded from the transducer at the moment the forelimb grip was overcome by the examiner. Five trials were performed during each phase of the cooling cycle and the mean (±SEM) across the five trials were used for analyses.

3.3.10 Intracortical microstimulation

ICMS procedures and analyses were conducted as described in chapter 2, with the following adaptations. Glass-coated platinum/iridium microelectrodes with an input impedance of 0.5 ± 0.1 MΩ (1000 Hz, 10 nA) were used (FHC Inc., Bowdoin, ME) were used. Electrode impedance was monitored throughout mapping experimentation and electrodes were discarded when impedance measurements dropped below 0.3 MΩ. LD-ICMS stimulation consisted of 500-ms trains of 200-μs biphasic (cathodal lead) pulses, delivered at a frequency of 333 Hz and an intensity of 100 μA. Biphasic current was used to minimize damage that could occur during long-duration stimulation trains (Asanuma & Ward, 1971; Graziano et al., 2002). Pulse trains were delivered in 0.2 Hz intervals (up to a maximum of 6 per site) to ensure the stability of evoked responses and sites in which movement was not reliably evoked in >50 % of stimulation trials were considered non-responsive.

3.3.11 Movement classification and motor map topography

Movements evoked under ICMS were monitored visually during electrophysiological mapping and video-recorded for subsequent analysis (30 frames/sec, 1,000 Hz shutter speed, Canon HDC-HS60). A light-emitting diode synchronised with stimulator output was fixed to the stereotaxic frame in the camera field of view. Video-recorded movements were characterized with VLC software (http://www.videolan.org). Frame-by-frame analysis of digitized joint positions with ImageJ (NIH) and Canvas imaging software (9.0.1, ACD systems Inc., Miami, FL) was used when movements were too difficult to visually characterize and for determining the effect of varying stimulation duration and intensity on movement amplitude and sequencing.

Forelimb map topography was assessed by analyzing the nature, number, and location (referenced to bregma) of response-positive stimulation sites. Canvas imaging software was used to record the location of stimulation sites in frontal and sagittal planes using a grid of 500 μm squares, calibrated to bregma, overlaid on the digital photograph of the cortical surface. Penetrations were performed at the intersections of the grid lines and in the center of each square to give an interpenetration distance of 354 μm. Each responsive site was taken to represent 0.125 mm^2 of cortical surface (354 x 354 μm).

3.3.12 Statistical analyses

Analysis of Variance (ANOVA) was performed on movement representation topography analyses with Tukey post-hoc tests used for multiple comparison testing. Independent student *t*-tests were used in single measure two-sample comparisons of forelimb map area measurements, and drug doses delivered during ICMS. One-way repeated measures ANOVA were performed on behaviour analysis for grip strength, vermicelli handling, sunflower seed eating, and end-point single-pellet reaching measures for RFA-cooled and CFA-cooled groups. Dunnett's posthoc tests contrasting cooling and rewarm conditions to baseline were performed when a significant main effect was observed. Paired samples *t*-tests were used to asses reach training progression between the first and last three days of single-pellet pretraining as well as pre- and post-implantation reaching success. Kruskal-Wallis with Mann-Whitney U posthoc tests were used to assess cooling-induced (cooling – baseline error scores) differences reach subcomponent error scores between RFA-cooled and CFA-cooled. All analyses were two-tailed. An *a priori* alpha level of .05 was used. Statistical analyses were conducted using GraphPad Prism 5

(GraphPad Software Inc., La Jolla, CA). Data are presented as mean ± SEM unless otherwise noted. Asterisks in figures represent significance level: * $p < .05$ ** $p < .01$, *** $p < .001$.

3.4 Results

3.4.1 Characterization of forelimb movements and cortical movement topography derived with long-duration intracortical microstimulation.

A total of 377 forelimb-responsive sites in 10 experimentally-naïve rats was probed using LD-ICMS. Nine distinct forelimb movement patterns were observed and are depicted in Figure 3-2. Movements were characterized as either simple when involving muscle contraction about a single joint, or complex when involving muscle contraction about multiple joints. Simple movements typically involved flexions of the elbow or digits and extensions of the wrist. These movements were similar to the brief twitches commonly observed with short-duration ICMS (Neafsey et al., 1986); however, muscle contractions were maintained for the duration of the stimulation trains. Less common movements elicited, that were not observed in short-duration ICMS, included supination of the hand and extension of the elbow. Four complex, multiple joint, movements were observed and classified as forelimb advances, elevations, grasps and retractions. Forelimb advances were characterized by synchronous rostral displacement of the forelimb involving flexions of the shoulder and elbow, and extension of the wrist. Forelimb elevations were characterized by combined flexion of the elbow and extension of the wrist. Elevation movements were qualitatively similar to advances, but did not involve rostral displacement of the forelimb. Grasping movements where characterized by flexion of the wrist

Figure 3-2. Movement patterns elicited by long-duration intracortical microstimulation (a-i). Movements were classified as either simple when involving a single forelimb joint, or complex when involving multiple forelimb joints. Complex movements were classified as (a) elevations involving flexion of the elbow followed by extension of the wrist, (b) advances involving forward displacement of the elbow and shoulder with wrist extension and hand opening, (c) grasps involving flexion of the wrist and simultaneous digit contraction and hand closure, and (d) retractions involving caudal displacement of the elbow and shoulder. Simple movements consisted of flexions of the (e) digits or (g) elbow, extensions of the (f) elbow or (i) wrist, as well as (h) supinations of the forelimb.

Figure 3-2: Forelimb movements evoked with LD-ICMS

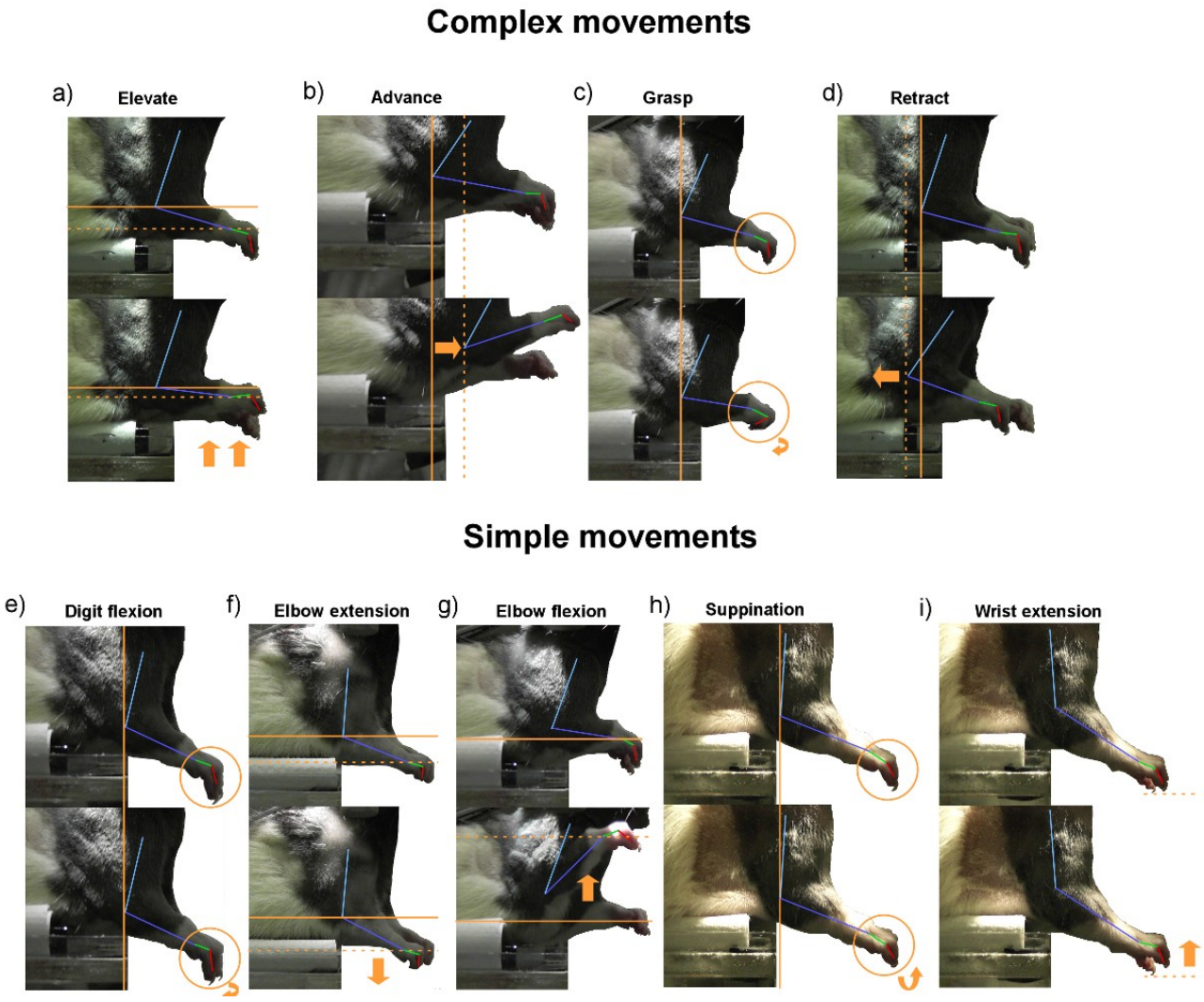

and contraction of the digits. Retractions were characterized by caudal displacement of the forelimb involving shoulder extension and elbow flexion and wrist extension. To contrast forelimb movement topography derived by LD-ICMS and SD-ICMS, three rats were mapped under both stimulation paradigms. A representative motor map is provided in Figure 3-3. Long-duration ICMS evoked forelimb movements within previously defined rostral (RFA) and caudal (CFA) forelimb motor cortex, separated by an intervening cortical strip of neck, whisker, jaw, or non-responsive stimulation sites (Neafsey & Sievert, 1982; Neafsey et al.,1986). Forelimb movement representations were bounded by non-forelimb and non-responsive stimulation sites as previously reported with short-duration ICMS (Donoghue & Wise, 1982; Neafsey et al., 1986; Brown et al., 2011). Total forelimb map was not found to differ between LD-ICMS (5.3 ± 0.4 mm^2) and SD-ICMS (5.0 ± 0.7 mm^2) protocols (t_{11} = 0.37, p > .05; Fig. 3-4a). Complex movements were found exclusively with LD-ICMS and accounted for 52.2 ± 2.8 % of all responsive forelimb sites (Fig. 3-4b, 3-4c)

We next sought to determine the effect of varying stimulation train duration and intensity on the nature of evoked forelimb movements (Fig. 3-4d, 3-4e). Complex forelimb movements were readily elicited with stimulation trains of 500 ms at intensity of 100 μA. Train durations less than 300 ms and stimulation intensities less than 100 μA commonly evoked movement across a single joint involving flexions of the elbow or extensions of the wrist. Train durations that exceeded the time required for the elicited movement resulted in the final movement posture being held for the duration of the stimulation. This typically occurred at durations longer than 500 ms. Stimulation at intensities higher than 100 μA resulted in a increase of the peak amplitude, but not quality, of evoked responses.

Figure 3-3. Representative forelimb movement representation topography derived in the same rat under long-duration and short-duration intracortical microstimulation. The duration of stimulation trains alters the evoked forelimb responses elicited within the rostral (RFA) and caudal (CFA) forelimb areas. Complex movements, involving coordinate activity among multiple forelimb joints, are observed under long-duration microstimulation.

Figure 3-3. Representative forelimb motor maps elicited under SD-ICMS or LD-ICMS

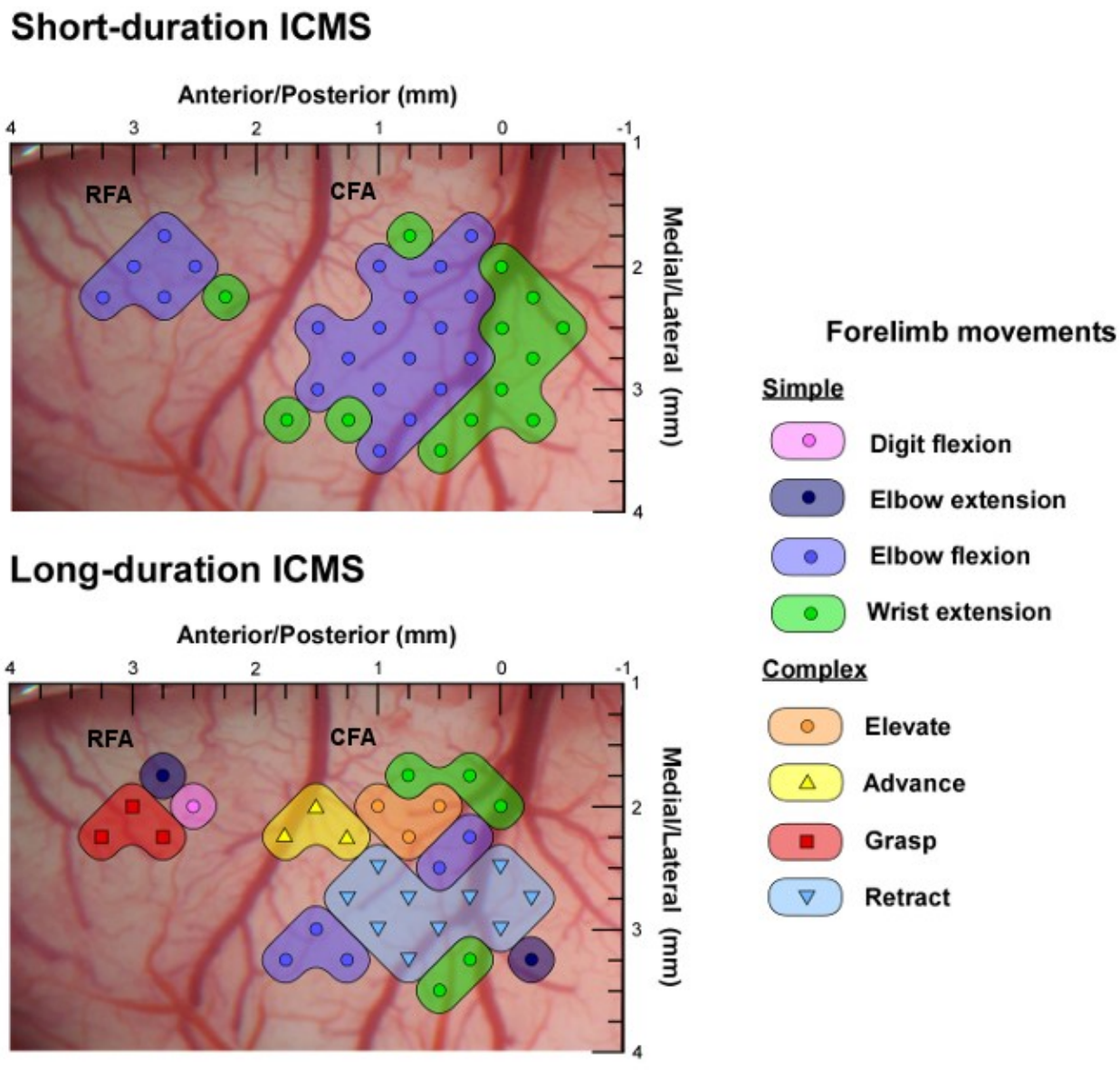

Figure 3-4. Comparison of forelimb movements evoked with short-duration and long-duration intracortical microstimulation. (a) Total forelimb map area does not significantly differ between short-duration and long-duration microstimulation ($p > .05$). (b) Long-duration microstimulation evokes both simple and complex movements in equivalent proportions ($p > .05$). (c) Size distribution of forelimb movements elicited under short-duration and long-duration microstimulation. Elbow flexions remain the most common movement elicited under both stimulation conditions. Sample evoked motor responses to balanced biphasic stimulation trials of varied train duration (d) and intensity (e) plotted as maximal displacement from baseline during stimulation. Movements were video recorded at 30 frames/sec (1/1000 s shutter). Frame-by-frame analysis was performed using ImageJ software (NIH). Movement across a single joint (simple movement) elicited at lower train durations and intensities readily transitioned to movements across multiple joints (complex movements) at train durations ≥ 500 ms and intensities of ≥100 μA**.**

Figure 3-4: Forelimb motor map area and stimulation parameter assay

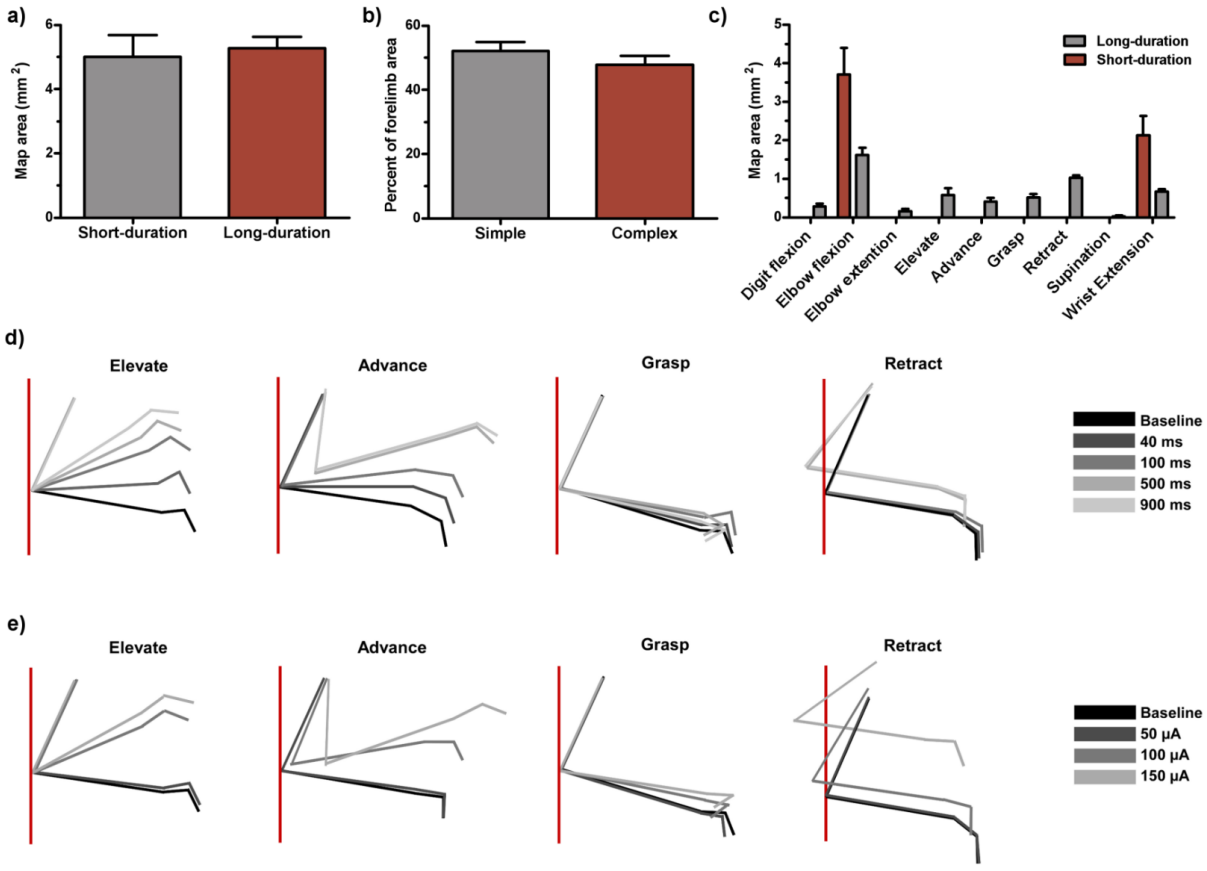

A clear topography of complex movement representations was found along the rostrocaudal map axis across rats to LD-ICMS (Figs. 3-3, 3-5). Grasping movements were situated most anterior and exclusively in the RFA. Mean coordinates of grasp-responsive stimulation sites were found to be 3.2 ± 0.1 mm anterior to bregma. Advances were concentrated in the anterior aspect of CFA (1.5 ± 0.2 mm). Retractions (0.8 ± 0.1 mm) and elevations (0.7 ± 0.1 mm) were clustered along the lateral and medial posterior aspect of CFA, respectively. Simple movement representations were found to be distributed within CFA with no clear topography with the exception of digit flexions which were always localized to the RFA and grasp representation (Fig. 3-5). Topographic quantification of all movement area sizes and locations is provided in Table 1-1.

3.4.2 Forelimb movement representation topography following skilled motor learning

Rats were trained for 14 days on the single-pellet reaching task and movement representations were later derived using long-duration ICMS (Fig. 3-6a). Task acquisition and skilled motor learning was demonstrated by an increase in the number of reach attempts and the success rates of reach attempts during training (Fig. 3-6b, 3-6c). Rats made significantly (t_8 = 8.17, $p < .01$) more reach attempts during the last three days (65.2 ± 6.2) of training compared to the first three days (14.9 ± 4.0). Along with increased reach attempts, success rates increased with training. The percent success of reach attempts was significantly (t_8 = 6.78, $p < .01$) increased over the last three days (52.9 ± 3.2%) of training compared to the first three days (17.9 ± 5.4%).

Skilled reach training was associated with a significant ($F_{11,102}$ = 38.87, $p < .001$) increase in the proportion of stimulation sites within forelimb movement representations that also

Table 3-1. Forelimb motor map topography

Group	Forelimb Movement[a]	Cortical Area (mm^2 ± SEM)	AP Coordinates (mm ± SEM)[b]	ML Coordinates (mm ± SEM)[c]
Naïve	*Complex*			
	Elevate	0.575 ± 0.175	0.689 ± 0.116	2.396 ± 0.158
	Advance	0.413 ± 0.095	1.547 ± 0.170	2.283 ± 0.102
	Grasp	0.513 ± 0.090	3.191 ± 0.107	2.326 ± 0.089
	Retract	1.025 ± 0.058	0.808 ± 0.070	3.165 ± 0.072
	Simple			
	Digit flexion	0.288 ± 0.070	3.238 ± 0.101	2.200 ± 0.102
	Elbow extension	0.194 ± 0.059	1.141 ± 0.480	2.447 ± 0.399
	Elbow flexion	1.613 ± 0.194	1.115 ± 0.122	2.682 ± 0.096
	Suppination	0.025 ± 0.025	0.000 ± 0.000	1.875 ± 1.875
	Wrist extension	0.663 ± 0.062	0.538 ± 0.196	2.887 ± 0.143
Reach-trained	*Complex*			
	Elevate	0.694 ± 0.140	0.794 ± 0.114	2.420 ± 0.085
	Advance	0.667 ± 0.143	1.616 ± 0.112	2.500 ± 0.084
	Grasp	0.472 ± 0.083	3.261 ± 0.039	2.511 ± 0.068
	Retract	1.111 ± 0.183	0.631 ± 0.085	3.347 ± 0.085
	Simple			
	Digit flexion	0.306 ± 0.059	3.101 ± 0.087	2.461 ± 0.115
	Elbow extension	0.167 ± 0.059	0.615 ± 0.342	2.694 ± 0.095
	Elbow flexion	1.097 ± 0.209	1.360 ± 0.053	3.082 ± 0.080
	Suppination	0.056 ± 0.056	2.063 ± 2.063	4.188 ± 0.000
	Wrist extension	0.444 ± 0.066	0.962 ± 0.320	2.893 ± 0.175

[a] Empty cells denote an absence of a particular movement for that group
[b] Anterior/Posterior (AP) coordinates are referenced to bregma in the coronal plane.
[c] Medial/Lateral (ML) coordiantes are referenced to the saggital suture

Figure 3-5. Cumulative distribution of forelimb movement patterns in 10 naïve rats derived with long-duration intracortical microstimulation. Complex movements exhibit a topographical clustering across rostrocaudal axis of the motor cortex: Gasping movements are localized most anteriorly and are exclusive to the rostral forelimb area; Advances are elicited caudally from grasps; Retractions are typically elicited from posterior lateral aspect of the caudal forelimb area; Elevations are elicited predominantly from posterior medial aspect of the caudal forelimb area. Simple movements are readily evoked from wide areas of the forelimb motor cortex, with the exception of digit flexions which co-localize with the grasp region of the rostral forelimb area.

Figure 3-5: Cumulative distribution of simple and complex movement topography

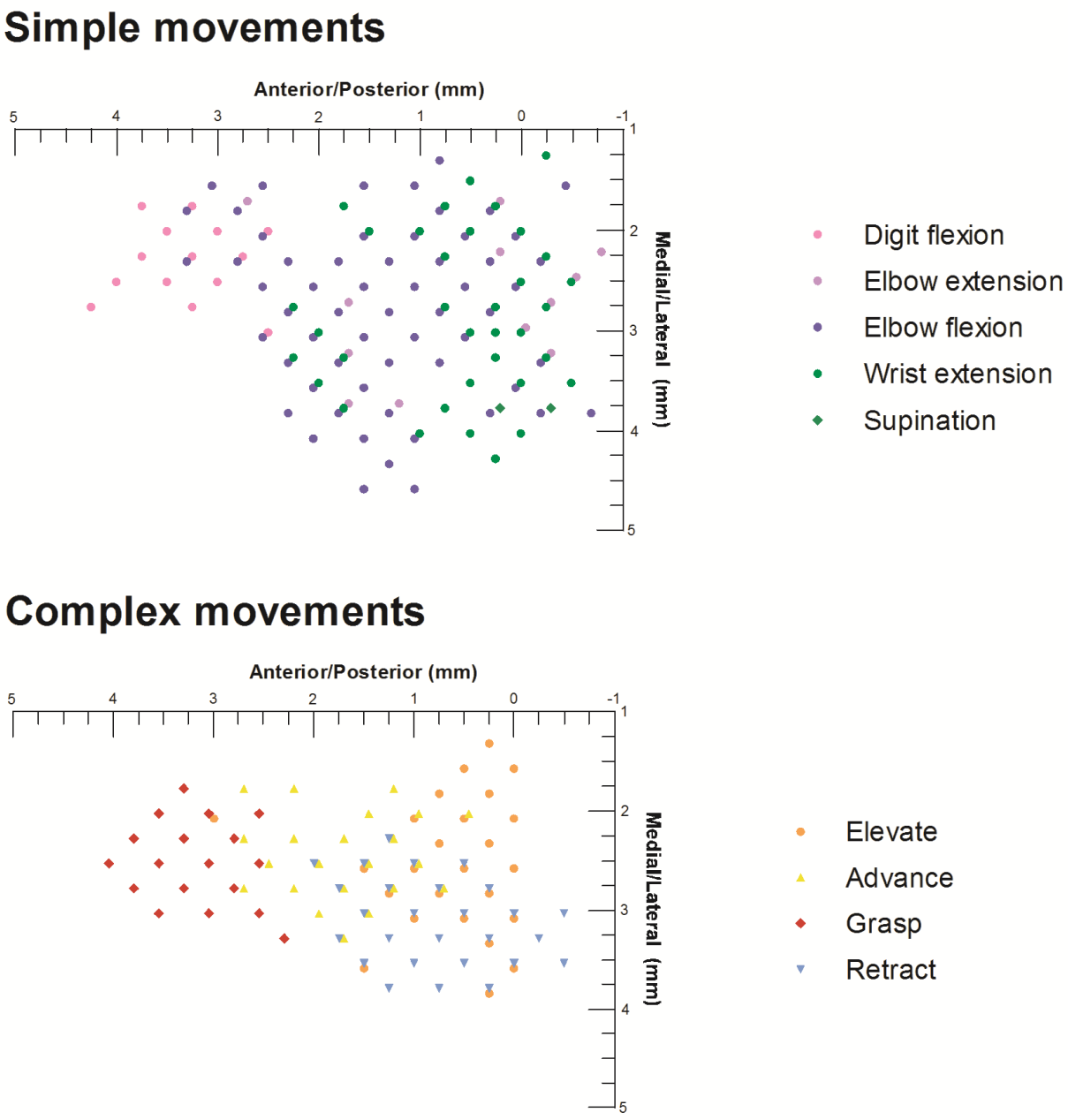

elicited non-forelimb movements (neck, jaw, whisker, tail, trunk, or hindlimb; Fig. 3-6f, 3-6g). 80.4 ± 7.6 % of forelimb-responsive stimulation sites in reach-trained rats were dual-responsive for non-forelimb movements relative to 22.2 ± 4.0 % in untrained controls. Post-hoc analyses revealed that the increased overlap of non-forelimb responsive sites within the forelimb motor map were attributed to significant ($p < .05$) increases in neck (42.6 ± 4.1 %) and jaw (13.5± 1.7 %) representations observed in trained rats relative to untrained controls (9.7 ± 2.5 % and 2.6 ± 0.7 %, respectively).

Reach training was not found to effect the nature or quality of complex forelimb movements. All complex and simple forelimb movements found in reach-trained rats were observed in untrained controls. Similarly, reach training did not alter either the size or location of forelimb movement representations (all $p > .05$; Fig 3-6d, 3-6e; Table 1). No differences in the amounts of either ketamine ($t_{17} = 1.4$, $p > 0.05$) or xylazine ($t_{17} = 1.7$, $p > 0.05$) administered for microstimulation procedures, as a function of body weight and duration of surgery, was observed between groups. Mean amounts of ketamine administered were 0.939 ± 0.035 mg/kg/min for reach-trained rats and 1.010 ± 0.037 mg/kg/min for untrained controls. Mean amounts of xylazine administered were 0.040 ± 0.002 mg/kg/min for reach-trained rats and 0.040 ± 0.002 mg/kg/min for untrained controls.

3.4.3 Behavioural assessment during selective deactivation of the CFA and RFA

3.4.3.1 Single-pellet reaching

During reach pretraining, task acquisition and skilled motor learning was demonstrated by an increase in the success rates and reach attempts made in the last three days of training compared to the first three days of training in both groups. CFA-cooled rats exhibited significant

Figure 3-6. Forelimb movement representations following skilled reach training. (a) Representative forelimb movement representation topography derived in a behaviourally naïve (left) and reach-trained (right) rat. The number of reach attempts (b) and percent success (c) during training were both significantly greater in the last three sessions compared to the first three ($p < .001$). (d) Reach-trained rats did not demonstrate ($p > .05$) larger forelimb movement representations as a whole (d) nor any specific increase in individual movement representation size (e). Although forelimb representation size between groups was equivalent there was a significant ($p < .001$) increase in the proportion of forelimb movement representations that also elicited non-forelimb movements following training (f). Post hoc analyses revealed that jaw and neck movements overlapping within the forelimb movement representations in reach-trained rats were significantly ($p < .05$) increased.

Figure 3-6. Motor map following skilled reach training

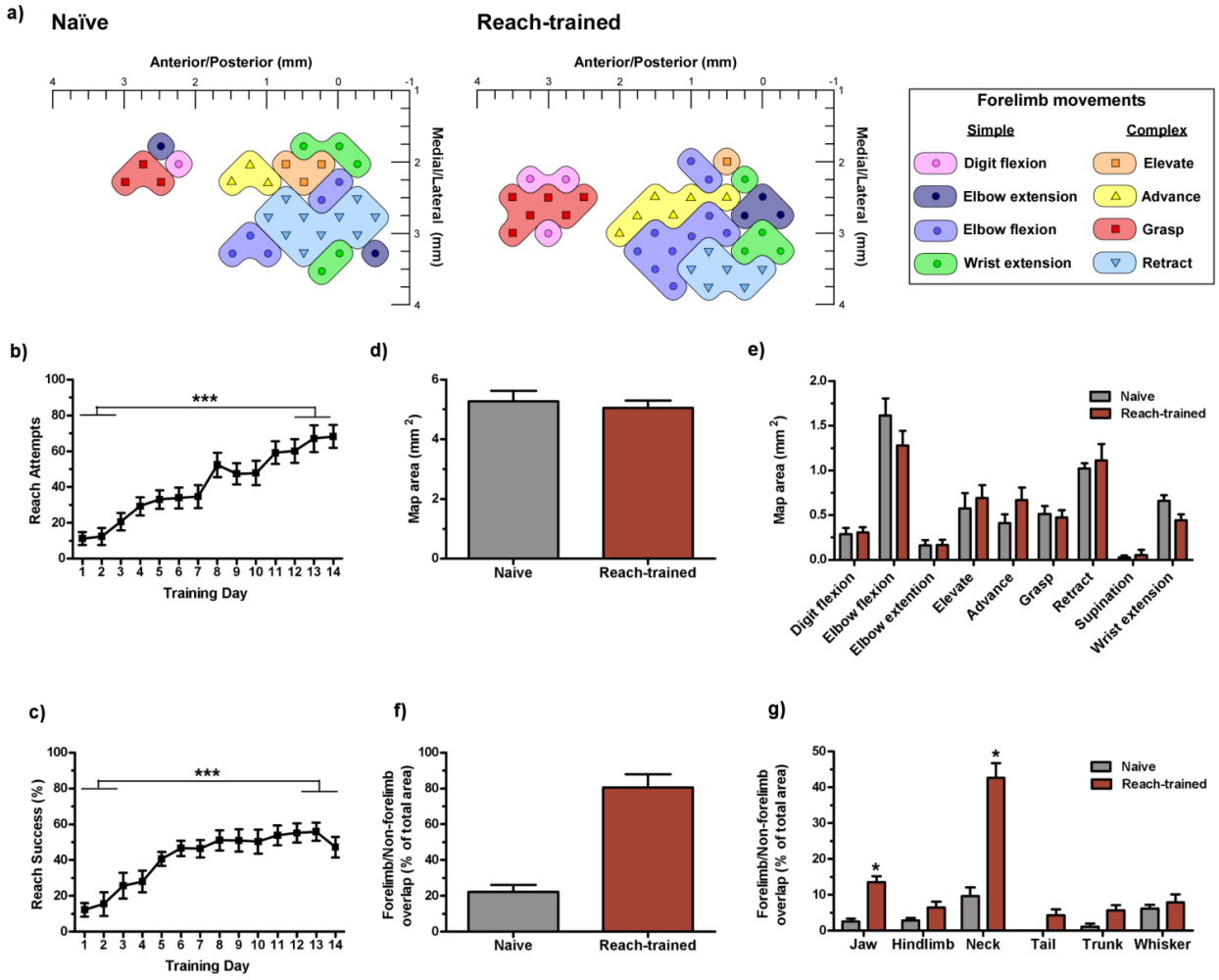

increases in reach success (first three days: 17.2 ± 3.7 %, last three days 50.9 ± 2.5, $t_7 = 7.69$, $p < .001$) and attempts (first three days: 12.8 ± 4.3, last three days 42.9 ± 2.7, $t_7 = 7.01$, $p < .001$) during training. Similarly, RFA-cooled rats exhibited significant increases in reach success (first three days: 20.46 ± 5.1 %, last three days 54.1 ± 5.5, $t_8 = 4.61$, $p < .01$) and attempts (First three days: 11.0 ± 1.6, Last three days 46.5 ± 4.5, $t_8 = 6.70$, $p < .001$) during training.

Reaching performance is depicted in figure 3-7. CFA-cooled rats exhibited significant differences in reaching success rates between cooling cycles ($F_{2,14} = 21.11$, $p < .001$). Posthoc analyses revealed a significant reduction ($p < .05$) in success rates during cooling (40.43 ± 4.9) but not rewarm (57.7 ± 4.5, $p > .05$) relative to baseline (57.0 ± 5.8). RFA-cooled rats also exhibited significant differences in reaching success rates between cooling cycles ($F_{2,16} = 20.75$, $p < .001$). Posthoc analyses revealed a significant reduction ($p < .05$) in success rates during cooling (37.0 ± 7.7) but not rewarm (44.5 ± 7.6, $p > .05$) relative to baseline (48.1 ± 6.1). A imilar pattern emerged for reach attempts in which CFA-cooled rats exhibited significant differences between cooling cycles ($F_{2,14} = 6.78$, $p < .01$). Posthoc analyses revealed a significant reduction ($p < .05$) in attempts during cooling (31.9 ± 2.2) but not rewarm (35.4 ± 2.9, $p > .05$) relative to baseline (41.0 ± 3.185). RFA-cooled rats also exhibited significant differences in reach attempts between cooling cycles ($F_{2,16} = 7.63$, $p < .001$). Posthoc analyses revealed a significant reduction ($p < .05$) in reaches made during cooling (23.9 ± 2.8) but not warming (29.56 ± 3.0, $p > .05$) relative to baseline (34.6 ± 3.0). No differences ($p > .05$) were observed between pre-implantation success rates during the last three days of training and post-implantation success rates in the baseline cooling cycle in either group.

Although cooling was associated with similar reductions in reaching performance during cooling deactivation of both CFA and RFA groups, assessment of cooling-induced error scores

Figure 3-7. Single-pellet reaching endpoint success and attempts. Behavioural performance with repeated testing sessions under baseline, cortical cooling, and rewarm conditions. Cortical cooling was associated with significant reductions in mean (± SEM) reaching attempts and success in both RF-cooled (a,c) and RFA-cooled (b,d) groups. *$p < .05$, ** $p < .01$, ***$p < .001$.

Figure 3-7. End-point success in skilled reaching ability during cooling

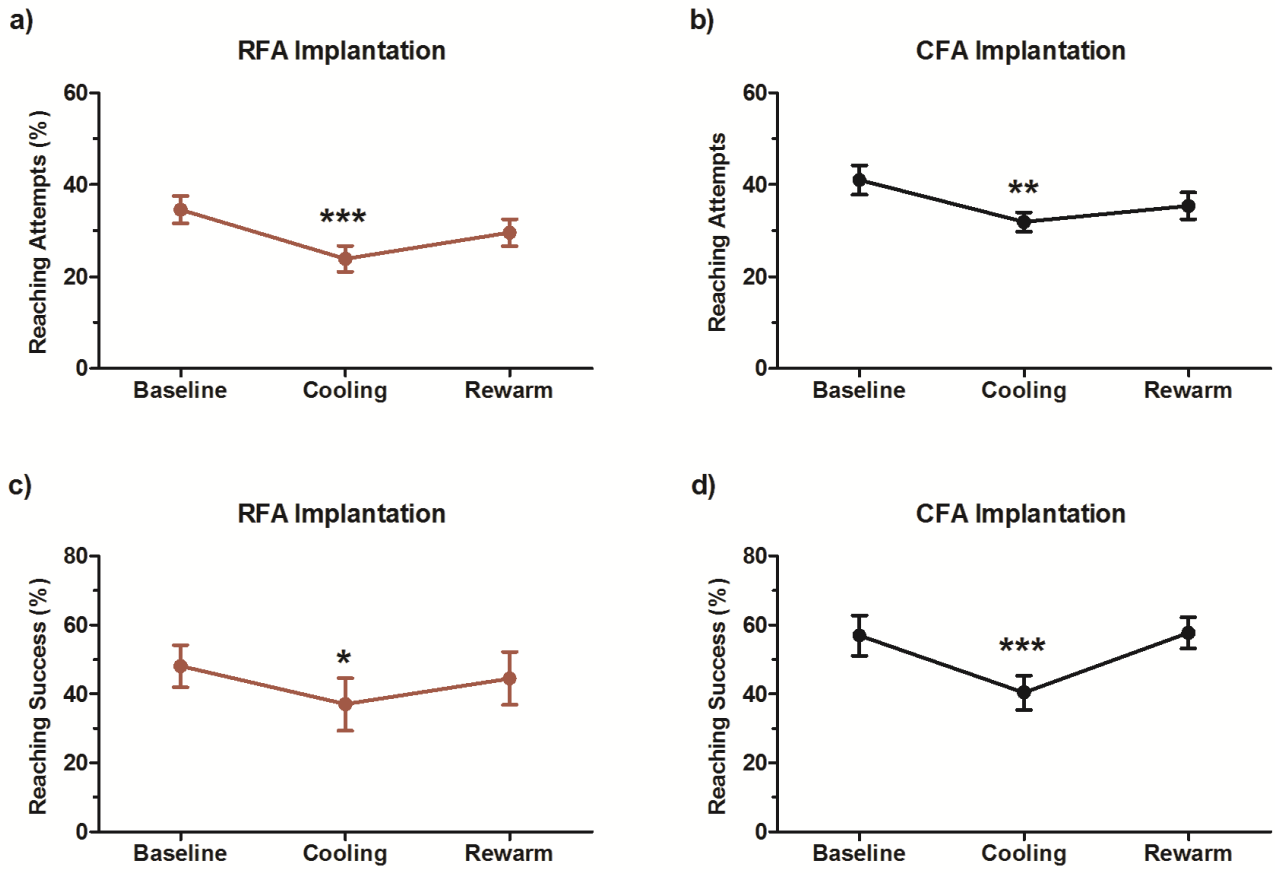

in the qualitative assessment of reaching movement subcomponents revealed a significant difference between groups (H_{20} = 52.07, p < .001, Fig. 3-8). Relative to baseline performance, cooling in RFA-cooled rats was associated with significantly higher mean error scores (0.527 ± 0.0785; U = 1.00 p < .001) on the grasp subcomponent compared to CFA rats (0.050 ± 0.046). Under baseline and rewarm conditions rats typically clasped the food pellet securely within the hand. During cooling deactivation of the RFA, food pellets were often held precariously between digits 2-3 or 4-5. Conversely, there were trends for increased mean error scores for elbow to midline (U = 22.5, p < .0597) and advance (U = 22.5, p < .0586) subcomponents in CFA-cooled (0.088 ± 0.044 and 0.038 ± 0.018, respectively) rats relative to RFA-cooled rats (0.0 ± 0.0 and 0.0 ± 0.0, respectively). During cooling deactivation of the CFA the elbow was not consistently abducted towards midline requiring an adjustment of reaching postures. Advances in a set of CFA-cooled rats were found to terminate prematurely, requiring an adjustment during arpeggio and grasping. No significant error score differences found were found between groups for the remaining reach movement subcomponents (all p > .05; Fig 3-8.)

3.4.3.2 Vermicelli handling

In CFA-cooled rats, no differences ($F_{2,14}$ = 0.95, p = .41) in the asymmetry ratio were found between baseline (47.8 ± 1.4 %), cooling (47.3 ± 1.7 %), and rewarm (49.2 ± 1.2 %) cycles (Fig. 3-9a). A significant main effect was observed in the asymmetry ratio of forelimb manipulations between cooling cycles in RFA-cooled rats ($F_{2,16}$ = 22.31, p < .001, Fig. 3-9b). Dunnett's post hoc testing revealed significant (p < .001*)* reductions in the asymmetry ratio, and consequently contralateral forelimb manipulations made in RFA-cooled rats during the cooling (32.5 ± 4.0 %) cycle compared to baseline (49.6 ± 1.4 %). No differences in the asymmetry ratio

Figure 3-8. Qualitative comparison of the grasping movement subcomponent in representative rats during acute cooling of the RFA and CFA. Under baseline and rewarm conditions rats in both groups typically clasp the food pellet securely within the hand. During cooling deactivation of the RFA, food pellets were often held between digits. A significant increase in the mean (± SEM) error score of the grasping movement was observed during cooling (baseline error scores subtracted) of the RFA compared to the CFA). ***$p < .001$.

Figure 3-8. Qualitative assessment of reaching performance during cooling

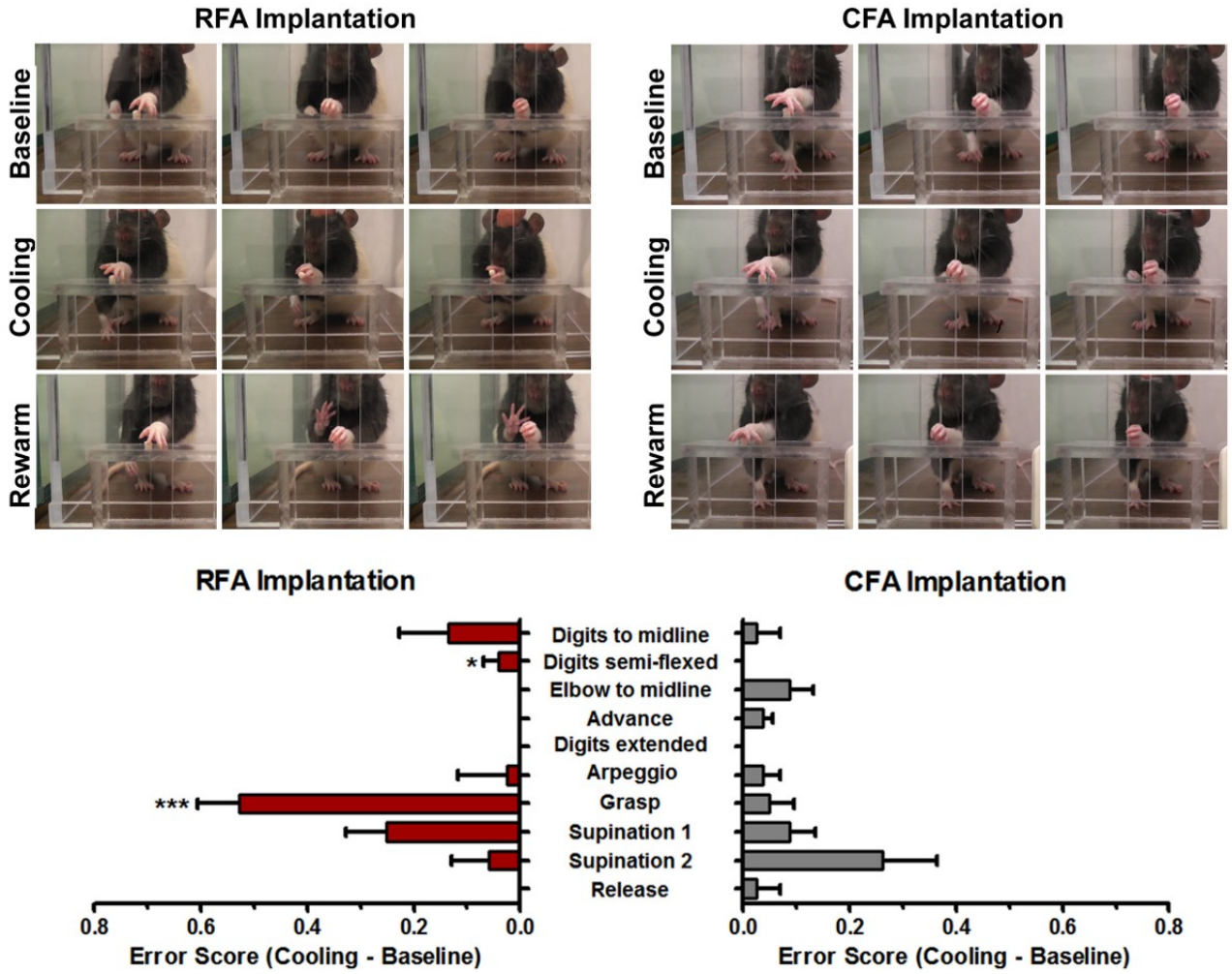

for rewarm (49.4 ± 1.9 %) was found relative to baseline ($p > .05$). Additionally, no differences ($p > .05$) in the time to eat the pasta strands was observed between cooling cycles for either CFA or RFA rats (Fig. 3-9c, 3-9d). CFA-cooled rats required 21.4 ± 2.9 s during baseline, 22.9 ± 3.4 s during cooling and 19.9 ± 3.5 s during rewarm to consume all pasta strands. RFA-cooled rats required 31.1 ± 6.0 s during baseline, 31.6 ± 6.7 s during cooling and 30.6= ± 6.6 s during rewarm to consume all pasta strands.

3.4.3.3 Sunflower Seed eating

No differences ($p < .05$) in the number of shell pieces between cooling cycles were observed for either CFA-cooled or RFA-cooled groups (Fig 3-9e, 3-9f). Mean shell pieces in CFA-cooled rats were 11.1 ± 0.5 during baseline, 12.4 ± 1.1, during cooling and 11.9 ± 0.8 s during rewarm cycles. Mean shell pieces in RFA rats were 11.1 ± 0.6 during baseline, 11.9 ± 0.5, during cooling and 11.4 ± 0.4 s during rewarm cycles.

A significant main effect was observed in the time required to eat all seeds between cooling cycles in CFA-cooled ($F_{2,14} = 6.49$, $p < .05$) but not RFA-cooled groups ($F_{2,16} = 1.75$, $p = .21$)(Fig. 3-9g, 3-9h). Dunnett's post hoc testing revealed significant ($p < .05$) reductions in contralateral forelimb grip strength in CFA-cooled rats during the cooling (55.0 ± 5.3 g) and rewarm (50.5 ± 4.9 g) cycle compared to baseline (49.9 ± 4.8 g). RFA-cooled rats required 48.3 ± 4.4 s during baseline, 55.9 ± 6.2 s during cooling and 49.2 ± 5.2 s during rewarm to consume all seeds.

Figure 3-9. Performance in vermicelli handling, sunflower seed manipulation, and grip strength tests. (a-d) Vermicelli pasta asymmetry ratios and handling times (mean ± SEM) in CFA-cooled and RFA-cooled groups under baseline, cortical cooling, and rewarm conditions. A lower asymmetry ratio reflects reduced contralateral-to-cryoloop forelimb manipulations and hand disuse during eating. A significant decrease in the asymmetry ratio was observed in RFA-cooled but not CFA-cooled rats. The time taken to eat the pasta did not differ across cooling cycles for either groups. (e-h) Sunflower seed shell fragments and eating times during baseline, cooling, and rewarm cycles in CFA-cooled and RFA-cooled groups (mean ± SEM). A significant increase in the time taken to consume the seeds was observed during cooling deactivation of the CFA but not the RFA. The number of shell fragments across cooling cycles did not differ for either group. (i,j) Grip strength (gm) assessment of the contralateral forelimb during baseline, cooling, and rewarm cycles in CFA-cooled and RFA-cooled groups. Cortical cooling was associated with significant decreases in mean (± SEM) grip strength in both CFA-cooled and RFA-cooled deactivations groups that persisted during assessment in rewarm conditions. $*p < .05$, $***p < .001$.

Figure 3-9. Behavioural assessment during cooling

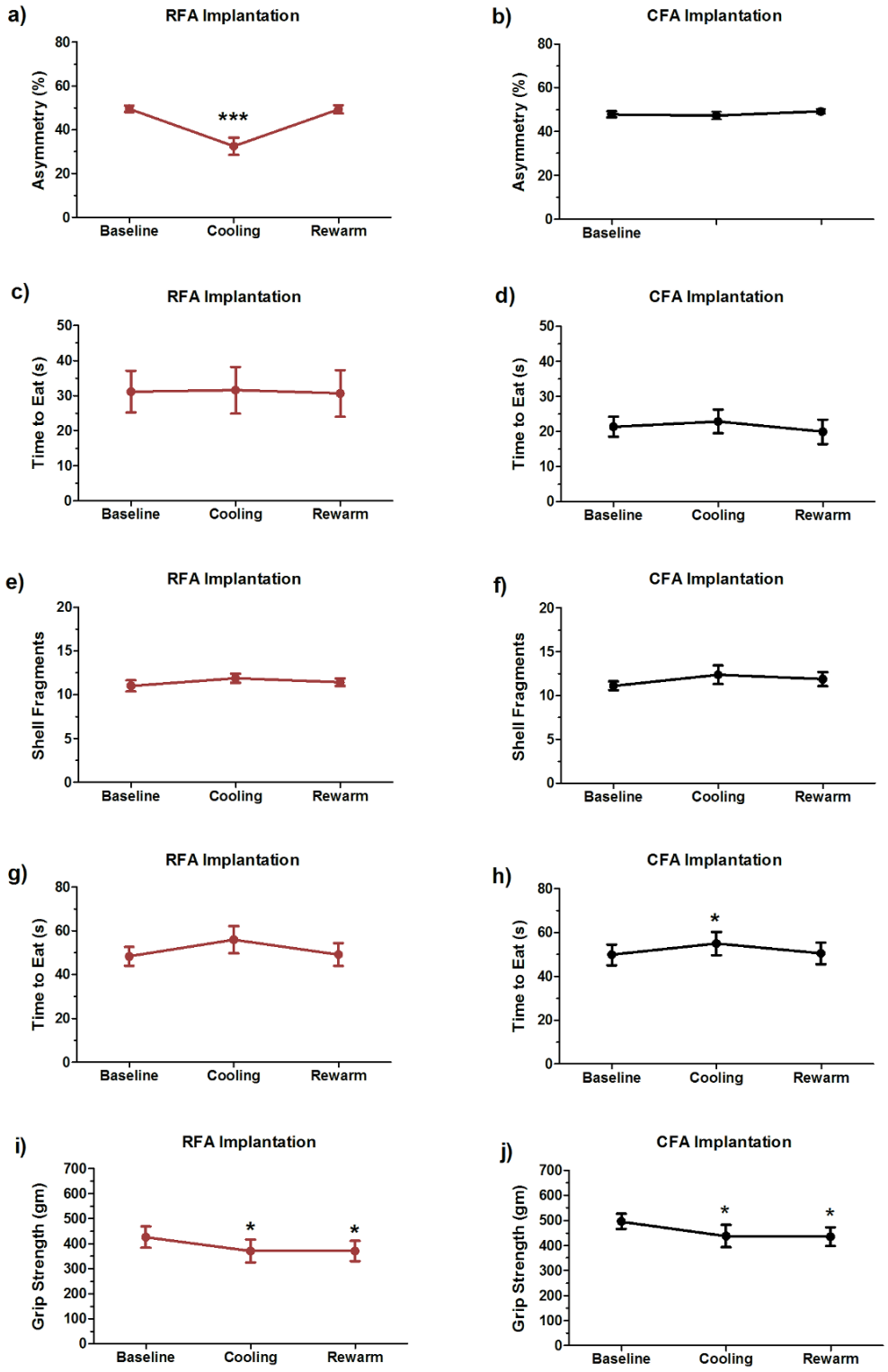

3.4.3.4 Grip strength

A significant main effect was observed in forelimb grip strength between cooling cycles in both CFA-cooled ($F_{2,14} = 6.66$, $p < .01$) and RFA-cooled groups ($F_{2,14} = 8.69$, $p < .01$)(Fig. 3-9i, 3-9j). Dunnett's post hoc testing revealed significant ($p < .05$) reductions in contralateral forelimb grip strength in CFA-cooled rats during both cooling (427.2 ± 45.1 g) and rewarm (434.8 ± 37.2 g) cycles compared to baseline (495.6 ± 30.63 g). Similarly, contralateral forelimb grip strength was significantly ($p < .05$) reduced in RFA-cooled rats during both cooling (370.5 ± 44.9 g) and rewarm (370.7 ± 40.64 g) cycles compared to baseline (426.0 ± 42.6 g). No differences in baseline grip strength was observed between CFA-cooled and RFA-cooled groups ($p > .05$).

3.4.4 Cryoloop placement verification and movement representation integrity

Following behavioural testing, rats were subjected to long-duration ICMS to verify cortical movement representation integrity and appropriate cryoloop placement targeting the CFA and RFA forelimb areas. In two rats, movement representations were unable to be derived due to a headcap loss following grip strength testing (RFA-cooled group) and cortical damage arising from cryoloop extirpation (CFA-cooled group). In all other cases the cortex was viable allowing forelimb movement derivation of either the CFA or RFA which was found to be localized within expected cooling deactivation isotherms (Fig. 3-10). No differences ($p > .05$) were observed in the size of either the CFA (4.3 ± 0.2 mm^2, 3.9 ± 0.2 mm^2) or RFA (1.0 ± 0.1 mm^2, 0.8 ± 0.1 mm^2) between unimplanted and cryoloop implanted groups.

Figure 3-10. Representative forelimb movement representations derived following CFA and RFA cryoloop implantation groups. Long-duration ICMS was used to confirm cortical map integrity following cryoloop implantation and behavioural testing. No differences in the size of either the RFA or CFA was observed between implanted and unimplanted groups ($p > 05$).

Figure 3-10: Cryoloop post-implantation assay

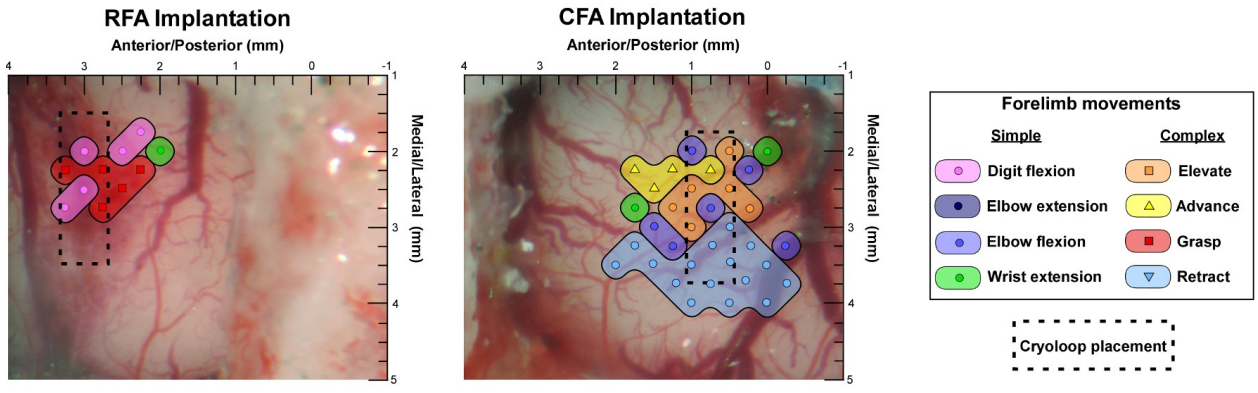

3.5 Discussion

Microstimulation studies have implicated two possible interpretations for the functional organization of motor cortex. A somatotopic mapping of body musculature is revealed using short-duration stimulation (SD-ICMS, < 50 ms; Asanuma and Rosén, 1972; Andersen et al., 1975; Donoghue et al., 1992); whereas complex, multi-joint, movements are evoked with long-duration stimulation on a behaviourally relevant time scale (LD-ICMS, ~500 ms; Graziano et al., 2002, 2005; Haiss and Schwarz, 2005; Gharbawie et al., 2011). We document a specialization and segregation of complex movement representations eliciting grasp behaviour in rostral (RFA) and elevate, advance and retract behaviours in the caudal (CFA) forelimb cortical motor areas in the rat under LD-ICMS indicating a functional dissociation between the two motor areas that is not observed under SD-ICMS. To investigate the functional contribution of these complex movement representations in the behaving rat, we provide the first report of selective, acute and reversible forelimb grasping deficits during cortical cooling deactivation of forelimb grasping, but not elevate, advance or retract movement representations. Our results provide causal support for a movement, rather than muscle encoding functional network organization of motor cortex output revealed by long-duration microstimulation.

Stimulation of motor cortex on a behaviourally relevant time scale, approximating both the duration of reaching and neuronal discharge patterns recorded during reaching in monkeys (Georgopoulos et al., 1982), has been purported to provide insight on its functional organization that is otherwise unattainable using traditional short-duration stimulation trains evoking brief twitches of somatic musculature (Graziano et al., 2002). Long duration microstimulation of motor cortex in monkeys evokes different classes of ethologically relevant movements and

postures from different cortical subregions reminiscent of reaching-to-grasp, digital-manipulation, feeding, climbing and defensive behaviours (Graziano et al., 2002, 2005; Haiss and Schwarz, 2005; Stepniewska et al., 2009). Within a given complex movement representation area, a topographical organization of body posture is observed. In the arm representation of monkeys, for example, stimulation of dorsal cortex results in the arm being driven to lower body space, stimulation of ventral cortex drives the hand into upper body space, and stimulation of intermediary cortex drives the hand towards midline body space (Graziano et al., 2002). We report a topographic organization of reach-to-grasp behaviour in rat forelimb motor regions using long-duration electrical stimulation that is not observed under short-duration stimulation protocols. Four distinct complex forelimb movement representations were noted, driving the forelimb towards different postures comprising forelimb elevation, advancement, grasping and retraction. Complex movements were found to exhibit marked rostrocaudal topography with spatial segregation. Grasps were exclusively elicited within the RFA (Neafsey & Sievert, 1982), reaches were observed within the rostromedial aspect of the CFA, retractions localized to the caudolateral aspect of the CFA, and elevations predominantly found in the caudomedial region of the CFA. Forelimb movements were evoked with short-latency following stimulus onset, held for the duration of the stimulation train, and were similar to those previously reported (Ramathanan et al., 2006; Bonazzi et al., 2013)

The functional role of observed complex movement representations suggested by microstimulation results was then assessed in the behaving rat by use of chronically implanted subdural cortical cryoloops (Lomber et al., 1999), providing temporary and reversible functional deactivation of either the RFA or CFA. We report for the first time a specific motor deficit resultant from the reversible deactivation of a complex movement representation in service of

that behaviour. Although cortical cooling deactivation of both forelimb motor areas was associated with significant deficits in single-pellet reaching success rates and attempts, a specific impairment in the grasping subcomponent of reaching (Whishaw et al., 2003) was observed solely during RFA deactivation silencing grasping movement representations. CFA deactivation, on the other hand, was associated with trends for increased impairments of abducting the elbow towards midline and reach advance. Cortical cooling of the RFA was also associated with a significant specific deficit in the vermicelli handling test exhibited by a reduced ratio of contralateral forelimb manipulations that was not demonstrated during cooling of the CFA. These deficits were fully reversible when assessed following passive cortical rewarming to baseline temperatures. Cooling deactivation of the CFA was associated with a specific impairment in the sunflower seed task exhibited by a significant increase in the time required to consume the seeds. Although seemingly a distal forelimb motor task, it has primarily been shown to rely on cranial motor functions of the tongue and jaw to shell the seeds with the forelimbs serving to support the seeds in a proper position for consumption (Whishaw et al., 1998; Prine et al., 2013). As the CFA has shown to preferentially elicit complex coordinated forelimb movements involving proximal limb musculature in concert with neck and jaw activation (Ramanathan et al., 2006; Bonazzi et al., 2013) it could be expected to be more sensitive to CFA rather than RFA dysfunction in this test.

Although cooling deactivation did not result in severe behavioural impairment particularly with the CFA group, it is important note that at the temperatures employed in this study, cooling results in a synaptic (< 20°C; Lomber et al., 1999) but not a conduction (< 0°C; Bénita and Condé, 1972) block localized to within 1 mm of the loop. ICMS has been shown to elicit neuronal activation millimetres away from the stimulation site, even at low (< 10 μA)

intensities, a finding ascribed to distal fiber activation (Histed et al., 2009). Movement representations derived via ICMS may slightly under-represent underlying somatic activation. As the cortical deactivation area used in this experiment was selected to silence the much smaller RFA, it is plausible that an incomplete inactivation of the CFA was achieved in some rats. None the less, a significant deficit in skilled reaching performance was observed during CFA cooling. Contralateral forelimb grip strength reductions during cooling we seen in both RFA and CFA rats and persisted during cortical rewarming. While grip strength reductions may reflect mild paretic effects from motor cortical inhibition, persistence of the impairment despite return of cortical temperature to baseline could either reflect a lag for reestablishment of network activity mediating movement force encoding or habituation to the test. Adaptation of cooling deactivation for chronic use in rats was well tolerated with intact movement representations probed with ICMS following behavioural assessment. Importantly, no differences in either reaching performance prior to and following cryoloop implantations, or the size of CFA and RFA between unimplanted and implanted rats were observed indicating that cryoloop implantation procedure itself was not related to the behavioural deficits noted during cooling deactivation. Effective deactivation was confirmed by the abolishment of ICMS responses during acute cooling, indicating similar isotherm deactivation thresholds as reported in cats (Lomber et al., 1999), guinea pigs (Coomber et al., 2011) and rats (Antunes and Malmiera, 2011).

The topography of complex movement representations observed presently with a segregation of forelimb grasping (RFA) from forelimb reaching (CFA) lends support to an intriguing theory on the differential evolutionary origins for grasp and reach behaviour in mammals. Dual visuomotor channel theory (Jeannerod, 1981) proposes that separate neural

circuitry mediating forelimb reaching and grasping evolved simultaneously in the primate lineage from a demand to locomote and feed in an arboreal environment and are unified under visual control for coordinated movement. Karl and Whishaw (2013) have recently proposed that forelimb reach abilities, predating primates, were instead derived independently with reaching exapted from the stepping movements of locomotion (limb elevation, advance, retract) and grasping from food handling behaviour. Although the RFA and CFA exhibit a fractured somatotopy of forelimb representation under SD-ICMS, a functional dissociation between the two motor areas is revealed under LD-ICMS supporting this later theory with forelimb elevation, advancement, and retraction elicited from the CFA and grasping from the RFA. These two forelimb motor areas may then be analogous to the independent circuitry for reaching and grasping observed in primates (Kaas et al., 20011; Gharbawie et al., 2011) and cats (reviewed in Alstermark and Isa, 2012) and serve distinct functional, rather than hierarchical (Rouiller et al., 1993) roles in motor control. It is worthy to note that orofacial representations are found to border the RFA laterally (Neafsey and Sievert, 1986), suggesting that the topographic distribution of adjacent complex movement representations organized for behavioural function (i.e., food handling and eating) extends even to disparate body parts.

Collectively, these data are the first to provide causal support for a functional organization of motor cortex based on complex movement representations, rather than muscle somatotopy. Long-duration microstimulation has been suggested to reveal an integrative assay of three-dimensional movement encoding arranged to fit on the two-dimensional cortex according to a 'nearest neighbour' schema (Graziano and Aflalo, 2007), incorporating the multiple and overlapping somatotopic muscle representations (Luppino et al., 1991, Schieber, 2001). Although network activation and recruitment properties from microstimulation are not

fully understood, distinct complex movement representations have been shown to involve segregated corticofugal projections (Harrison et al., 2012). This is perhaps surprising noting that while proximal and distal forelimb musculature in the rat is separately innervated by C4 and C8 spinal segments, respectively (McKenna et al., 2000), they are intermixed at the cellular level in the cortex (Wang et al., 2001). This functional parcellation of complex movement representations into distinct zones within forelimb motor areas, then, presumably results from differences in intrinsic intracortical circuitry as well as afferent and efferent projection pathways (Li et al., 1990; Rouiller et al., 1993; Haiss and Schwarz, 2005; Harrison et al., 2012).

Chapter Four:

Impaired selection specificity in complex movement representations following repeated seizures

Andrew R. Brown[1,2], Gerard M. Coughlin[3] G. Campbell Teskey[1,3,4]

[1]*Hotchkiss Brain Institute*, [2]*Department of Neuroscience,* [3]*Department of Psychology,*

[4]*Department of Cell Biology and Anatomy, University of Calgary, Alberta, Canada*

First author contributions: experimental design, electrode implantation and electrophysiological mapping surgery, data analysis, manuscript preparation.

4.1 Abstract

Repeated frontal lobe seizures are associated with larger neocortical movement representations (motor maps) in addition to concomitant interictal motor deficits in both clinical populations with epilepsy and in experimental models of epilepsy. However a functional relationship between motor map reorganization and specific behavioural impairment has yet to be established. To investigate the functional mechanisms underlying seizure-induced cortical plasticity, we used "behaviourally relevant" long-duration intracortical microstimulation (LD-ICMS) to test the hypothesis that repeated seizure activity would be associated with alterations in evoked motor responses and complex movement representation topography. We document that callosal kindling in Long-Evans rats is associated with increased overlap of adjacent forelimb movement representation areas derived under LD-ICMS. In a second experiment, forelimb movement representations were derived under the condition of reduced intracortical inhibition with focal application of the $GABA_A$ receptor antagonist bicuculline methiodide recapitulating the larger maps observed following kindling, but eliciting different movements consisting of brief forelimb twitches. Collective evidence suggests that repeated seizures result in a loss of cortical movement encoding specificity that may underlie the interictal motor deficits follow repeated seizures.

4.2 Introduction

The functional reorganization, or plasticity, of motor and sensory cortices is an integral component for the encoding of experience and learning (Nudo et al., 1996; Kilgard & Merzenich, 1998; Sanes & Donoghue, 2000; Lomber et al., 2010), but can also be detrimental to neural function when brought on by pathology (Teskey et al., 2008; Mao & Pallas, 2012; Hubsch et al., 2013). Some individuals with frontal lobe epilepsy show alterations in corticomotor organization demonstrated as increased size and mosaicism of neocortical movement representations (Motor maps)(Umatsu et al., 1992; Branco et al., 2003; Hamer at el., 2005) as well as interictal disruptions in movement execution and motor coordination (Hemstaedter et al., 1996; Upton and Thompson 1997; Hernandez et al., 2002). Experimentally-induced repeated seizure activity in rats with chronic electrical kindling of the corpus callosum, amygdala, or hippocampus increases the total size of forelimb neocortical movement representations derived with short-duration intracortical microstimulation (SD-ICMS) with a proportional representation of distal (digit, wrist) to proximal (elbow, shoulder) musculature (Teskey et al., 2002; Van Rooyen et al., 2006; Teskey et al., 2008), and is associated with forelimb motor deficits (Henry et al., 2008; Flynn et al, 2010). Two separate representations of the forelimb are normally found in the rat motor cortex, the rostral (RFA) and caudal (CFA) forelimb areas, separated by an intervening strip of craniofacial representation (Neafsey and Sievert, 1986). Kindling-induced larger maps results in a merging of the RFA and CFA, forming a contiguous forelimb representation in addition to a dramatic posterolateral expansion that has been termed the posterior forelimb area (PFA)(Henderson et al., 2011). Movement representation plasticity following kindling has been attributed to anatomical and physiological alterations in synaptic

efficacy within layer V of sensorimotor cortex (Teskey et al., 2002; 2005), with larger maps observed following long-term potentiation (LTP)(Monfils et al., 2004), smaller maps following long-term depression (Teskey et al., 2007) and a reversal of kindling-induced larger maps achieved with low-frequency stimulation promoting long-term depression (LTD)(Ozen et al., 2009). Rapid changes in the size and organization of movement representations can be observed within minutes following pharmacological disinhibition of pre-existing lateral excitatory horizontal connections within layer V (Jacobs and Donoghue, 1991) or hours following a single episode of status epilepticus (Young et al., 2009). Motor map expansion, therefore, likely reflects an unmaking of latent motor circuitry that is not normally activated with microstimulation, but is revealed under conditions of decreased intracortical inhibition or enhanced excitatory drive.

Despite the substantial evidence demonstrating motor map reorganization following repeated seizures, it is not clear how such reorganization relates to specific behavioural impairment. This may be due to the minimal stimulus approach of SD-ICMS utilizing movement threshold intensities (typically > 60 μA) and brief stimulation trains (>50 ms) to probe cortical output function. Microstimulation at higher intensities (~100 μA) using longer train durations (~500 ms, long-duration ICMS, LD-ICMS), closely matching the time-scale of cortical motorneuron activity during natural movement, promotes transsynaptic cortical activation (Tolias et al., 2005) and has been shown to evoke complex and coordinated movements similar to those of natural behavior in primates (Graziano et al., 2002, 2005; Heiss and Schwarz, 2005; Gharbawie et al., 2011) and rodents (Ramanthan et al., 2006; Harrison et al., 2012; Bonazzi et al., 2013). LD-ICMS has been suggested to reveal aspects of functional cortical movement encoding that is unattainable with SD-ICMS (Graziano, 2009). In the rat, LD-ICMS evokes reach-to-grasp behaviour with movement subcomponents clustering separately within the RFA

and CFA forelimb regions. Importantly, an association between the integrity of specific complex movement representations elicited with LD-ICMS and forelimb motor ability have been reported. Reversible deficits in forelimb grasping are observed during selective deactivation of cortical grasping "RFA" representations (Chapter 3), and the degree of functional recovery in skilled reaching ability after cortical injury to forelimb retraction representations is correlated with their re-expression following rehabilitative training (Ramanathan et al., 2006).

In the current study, we employed LD-ICMS to derive forelimb movement representations in Long-Evans rats following chronic callosal kindling to test the hypothesis that functional plasticity in motor cortex would be reflected by alterations in the nature of evoked forelimb motor responses and complex movement representation topography. A second experiment was conducted to determine whether the larger movement representations observed following kindling can be recapitulated under the cortical disinhibition achieved by administration of the $GABA_A$ receptor antagonist bicuculline methiodide. We show that expanded PFA motor regions evoke qualitatively distinct twitches in forelimb musculature under LD-ICMS. Collective findings suggest to us that motor deficits arising from repeated frontal seizures may be attributed neural reorganization resulting in impaired movement selection specificity within cortical movement representations and not simply a loss of inhibition.

4.3 Materials and Methods

4.3.1 Rats and experimental groups

Thirty three adult male Long-Evans rats weighing 269-473g at the time of electrophysiological mapping were used in this study. In the first experiment rats were assigned

to one of two groups receiving either 20 daily sessions of kindling (kindle, n=7) or sham-kindling (sham-kindle, n=5) delivered to the corpus callosum prior to LD-ICMS electrophysiological mapping. In a second experiment, forelimb movement representations were derived under cortical bath application of either physiological saline (0.9%) or bicuculline methiodide using either SD-ICMS (n=5, within subjects design) and LD-ICMS (saline treatment n=10 from Chapter 3; bicuculline treatment n=6). Rats were obtained from Charles River (Saint-Constant, QC) and housed individually in clear plastic cages in a colony room maintained on a 12h light/dark cycle (lights on at 07:00) at 21°C. Upon arrival, rats were gently handled once per day for five days to minimize stress during behavioural testing and electrophysiological mapping. Experimentation was conducted between 08:00 and 22:00h. Rats were provided free access to food and water (Prolab RMH 2500 lab diet, PMI Nutrition International, Brentwood, MO, USA) throughout the duration of their housing except for an overnight food restriction prior to ICMS procedures. All procedures involving rats used in this study strictly adhered to the guidelines of the Canadian Council on Animal Care and were approved by the Health Sciences Animal Care Committee of the University of Calgary. All efforts were made to adhere to the principles of reduction, refinement, and replacement in experimental design (Russell & Burch, 1959), with every attempt made to limit the number of subjects and minimize animal suffering.

4.3.2 Intracortical microstimulation

ICMS procedures and analyses were conducted as described in chapter 3.

4.3.3 Bicuculline application

A 30 µl solution of 50 µM bicuculline methiodide (Sigma-Aldrich, Oakville, ON) was applied directly to the cortical surface, covering the entirety of cortex exposed by the craniotomy. This protocol has been previously reported to provide effective $GABA_A$ receptor blockade throughout all cortical layers (Stojic et al., 2000). Electrophysiological mapping started 30 minutes following the initial infusion and additional doses were given at 30 minute intervals. In cases where contralateral forelimb clonus was evident, mapping and additional bicuculline administrations were halted until the clonus subsided. The cortex was kept moist with intermittent application of physiological saline. Bicuculline and saline solutions were kept at 34° C.

4.3.4 Chronic electrode implantation

Electrode implantation protocol was adapted from Teskey et al. (2002). Twisted wire bipolar stimulating and recording electrodes were constructed from Teflon-coated stainless steel wire (A-M Systems, Everett, WA). Insulation was removed from the ends of the wire, and gold-plated amphenol pins were attached. Electrode poles were separated by 0.5 mm. Prior to implantation, animals were anaesthetized with isoflourane (5% induction, 1-2% maintenance; VIP-3000 Vaporizer, Matrix, Orchard Park, NY) and the scalp was shaved. Depth of anaesthesia was monitored throughout implantation, and isoflourane levels were adjusted to maintain an adequate level of anaesthesia.

Animals were secured in a stereotaxic frame (Kopf, Tujunga, CA), with the incisor bar set to skull flat. A heating pad was used to maintain body temperature. A longitudinal incision was made to expose the skull. Seven holes were drilled into the skull for the stimulating

electrode, the recording electrode and five stainless steel anchor screws. The stimulating electrode was implanted into the corpus callosum: 1.0 mm anterior to bregma, 0.5 mm lateral to midline, and 4.4 mm below bregma The recording electrode was implanted into the sensorimotor cortex: 1.0 mm anterior to bregma, 4.0 mm lateral to midline, and 2.7 mm below bregma. Electrophysiological monitoring was conducted during the implantation to ensure that dorsal-ventral placements yielded optimal evoked response amplitude.

Gold-plated amphenol pins were inserted into a nine-pin McIntyre plug (Molino and McIntyre, 1972; Ginder Science, Ottawa, ON). The plug was then secured to the skull using dental cement. The left frontal and parietal bones were left free of dental cement and screws to facilitate the later craniotomy. The scalp was sutured around the headcap composed of the dental cement and McIntyre plug. Rats were given a topical application of Xylocaine jelly (2%) analgesic around the incision. Rats were provided with a 7-day post-surgery recovery period, during which no experimental procedures were performed.

4.3.5 Kindling

Kindling was performed in awake, freely moving rats. Seven days following electrode implantation, an afterdischarge threshold (ADT) was determined for each rat in the kindling group. The ADT's were defined as the weakest current required to induce an afterdischarge (AD). Current delivered to the callosum started at 100 μA , increasing in steps of 50 μA every 60 s until an AD of at least 4 s was elicited.

Kindling stimulation was delivered through the electrode placed in the callosal white matter. Kindled animals received 20 daily sessions of kindling stimulation, including ADT determination. This stimulation consisted of a 1 s train of 60 Hz biphasic rectangular wave pulses

of 1 ms duration, which were separated by 1 ms. The stimulation intensity was 100 μA greater than the ADT for that individual. During both ADT determination and kindling sessions, an electrographic recording was obtained from both electrodes. The recorded signals were filtered at half amplitude, below 0.3 Hz and above 300 Hz, and then amplified 1000 or 2000 times (Grass Neurodata Acquisition System Model 12). In addition, seizure behaviour was observed and coded according to the five stage scale of Racine (1972). Sham-kindle rats were implanted but did not receive kindling stimulation. Immediately following electrophysiological mapping, rats were sacrificed via perfusion of sodium pentobarbital though the heart. Brains were extracted and fixed in formalin, sliced visually inspected to confirm placement of recording and stimulating electrodes.

4.3.6 Statistical analyses

Parametric one-way Analysis of Variance (ANOVA) were performed on movement representation topography analyses with Tukey post-hoc tests used for multiple comparison testing. Independent student *t*-tests were used in single measure two-sample comparisons of forelimb map area measurements, and drug doses delivered during ICMS. Non-parametric two-sample comparisons were conducted with Mann-Whitney tests. All analyses were two-tailed. An *a priori* alpha level of .05 was used. Statistical analyses were conducted using GraphPad Prism 5 (GraphPad Software Inc., La Jolla, CA). Data are presented as mean ± SEM. Asterisks in figures represent significance level: * $p < .05$ ** $p < .01$, *** $p < .001$.

4.4 Results

4.4.1 Kindling

Progression of mean seizure stage and AD duration was observed over 20 daily kindling sessions (Fig. 4-1). During the first three kindling sessions, rats exhibited a mean seizure stage of 2.6 ± 0.3 which significantly increased (t_{12}= *4.39,* $p < .001$) to 4.4 ± 0.3 over the last three kindling sessions. AD durations were 11.9 ± 1.8 s over the first three kindling sessions and significantly (t_{12}= *4.15,* $p < .01$) increased to 28.7 ± 3.7 s during the last three sessions.

4.4.1.1 Forelimb movement representation topography following callosal kindling

Representative forelimb movement representations of a kindled and sham rat are depicted in Figure 4-2. Kindling was associated with a significant (t_{10}= *4.93,* $p < .001$, Fig. 4-3a) increase (~100 %) in total forelimb movement representation area (8.16 ± 0.66 mm^2) compared to sham-kindle controls (4.10 ± 0.25 mm^2). Kindling was associated with increased movement representation mean areas for all movement categories except forelimb advance (Fig 4-3b; Table 4-1). Tukey post-hoc analysis revealed a specific increase in the size of elbow flexion movement representations a significant contributing factor ($p < .05$) in the larger forelimb movement representations observed in kindled rats. No differences in the mean anterior/posterior or medial/lateral coordinates of individual forelimb movement representations was observed between kindled rats and sham controls (all $p > .05$; Table 1), suggesting a proportional expansion in both axes.

Kindling was associated with eliciting novel movement combinations under LD-ICMS in addition to those previously reported (Chapter 2). Novel movements consisted of combinations in individual simple and complex movements observed in sham-kindle controls that co-occurred during individual stimulation trials in kindled rats (Fig. 4-2). The co-occurrence of two forelimb

Figure 4-1. Kindling afterdischarge duration and seizure stage scores. (a)Representative AD from the cortex of a kindled rat on the 8th kindling session, with an AD duration of 19.6s and a seizure stage of 4. (c-d) Progression of seizure stage and AD duration, respectively, over the course of the kindling sessions. Significant ($p < .05$) increases in both behavioural stage and AD duration were observed over the course of kindling.

Figure 4-1: Kindling afterdischarge duration and seizure stage scores

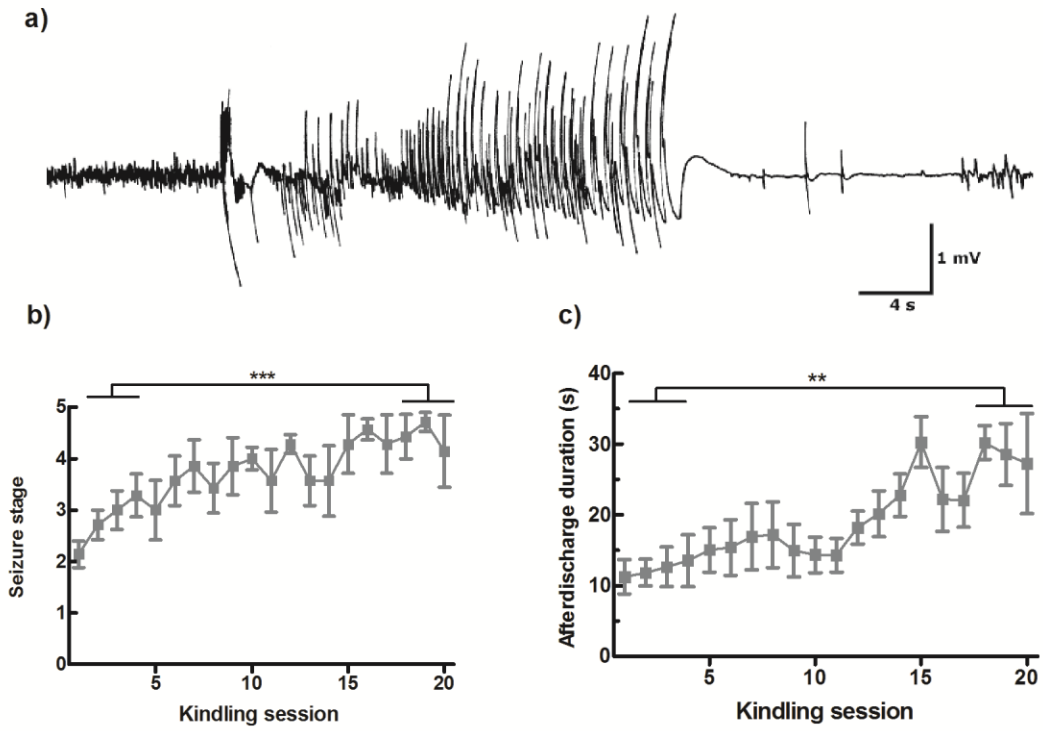

Figure 4-2. Representative forelimb movement representations derived in a sham-kindled (top) and kindled (rat) rat. Kindling was associated with markedly larger forelimb movement representations as well as the elicitation of dual forelimb-responsive stimulation sites.

Figure 4-2: Representative motor maps in kindle and sham-kindle groups

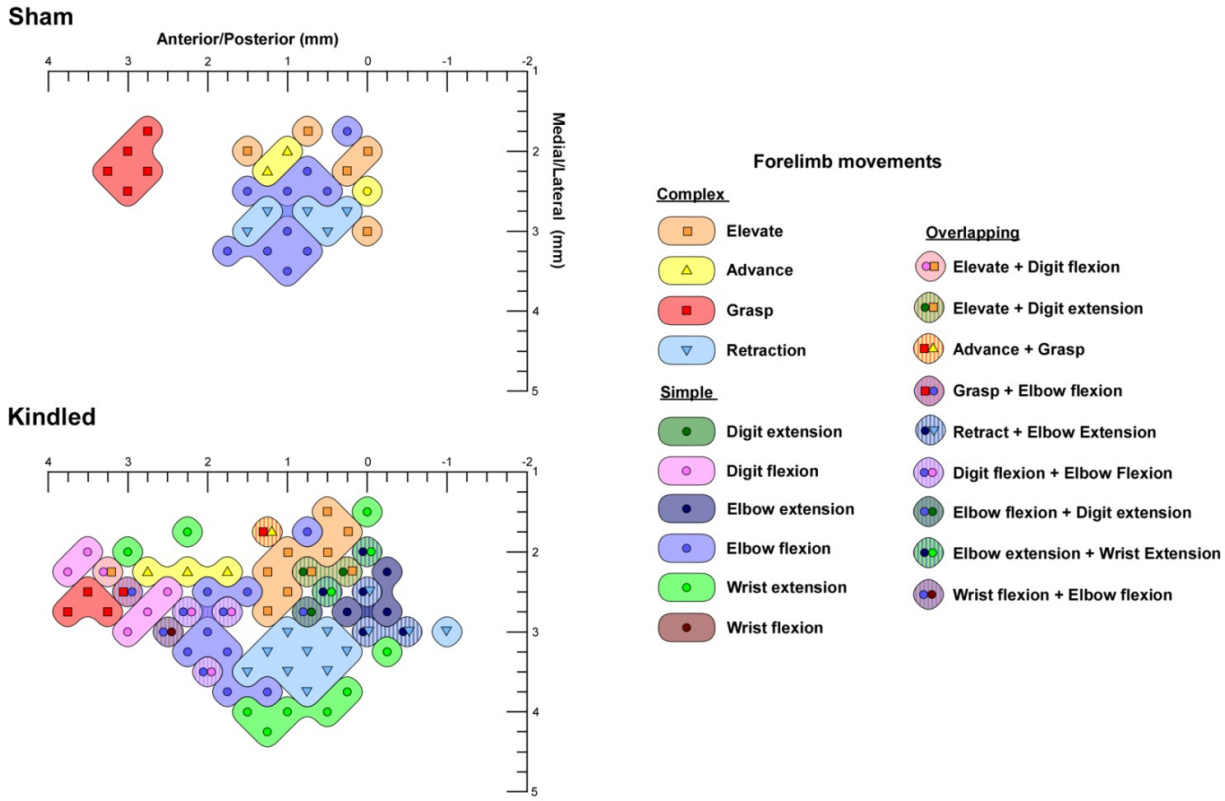

Figure 4-3. Kindling resulted in significant ($p < .05$) increases in forelimb movement representation area (b, c) in addition to the appearance of ipsilateral forelimb responses not observed in sham rats (d). (e) Kindling was also associated with a significant ($p < .05$) increase in dual-responsive stimulation sites elicited co-activation of forelimb/forelimb and forelimb/non-forelimb movements.

Figure 4-3: Motor map areas and overlap

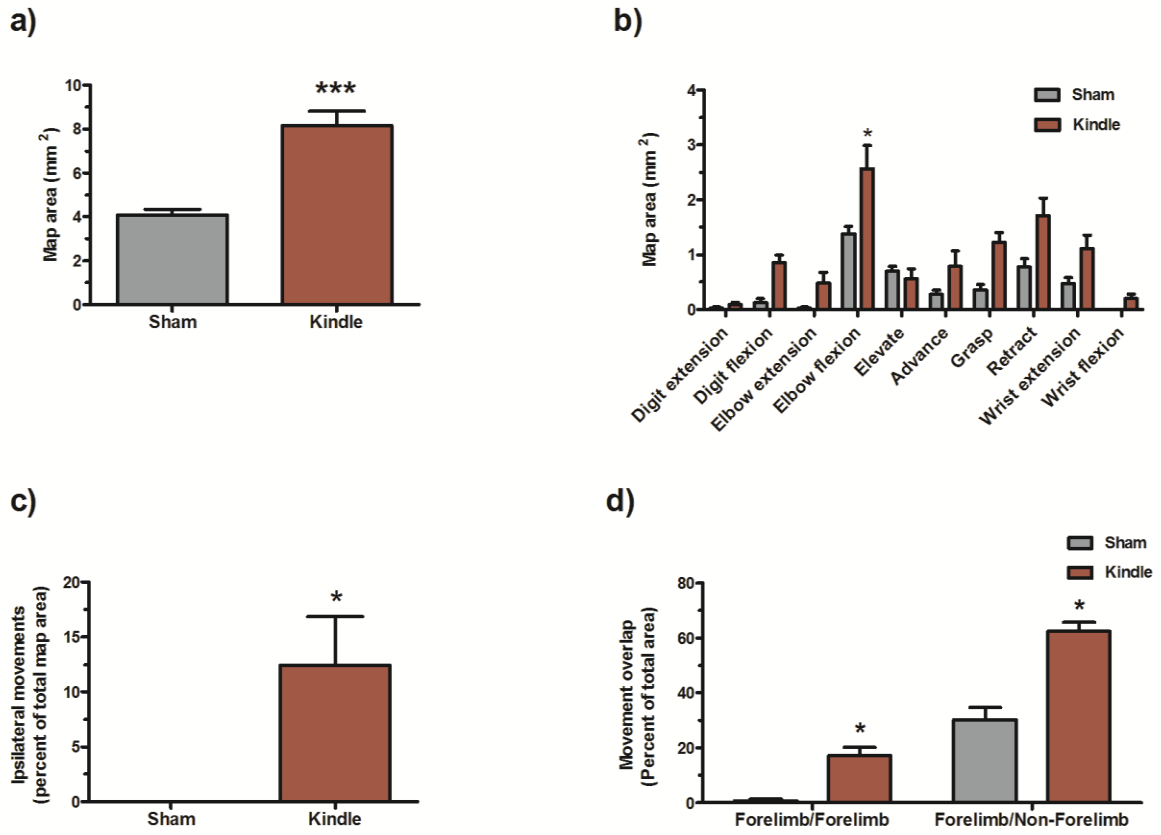

Table 4-1. Forelimb motor map topography

Group	Forelimb Movement[a]	Cortical Area (mm2 ± SEM)	AP Coordinates (mm±SEM)[b]	ML Coordinates (mm±SEM)[c]
Naïve	*Complex*			
	Elevate	0.575±0.175	0.6893±0.1155	2.396±0.1584
	Advance	0.4125±0.09511	1.547±0.1695	2.283±0.1016
	Grasp	0.5125±0.09024	3.191±0.1066	2.326±0.08866
	Retract	1.025±0.05833	0.8078±0.06966	3.165±0.07174
	Simple			
	Digit extension	0.025±0.025	2.75±2.75	2.75±0
	Digit flexion	0.2875±0.06985	3.238±0.1011	2.2±0.1024
	Elbow extension	0.1941±0.05907	1.141±0.4803	2.447±0.3988
	Elbow flexion	1.613±0.1941	1.115±0.1222	2.682±0.09623
	Suppination	0.025±0.025	0±0	1.875±1.875
	Wrist extension	0.6625±6.625	0.5383±0.1956	2.887±0.1433
	Wrist flexion			
Sham-kindle	*Complex*			
	Elevate	0.7±0.08478	0.55±0.1159	2.993±0.0547
	Advance	0.275±0.07289	1.427±0.1322	2.156±0.06883
	Grasp	0.35±0.1075	3.097±0.1351	2.147±0.07366
	Retract	0.775±0.1551	0.7202±0.1939	2.833±0.02182
	Simple			
	Digit extension	0.025±0.025	2.75±2.75	2.75±0
	Digit flexion	0.125±0.06847	3.333±0.2205	2.278±0.222
	Elbow extension	0.025±0.025	0.25±0.25	2±2
	Elbow flexion	1.375±0.1369	1.166±0.1982	2.687±0.0836
	Suppination			
	Wrist extension	0.475±0.1075	0.4792±0.3206	2.511±0.2186
	Wrist flexion			
Kindle	*Complex*			
	Elevate	0.5536±0.1847	0.621±0.2613	2.508±0.2266
	Advance	0.7857±0.2857	1.719±0.1543	2.437±0.1026
	Grasp	1.232±0.1734	3.018±0.1878	2.667±0.07682
	Retract	1.714±0.3178	0.3038±0.1287	3.331±0.1353
	Simple			
	Digit extension	0.089291±0.04494	1.00±0.6292	2.500±0.3819
	Digit flexion	0.8571±0.1376	2.207±0.1522	2.956±0.0963
	Elbow extension	0.4821±0.1975	0.5167±.5020	2.820±0.1404
	Elbow flexion	2.571±0.4207	1.242±0.1601	2.993±0.0547
	Suppination			
	Wrist extension	1.107±0.2446	0.8009±0.3914	3.273±0.1486
	Wrist flexion	0.1964±0.08988	1.688±0.5059	2.771±0.1867
Bicuculline	*Complex*			
	Elevate	0.4583±0.1431	0.6563±0.2941	2.589±0.2155
	Advance	0.5625±0.1505	1.604±0.2366	2.442±0.0738
	Grasp	0.2917±0.0527	2.486±0.5638	2.819±0.3461
	Retract	1.229±0.3153	0.2906±0.2906	3.195±0.1303
	Simple			
	Digit extension			
	Digit flexion	0.6667±0.1667	3.187±0.1933	2.542±0.1269
	Elbow extension	0.04167±0.04167	1.875±1.875	2.875±0
	Elbow flexion	2.313±0.4315	0.9569±0.196	2.519±0.0943
	Suppination	0.04167±0.02635	1.125±0.625	3.625±0.125
	Wrist extension	0.1875±0.0427	0.3403±0.3771	3.236±0.2559
	Wrist flexion			
	Twitches			
	Elbow	3.979±0.7702	-0.6677±0.1823	3.587±0.2068
	Shoulder	0.6667±0.157	-0.9825±0.1579	2.765±0.1125
	Wrist	0.4583±0.1954	-0.5347±0.3521	3.796±0.1251

[a] Empty cells denote an absence of a particular movement for that group

[b] Anterior/Posterior (AP) coordinates are referenced to bregma in the coronal plane.

[c] Medial/Lateral (ML) coordinates are referenced to the saggital suture

movements (simple or complex) at the same stimulation site were considered as points of dual forelimb representation (forelimb/forelimb movement overlap). Dual forelimb representations accounted for a significantly (t_{10}= *4.49,* $p < .01$, Fig. 4-3c) larger proportion of the total forelimb map area in kindled rats (21.08 ± 2.25 %) compared to sham controls (0.57 ± 0.57 %). Most commonly, dual forelimb representations were observed as adjacent bordering forelimb representation movements being evoked within a given representation. For example, elbow flexion representations are typically observed medially to forelimb retraction representations. In kindled rats, stimulation sites bordering these two representations elicited flexions of the elbow during forelimb retraction. Overlap of forelimb movement representations was particularly prominent in posterior RFA and anterior CFA regions. Normally separated by an intervening strip of craniofacial representation (Neafsey and Sievert, 1986), the larger forelimb map following kindling has been shown to result in a fusion of these two areas (Teskey et al., 2002). Contiguous forelimb representations between RFA and CFA were also observed presently with the co-occurrence of both forelimb grasping and digit flexions (restricted to the RFA in sham-kindled rats) and forelimb elbow flexions and advances (restricted to the CFA in sham-kindled rats) being observed from cortical territory evoking crianiofacial representations in sham-kindled rats. Dual forelimb-responsive sites within forelimb movement representations in kindle rats also took the form of bilateral forelimb movements. Kindled rats exhibited a significantly (Mann-Whitney U = 2.5, $p < .05$) greater proportion of bilateral forelimb movements (12.48 ± 4.45 %) compared to sham controls in which they were absent (0.0 ± 4.45 %). Bilateral forelimb responses were typically evoked the same movement in both forelimbs (e.g., elbow flexion/elbow flexion), however, antagonistic muscle synergies were also observed between forelimbs (e.g., elbow flexion/elbow extension). Stimulation sites evoking dual forelimb and

non-forelimb responses (i.e., jaw opening with forelimb grasp) were also commonly observed in kindled rats. Overlap of forelimb/non-forelimb representation, quantified as a proportion of total forelimb representation area eliciting a dual representation of non-forelimb body movements was found to be significantly (t_8= *6.3,* $p < .01$, Fig. 4-3e) larger in kindled rats (65.76 ± 3.37 %) compared to sham controls (30.29 ± 4.45 %).

No significant differences between groups were found in the amount of ketamine, $t(10) = 0.89$, $p = > .05$, or xylazine, $t(10) = 1.35$, $p > .05$, administered during ICMS . Rats in the kindled group received 0.90 mg/kg/min ± 0.041 mg/kg/min of ketamine, whereas those in the sham group were administered 0.97 mg/kg/min ± 0.017 mg/kg/min of ketamine. Likewise, kindled rats received 0.048 mg/kg/min ± 0.0019 mg/kg/min of xylazine, and control rats received 0.056 mg/kg/min ± 0.0058 mg/kg/min of xylazine.

4.4.2 Forelimb movement representation topography under bicuculline administration

Acute cortical application of bicuculline methiodide was not associated with the elicitation of dual-responsive forelimb movements within forelimb movement representations, and consequently did not increase movement representation overlap. Bicuculline treatment was associated with significant enlargement of forelimb movement representation areas under both SD-ICMS and LD-ICMS stimulation protocols relative to saline application ($F_{3,22} = 17.32$, $p < .001;$ Figs. 4-4,4-5a; Table 1). Total forelimb motor map area was increased from 4.4 ± 0.2 mm^2 in saline-treated to 9.5 ± 0.2 mm^2 in bicuculline-treated rats under SD-ICMS and from 5.3 ± 0.4 mm^2 to 10.9 ± 1.0 mm^2 under LD-ICMS (both $p < .05$). Larger movement representations following kindling were proportional under both stimulation protocols as no differences in forelimb map area were observed between LD-ICMS and SD-ICMS groups during either saline

Figure 4-4. Representative forelimb movement representations derived with short-duration and long-duration microstimulation under application of saline vehicle and bicuculline methiodide. Bicuculline significantly ($p < .05$) increased the size of the forelimb motor area under short-duration microstimulation, but did not result in the generation of novel movements. Bicuculline significantly ($p < .05$) increased the size of the forelimb motor area under long-duration microstimulation, and resulted in novel movement twitches of the forelimb that did not persist for the entire stimulation train.

Figure 4-4: Motor map topography

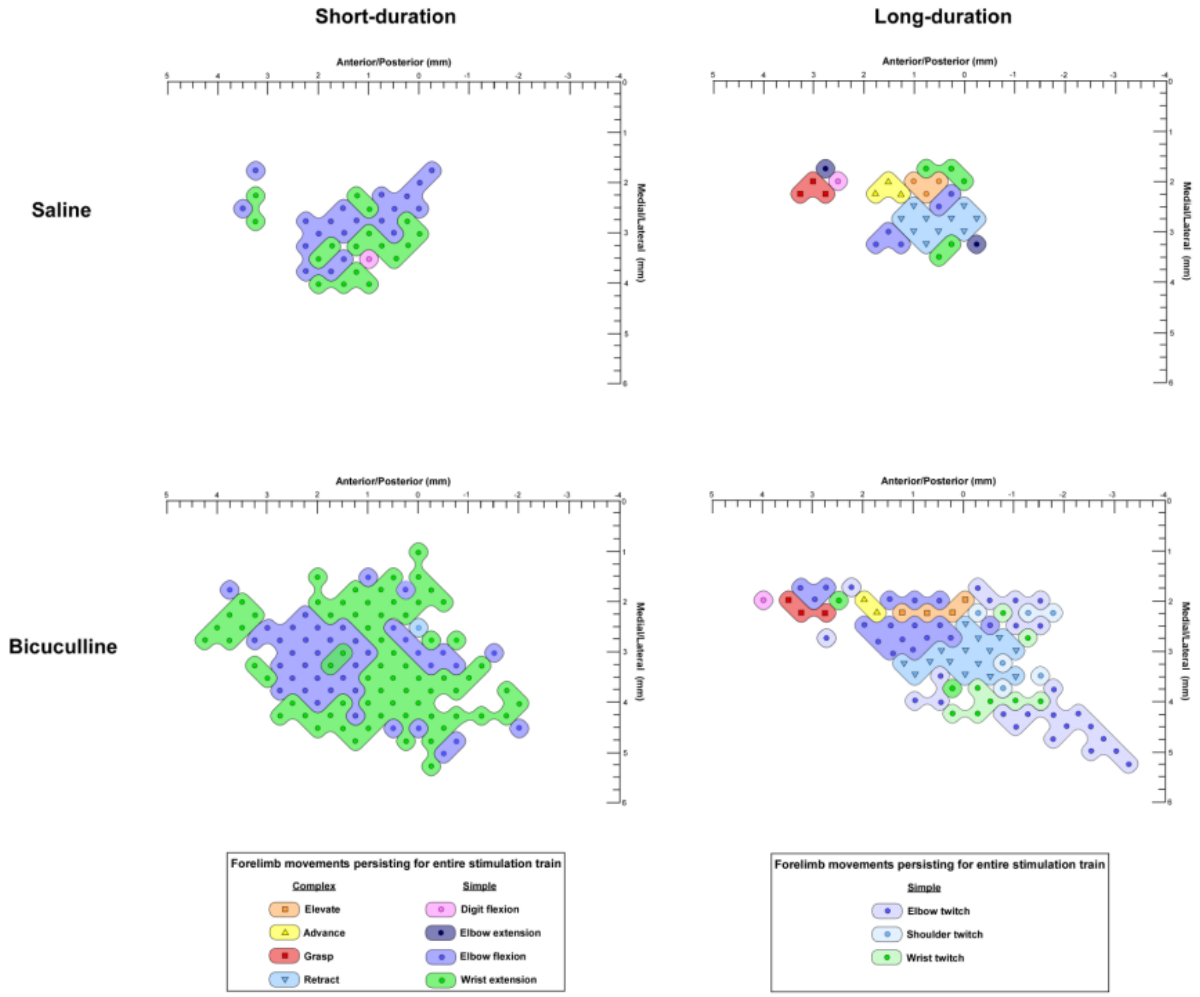

Figure 4-5. Increased forelimb movement representation area following bicuculline administration. (a) Bicuculline significantly increased total forelimb movement representation area under both short-duration and long-duration microstimulation protocols. (b) Increased forelimb movement representation area was not associated with expansion of existing movement representations observed under saline administration. (c) Increased forelimb movement representation area observed with bicuculline administration was specifically attributed ($p < .05$) to the elicitation of novel forelimb twitches.

Figure 4-5: Motor map areas observed under saline and bicuculline

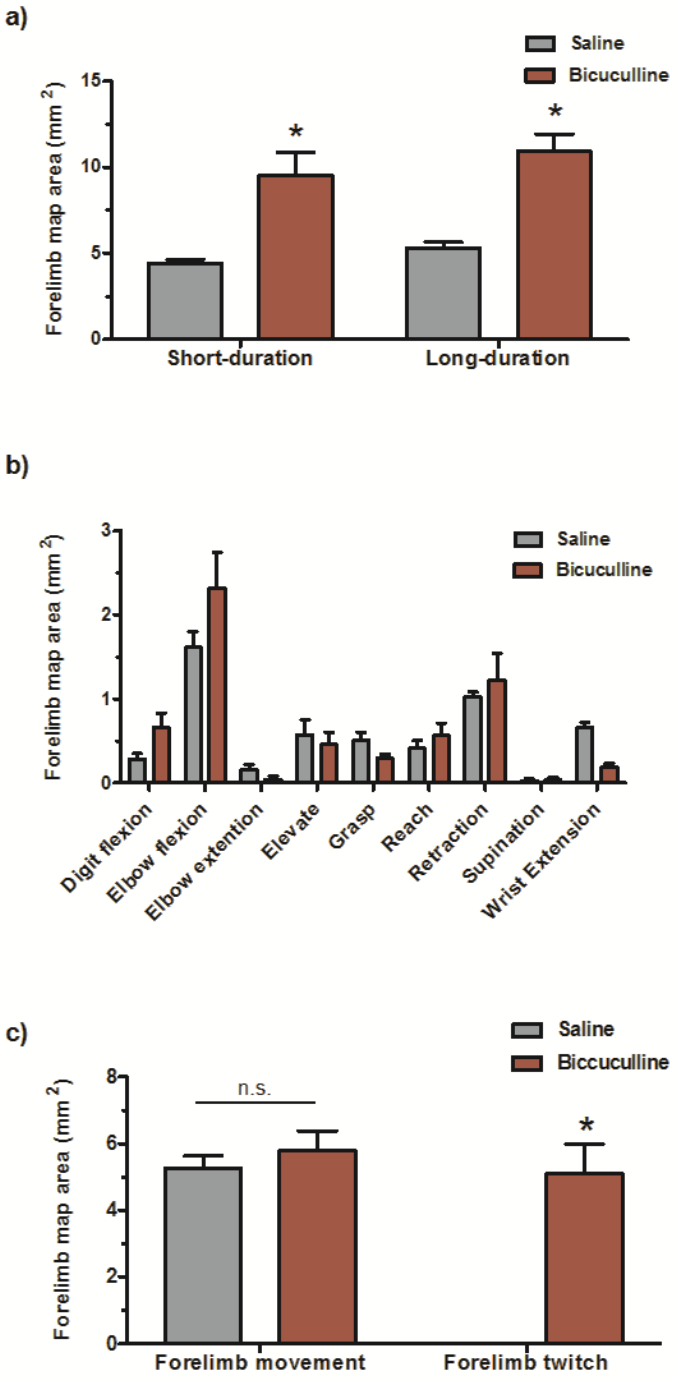

or bicuculline treatment ($p > .05$). Increased movement representation size under both stimulation protocols involved a caudolateral expansion of forelimb-responsive sites into previously reported PFA (Henderson et al., 2001) as well as an anterior fusing the RFA and CFA.

Despite a dramatic increase in total map area derived with LD-ICMS under bicuculline administration, no differences were observed in either the size or location of complex forelimb representations between bicuculline and saline groups (all $p > .05$; Table 1). Enlarged forelimb movement representation area elicited with LD-ICMS under bicuculline administration was instead found to be mediated by the emergence of novel rapid twitches of the elbow, shoulder, and wrist (akin to those observed of SD-ICMS) that can be differentiated from typical LD-ICMS responses in their very short duration (< 50 ms), terminating prior to the end of the stimulation train (500 ms). Increased forelimb movement representation area during bicuculline administration derived with LD-ICMS can be wholly attributed to these forelimb twitches (Fig. 4-5b,4-5c). No differences in the amounts of either ketamine ($t_{14} = 0.2$, $p > 0.05$) or xylazine ($t_{14} = 1.1$, $p > 0.05$) administered for microstimulation procedures, as a function of body weight and duration of surgery, was observed between LD-ICMS groups under saline or bicuculline treatments. Mean amounts of ketamine administered were 1.01 ± 0.037 mg/kg/min for saline-treated and 1.00 ± 0.017 mg/kg/min for bicuculline-treated rats. Mean amounts of xylazine administered were 0.040 ± 0.002 mg/kg/min for saline-treated and 0.044 ± 0.002 mg/kg/min for bicuculline-treated rats. The mean amount of bicuculline administered to LD-ICMS rats was 0.063 ± 0.001 mg/kg/min and did not significantly differ ($t_9 = 0.91$, $p > 0.05$) from that administered to SD-ICMS rats (0.072 ± 0.010 mg/kg/min).

4.5 Discussion

We demonstrate that repeated seizures induced significant increases in overlap between adjacent forelimb movement representations, resulting in the co-elicitation of dual forelimb movements evoked with long-duration intracortical microstimulation (LD-ICMS). Further, we show that increased movement representation overlap cannot be accounted for by reduced cortical inhibition. $GABA_A$ receptor antagonism provided by bicuculline administration was not associated with the elicitation of dual-responsive forelimb movement sites despite significantly a larger forelimb representations compared to saline application

Repeated callosal kindling was associated with significant increases in both afterdischarge durations recorded from sensorimotor neocortex and behavioural seizure stage scores. A dramatic (~ 100 %) kindling-induced increase in total complex forelimb movement representation area was observed exhibited as a merging of rostral (RFA) and caudal (CFA) motor areas in addition to a posterolateral expansion of forelimb responses into previously defined posterior forelimb area (PFA; Henderson et al., 2011). Kindling has previously been shown to result in a persistent enlargement of forelimb movement representations derived with SD-ICMS (Teskey et al., 2002; Henderson et al., 2011) that is related to the spread of epileptiform discharges reaching sensorimotor cortex (van Rooyen et al., 2006) rather than being attributed to a direct effect of the electrical stimulation used to evoke seizures during kindling. We report that the same phenomenon is observed under LD-ICMS and that long-duration microstimulation can be used to provide insight towards the functional reorganization of motor cortex and its relation to concomitant changes in motor behaviour. Deficits in forelimb motor ability (Henry et al., 2008; Flynn et al., 2010) have been reported following kindling; however, it

has been difficult to relate specific behavioural impairment to changes in forelimb movement representations derived with SD-ICMS. Although an increase in the proportional representation of distal to proximal forelimb musculature is observed following kindling (Teskey et al., 2002) and is associated with deficits in skilled reaching performance in rats (Henry et al., 2008). Traditional interpretations on the organization of motor cortex stipulate a somatotopic mapping of body musculature (Penfield and Boldrey, 1937; Woolsey et al., 1952) that is revealed with SD-ICMS (Asanuma and Rosén, 1972) A novel theory proposed by Graziano et al., (2002) suggests an organization of motor cortex based on the encoding of coordinated, multi-joint movements towards specific body postures, clustered separately on the cortex according to movement type, that are revealed when stimulation is performed on a behaviourally relevant time-scale using LD-ICMS. In support of the latter hypothesis, reversible functional lesions of distinct complex movement representations derived under LD-ICMS have been shown to induce specific deficits in related motor performance that are inconsistent with a somatotopic mapping of body musculature (Chapter 3). It has been argued that during volitional movement there is not a uniform, simultaneous activation in all participating muscle groups (Graziano et al., 2009). According to this tip-of-the iceberg hypothesis, threshold stimulation mapping during SD-ICMS results in a the elicitation of simpler movements, across a single joint, being evoked by only allowing the strongest contributing muscle component of the cortically encoded movement to be observed. Increased proximal-to-distal forelimb muscle representation observed with SD-ICMS following repeated seizure activity (Teskey et al., 2002) may then not reflect observed interictal behavioural deficits (Henry et al 2008) as the stimulation paradigm used to derive corticomotor output reveals only the strongest subcomponent of the altered movement representation. Present results suggest that functional reorganization of motor cortex following repeated seizure activity

is related to a blurring between distinct complex movement representations resulting in overlap between otherwise segregate movement areas. In this interpretation, behavioural deficits may result from either a loss of movement selection specificity or conflicting movement selection recruitment within the forelimb motor areas which may underlie the behavioural disturbances following repeated frontal seizures.

The mechanistic underpinnings of motor map expansion and reorganization after seizures has received little attention, but may reflect persistent changes in the balance of cortical excitation mediated by alterations in glutamatergic and GABAergic signaling within layer V horizontal connections. Acute increases in cortical excitatory drive, induced by either disinhibition of recurrent GABAergic feedback onto layer V pyramidal cells with focal cortical application of bicuculline (Jacobs and Donoghue, 1991) or repeated microstimulation (Nudo et al., 1990), results in reversible expansion of motor responsive cortical territory indicating that cortical regions expand when pre-existing lateral excitatory connections are unmasked. Bicuculline administration has also been shown to reveal movement representations at earlier time-points during development than is otherwise observed (Young et al., 2012).Changes in AMPA, NMDA, and GABA receptor signalling, are known to be critical for persistent cortical plasticity (Collingridge et al., 2004) and are altered with kindling (McNamara et al., 1990; Gavrilovici et al, 2006). Structurally, kindling has been shown to increase excitatory perforated synapse density within layer V known to contain high quantities of AMPA and NMDA receptors (Ganeshina et al., 2004). Further, stimulation-induced potentiation of horizontal fibers within layer V sensorimotor cortex has also been demonstrated *in vitro* (Hess and Donoghue, 1994). Increased overlap of movement representation areas, in addition to encroachment of neighbouring craniofacial and hindlimb representations within forelimb motor regions observed

presently likely reflect kindling-induced potentiation of horizontal connections between neighbouring movement representations. Expansion of observed forelimb responsive sites between RFA and CFA and the emergence of a PFA observed under bicuculline administration and following kindling occur outside of known corticospinal projection areas (Wise et al., 1979). The PFA in particular, overlaps with forelimb and hindlimb representation within primary somatosensory cortex (Welker et al., 1971). The brief muscle twitches evoked from these areas under bicuculline suggest an unmasking of latent connectivity to corticofugal projection areas. That these areas were found to evoke complex movements following kindling highlights the capacity for persistent plastic reorganization of cortical circuitry. Although the topographic organization of movement representations is known to be sensitive to depth of ketamine anesthesia (Tandon et al., 2008) and ketamine is a known NMDA receptor antagonist (Harrison and Simmonds, 1985), no significant difference in the amount of ketamine delivered, as a function of mapping duration and body weight, was observed between groups.

A point of note on the finding that increased movement representation overlap observed following kindling is not accounted for by reduced cortical inhibition may be warranted, given the experimental design used in this study. While kindling was performed on the midline callosum, with seizure activity spreading to both sensorimotor cortices, bicuculline was administered soley to the mapped hemisphere. Anatomical and functional links between homotopic cortical areas have been reported (Kartje-Tillotson et al., 1985; Liang et al., 1993; Rouiller et al., 1993). Alterations in movement representations following kindling and under bicuculline administration may then be influenced by contralateral cortex. It has been reported that intrahemispheric input from contralateral cortex can modulate ipsilateral motor responses elicited by stimulation of the other cortex (Brus-Ramer et al., 2009). Increased bilateral

movements following kindling, then, likely reflect persistant changes in both hemispheres and alterations in intrahemispheric processing. Contralateral motor responses to microstimulation of a given hemisphere, however, have shown to be independent of contralateral cortical function (Brus-Ramer et al., 2009). We therefore restricted our investigations to contralateral movements observed under ICMS in order to avoid confounding influence from homotopic neocortex.

In summary, we demonstrate that kindling-induced expansion of forelimb movement representations elicited with LD-ICMS is associated with increased representational overlap between adjacent complex movement representations and that expanded movement representations likely arise from latent horizontal connectivity of motor circuits that can be revealed to their full extent under conditions of cortical disinhibition provided by a GABAergic antagonist. Increased overlap within cortical movement representations may reflect impaired corticomotor movement selection specificity leading to impaired movement coordination and execution associated with in clinical populations with frontal lobe epilepsy.

Chapter Five: General Discussion

The overarching goal of the present thesis was to investigate the functional organization of the motor cortex. Three investigations were conducted in pursuit of this goal, documented in experimental chapters 2-4, sharing a common interest in associating changes in cortical output function with changes in behaviour. I begin this chapter with a brief ordered review of conducted studies. I follow with a contextual discussion on what I take to be the major findings and limitations of this thesis to current understanding on motor cortex organization and function. I end with discussion of what I feel two important future directions and unresolved questions related to the investigation of motor cortex function and organization.

5.1.1 Summary of findings

Chapter 2 assessed whether therapeutic deep brain stimulation of the subthalamic nucleus, restoring forelimb motor deficits resulting from nigrostriatal degeneration in the 6-OHDA model of Parkinson's disease, would be correlated with a stimulation-bound rescue of lesion-induced changes in movement thresholds and forelimb representation areas. Bilateral intrastriatal 6-OHDA lesions are known to increase cortical forelimb movement thresholds and decrease the size of forelimb movement representations (Brown et al., 2009; Viaro et al., 2011). I show this to be the case and infer that acute changes in motor ability can be reflected in an assay of motor cortex output function using SD-ICMS.

Chapter 3 provided a causal test of conflicting predictions arising from the two dominant theories addressing the functional organization of motor cortex. The muscle somatotopy theory stipulates that motor cortex is functionally organized as an ordered representation of somatic

musculature (Asanuma, 1975). The movement theory proposes that motor cortex is grossly organized according to different "action" clusters serving species-typical classes of movement and, within each action cluster, finely ordered as a mapping of that movement within 3-dimenstional space reduced to fit within the constraints of a 2-dimentional cortex (Aflalo and Graziano, 2006). Ramanathan et al. (2006) provided the first report of complex movement representations derived in the rat demonstrating reach-to-grasp behaviour evoked from forelimb sensorimotor cortex under LD-ICMS, and our lab was starting to incorporate LD-CMS techniques at the time. I noted that grasping representations clustered in the RFA and after replicating the results of Ramanathan et al., (2006) devised the experimental design for chapter 3 with my supervisor according to the following logic: 1) under LD-ICMS, grasping behaviour is exclusively localized to the RFA; 2) under SD-ICMS, both the RFA and CFA contain complete forelimb joint representations (digit, wrist, elbow, shoulder); 3) acute deactivation of the RFA would be predicted to induce selective deficits in forelimb grasping ability according to the movement-based theory; 4) acute deactivation of the RFA would be predicted to induce either non-specific forelimb deficits (from inactivation of digit, wrist, elbow, and shoulder representations) or no forelimb deficits (from an intact forelimb representation remaining in the CFA). I then conducted the study with assistance from Dr. Lomber in adapting chronic cryoloop cooling deactivation techniques (Lomber et al., 1999) for use in the rat.

Selective cooling deactivation of the RFA, but not CFA, was found to result in specific deficits in forelimb grasping behaviour providing the first causal evidence supporting a movement-based functional organization of motor cortex. In control experiments (unreported), I also establish that cooling deactivation of the RFA also abolishes evoked forelimb responses to

microstimulation and that there is no reorganization of grasping representation to the CFA during RFA deactivation.

Chapter 4 was an application of LD-ICMS techniques undertaken to investigate the effect of repeated kindled-seizure activity on the functional organization of complex movement representations in forelimb sensorimotor neocortex as assessed by LD-ICMS. Functional neuroplasticity in sensorimotor neocortex following repeated seizure activity has been extensively studied (Teskey et al., 2002; 2005; 2008). Although kindled-seizures have been associated with reductions in movement thresholds and associated forelimb map unmasking elicited by threshold SD-ICMS in addition to forelimb motor deficits (reviewed in Teskey et al., 2008), it remains unclear how the two are related. For example, kindling is associated with an increase in the proportion of distal-to-proximal forelimb representation in addition to deficits in skilled reaching performance; however, skilled motor training in the same task is associated with similar movement representation reorganization and increased behavioural performance (Kleim et al., 1998).

I tested the hypothesis that kindling-induced potentiation of neocortical circuitry would be associated with increased synaptic efficacy between adjacent complex movement representations and would reflected as increased overlap under LD-ICMS. Increased overlap between adjacent forelimb-forelimb representations, in addition to adjacent craniofacial-forelimb representations was observed. In a second experiment I determine that this finding cannot be attributed to reductions in intracortical inhibition previously shown to acutely unmask and reorganize movement representations (Jacobs and Donoghue, 1991).

5.1.2 Major findings and limitations

5.1.2.1 Evidence for a movement-based functional organization of motor cortex

I feel that chapter 3 forms the core of this thesis. In chapter 3 I provide the first causal evidence in support of a movement-based functional organization of motor cortex in addition to an ancillary finding supporting a functional dissociation between RFA and CFA motor areas. Although there have been many microstimulation studies investigating a movement based organization for motor cortex (Graziano et al., 2002;2005; Haiss and Schwarz, 2005; Stepniewska et al., 2009; Harrison et al., 2002; Bonazzi et al., 2013), they have been primarily descriptive and correlational in nature.. Ramanathan et al. (2006) report that electrolytic lesions of retraction representations within the CFA of the rat is associated with deficits in skilled pellet reaching end-point success. Following rehabilitative training, a significant correlation between improved reaching success and the magnitude of retraction representation re-emergence was observed. This study provides excellent demonstration of specific motor cortical plasticity associated with recovery of function after brain injury. An important finding from the study reveals that complex movement representations do demonstrate activity-dependent plasticity following injury. Of interest, it is noted that behavioural training alone was not associated with reorganization of forelimb complex movement representations, a finding that I replicate in this thesis. I did observe significant overlap of craniofacial representation within forelimb representations; however, the authors do not report whether a similar result was observed.

A novel functional dissociation was also revealed between RFA and CFA in forelimb grasping and advance movements, respectively. The RFA has been suggested to be an equivalent of the primate premotor or supplementary motor (MII) region, with CFA being considered

primary motor cortex (MI) based on connectional properties (Rouiller et al., 1993). A hierarchical view of cortical motor control is not too meaningful in a movement-based interpretation of motor cortex organization where different motor regions serve distinct function roles in movement generation. I have explicitly avoided reference to motor hierarchy throughout this thesis to avoid ambiguity. None the less, both RFA and CFA are known to contain direct corticospinal projections to the cervical spinal enlargement (Wise et al., 1979). Circumscribed lesions of the CFA and RFA are known to induce contralateral somatosensory deficits in the bilateral-stimulation task with RFA lesions resulting in a more severe and enduring deficit (Barth et al., 1990). This may be attributed to cytoarchitecture differences in somatosensory overlap with RFA residing in agranular Agl and CFA exhibiting a mixed representation within agranular AgL and dysgranular SI (Donoghue and Wise, 1982).

I decided to use a reversible lesion deactivation technique to infer the functional roles of descrete cortical regions by assessing a loss of function during deactivation. An alternate approach would be to stimulate the cortex in the awake, behaving state in order to induce movement. It has recently been reported that electrical stimulation-evoked cortical firing, however, does not sum with natural activity, but rather blockes and replaces electromyographic activity recorded during a reaching task (Griffin et al., 2011). This phenomenon has been termed 'neural hijacking' (Griffin et al., 2011) and has been suggested to occur via two mechanisms (Cheney et al., 2013). The first is that electrical stimulation elicits indiscriminate orthodromic and antidromic activation of axons (Ranck, 1975). While orthodromic activation could be expected to sum with ongoing naturalistic activity, antidromic activation has the potential to block naturalistic afferent activity through collision of action potentials. A second mechanism for neural hijacking proposes that unnatural activation of GABAergic inhibitory interneurons evoked

with electrical stimulation, leading to inhibitory post-synaptic potentials in target projections, would reduce the potential for non-stimulus spike activity (Cheney et al., 2013). Due to neural hijacking, use of electrical stimulation to evoke movement in the awake, behaving state would be problematic at best to probe the functional organization of motor cortex. Neural hijacking does have its strenghts, however, and is used with great therapeutic effect in treating motor deficits in Parkinson's disease (Chapter 2). In that particular circumstance, blockade and hijacking of pathological natural activity resulting from nigrostriatal degeneration to disinhibit motor cortex is a desirable outcome.

A point of note for chapter 3 is that cooling deactivation would be expected to provide a synaptic rather than conduction block (Bénita and Condé H, 1972) of neural activity. Although activity in fibers of passage would be spared, ICMS has resulted in distal fiber activation millimetres from the electrode even at low stimulation intensities (Histed et al., 2009). However, there are known CFA projections coursing through RFA (Rouiller et al., 1993) and the use of a technique for a synaptic rather than conduction block is fully justified. I did use local infusions of tetrodotoxin to achieve complete block of neural activity in pilot work resulting in more severe behaviour impairment, in addition to muscimol to achieve a pharmacological synaptic block (both unreported). During repeated behavioural testing required for the experiment, however, I found a tapering of the drug effect on behaviour that could indicate either the development of drug resistance, a build-up of non-reversible after-effects or tissue damage from the repeated infusions. Cortical cooling deactivation provided an effective, quick, repeatable, and well-tolerated method for a reversible function lesion. Limitations of chapter 3 would be the lack of a more comprehensive test battery for expected CFA sensitive deficits of forelimb advance, reach, and retraction and a focus on a unilateral deactivation, between groups design.

Cortical cooling deactivation did not result in severe behavioural impairment, particularly with the CFA implanted rats. The interpretation of negative results presents a challenge by suggesting that either the treatment was without effect, the measures used were not a valid assessment of the hypothesis, or that the sample size or treatment effect magnitude lacked appriopriate statistical power to find an effect. In chapter 3, separate cooling deactivation of the RFA and CFA was used to dissociate the functional contribution of these two areas in skilled forelimb motor ability. The vermicelli handling test was used to assess specific distal forelimb grasping deficits and was predicted to show selective impairment in RFA-cooled, but not CFA-cooled rats. Negative results in CFA-cooled rats in this test indicate that the deficits observed in RFA-cooled rats are specific to deactivation of the RFA rather than forelimb motor cortex in general. In the single pellet reaching task both CFA- and RFA-cooled rats showed significant deficits in reaching endpoint success and the number of reaching attempts made. In a qualitative assessment of reaching subcomponent error scores, it was found that RFA-cooled rats were specifically impaired in keeping the digits semi-flexed and grasping while CFA-cooled rats did not show any differences in performance under cooling relative to baseline. I would argue that negative results in this case, given significant impairment in endpoint performance in both groups, may be a result of how the testing was conducted. Movement subcomponent error scores were pooled for five successful reach trials. Deficits in CFA-cooled rats, with deactivation of elevate, advance and retract representations, may have been so severe that they resulted in predominantly unsuccessful trials. In cases of successful trials, correct pellet retrieval requires minimal error rates in movement subcomponents. Collective inhibition of multiple complex movement representations would be expected to increase the proportion of unsuccessful reach attempts. As a result, my sample of successful trials for the qualitative assessment may not

reflect the true extent of the behavioural deficit that is demonstrated in end-point success measures. Aternatively, a trend ($.05 < p < .06$) for specific deficits in elbow-to-midline and advance observed CFA-cooled rats may indicate insufficient statistical power with the present sample size used. Although the sunflower seed test has been shown sensitive to large sensorimotor cortex damage following stroke (Kleim et al., 2007), present results suggest that this test may not be sensitive to subtle effects from focal synaptic block. An alternative explanation for negative results were presented in chapter 3 suggesting that movement representations derived via ICMS may slightly under-represent underlying somatic activation as ICMS has been shown to elicit neuronal activation millimetres away from the stimulation site, even at low (< 10 μA) intensities (Histed et al., 2009). As the cortical deactivation area used in this experiment was selected to silence the much smaller RFA, it is plausible that an incomplete inactivation of the CFA was achieved in some rats.

5.1.2.2 Threshold microstimulation remains a valuable tool to assess corticospinal activity

SD-ICMS was initially developed to provide an electrophysiological tract tracing of corticofugal projections and it excels at providing a direct assessment of corticospinal excitability. Indeed, the assessment in frontal output function in chapter 2 would not have been possible with the suprathreshold, long-duration stimulation trains of LD-ICMS.

5.1.2.3 Evoked responses with LD-ICMS are not likely a result of excessive current spread

There has been resistance and controversy over the use of LD-ICMS focusing on the long-duration stimulation trains causing damage, being un-physiological, and inducing excessive

current spread which results in widespread recruitment of muscle activation. Concerns of tissue damage are negated with the use of biphasic current (Tehovnik, 1996), and the use of long-duration stimulation trains do closely match naturalistic activity patterns in motor cortex neurons recording during behaviour (Georgeopoulos et al., 1982; Graziano et al., 2009). Concerns over excessive current spread have been raised since the time of Ferrier in which his use of longer duration alternating current trains was criticized as leading to current spread reaching the striatum and eliciting extra-pyramidal motor responses (Gross, 2007). SD-ICMS was developed precisely to avoid excessive current spread which was thought to lead to the 'artifacts' of overlapping movement representations elicited with surface stimulation that are now known to result from intrinsic cortico-motorneuron projection anatomy (Cheney and Fetz, 1985; Jankowska et al., 1975). Further, direct current spread from the electric field around the electrode tip has been grossly exaggerated and passive current spread, resulting in transsynaptic activation, occurs much more commonly than previously thought - even at low (< 10 μA) threshold intensities used in SD-ICMS (Histed et al., 2009). I present three further pieces of evidence that observed LD-ICMS responses are not due to excessive or indiscriminate current spread. 1) Evoked responses were stable under repeated stimulation over time. 2) In chapter 3, SD-ICMS and LD-ICMS movement representations were found to be evoked from the same cortical territory and no differences were observed between the sizes of each representation. 3) In chapter 4, bicuculline administration resulted in equivalent unmasking in movement representation sizes and identical responses were evoked with both stimulation protocols in the newly unmasked PFA.

5.1.3 Future directions

5.1.3.1 Engram for motor learning?

An intriguing finding by Ramanathan et al., (2006) and replicated presently in chapter 3 was that skilled motor learning in the single pellet reaching test was not associated with plastic reorganization of complex movement representations. Under SD-ICMS an increase in the proportion of proximal-to-distal movement representations is observed following training in this task and is thought to reflect a neural encoding of the motor memory trace (Kleim et al., 1998). How then or where is learning reflected? The capacity for a plastic reorganization of complex movement representations has been establish following recovery of function after injury (Ramanathan et al., 2006), yet is not seen in uninjured rats that demonstrate motor learning.

5.1.3.2 Connectional properties of complex movement representations

In the mouse, segregate corticofugal projections are observed between complex movement representations through the level of the internal capsule (Harrison et al., 2012), suggesting an anatomical basis for a movement-based organization of motor cortex. Although extrinsic connectional properties of rat forelimb motor regions are known (Rouiller et al., 1993), LD-ICMS indicates functional specificity of complex movement representations within forelimb motor regions that are likely supported by distinct connectivity patterns. Knowledge of the underlying anatomy serving complex movement representations will greatly aid behavioural and electrophysiological approaches towards a deeper understanding on the functional organization of motor cortex.

References

Abedi PM, Delaville C, De Deurwaerdère P, Benjelloun W, Benazzouz A (2013). Intrapallidal administration of 6-hydroxydopamine mimics in large part the electrophysiological and behavioral consequences of major dopamine depletion in the rat. Neuroscience 236:289-297.

Adkins DL, Boychuk J, Remple MS, Kleim JA (2006). Motor training induces experience-specific patterns of plasticity across motor cortex and spinal cord. J Appl Physiol 101: 1776-1782.

Aflalo TN, Graziano MS (2006). Possible origins of the complex topographical organization of motor cortex: reduction of a multidimensional space onto a two-dimensional array. J Neurosci 26: 6288-6297.

Aggleton JP, Passingham RE (1981). Syndrome produced by lesions of the amygdala in monkeys (Macaca mulatta). J Comp Physiol Psychol 95*:* 961–977.

Alaverdashvili M, Foroud M, Lim DH, Whishaw IQ (2008). "Learned baduse" limits recovery of skilled reaching for food after forelimb motor cortex stroke in rats: A new analysis of the effect of gestures on success. Behav Brain Res 188: 281-290.

Alexander GE, Crutcher MD, DeLong MR (1990). Basal ganglia-thalamocortical circuits: parallel substrates for motor, occulomotor, "prefrontal" and "limbic" functions. Prog Brain Res 85: 119-146..

Allred RP, Adkins DL, Woodlee MT, Husbands LC, Maldonado MA, Kane JR, Schallert T, Jones TA (2008). The vermicelli handling test: a simple quantitative measure of dexterous forelimb function in rats. J Neurosci Methods 170: 229-244.

Alstermark B, Isa Tadashi (2012). Circuits for skilled reaching and grasping. Annu Rev Neurosci 35: 559-578.

Andersen P, Hagan PJ, Phillips CG, Powell TPS (1975). Mapping by microstimulation of overlapping projections from area 4 to motor units of the baboon's hand. Proc Roy Soc B 188: 31-60.

Anderson T, Hu B, Iremonger K, Kiss ZH (2006). Selective attenuation of afferent synaptic transmission as a mechanism of thalamic deep brain stimulation-induced tremor arrest. J Neurosc. 26: 841-850.

Antunes FM, Malmiera MS (2011). Effect of auditory cortex deactivation on stimulus-specific adaptation in the medial geniculate body. J Neurosci 23: 17306-17316.

Armand J (1982). The origin, course and termination of corticospinal fibers in various mammals. Prog. Brain Res 57: 329-360.

Asanuma H, Arnold AP (1975). Noxious effects of excessive currents used for intracortical microstimulation. Brain Research 96: 103-107.

Asanuma H, Rosén I (1972). Topographical organization of cortical efferent zones projecting to distal forelimb muscles in the monkey. Exp Brain Res 14: 243-256.

Asanuma H, Sakata H. (1967) Functional organization of a cortical efferent system examined with focal depth stimulation in cats. J Neurophys 30: 35-54.

Asanuma H, Ward JE (1971). Patterns of contraction of distal forelimb muscles produced by intracortical stimulation in cats. Brain Res 27: 97-109.

Ashby P, Paradiso G, Saint-Cyr JA, Chen R, Lang AE, Lozano AM (2001). Potentials recorded at the scalp by stimulation near human subthalamic nucleus. Clin Neurophys 112: 431-437.

Barth TM, Jones TA, Schallert T (1990). Functional subdivisions of the rat somatic sensorimotor cortex.

Beck CH, Chambers WW (1970). Speed accuracy, and strength of forelimb movement after unilateral pramidotomy in rhesus monkeys. J Comp Physiol Psychol 70: 1-22.

Beevor CE, Horsley V (1887). A minute analysis (experimental) of the various movements produced by stimulating in the monkey different regions of the cortical centre for the upper limb, as defined by Professor Ferrier. Phil Trans Roy SocB: Biological Sciences 178: 153-167.

Beevor CE, Horsley V (1890). An experimental investigation into the arrangement of the excitable fibres of the internal capsule of the bonnet monkey (Macacus sinicus). Phil Trans Roy Soc B: Biological Sciences. 181: 49-88.

Ben V, Blin O, Brugeurolle B (1999). Time-dependent striatal dopamine depletion after injection of 6-hydroxydopamine in the rat. Comparison of single bilateral and double bilateral lesions. J Pharmacol 51: 1405-1408.

Bénita M, Condé H (1972). Effects of local cooling upon conduction and synaptic transmission. Brain Res 36: 133-151.

Beurrier C, Biolac B, Audin J, Hammond C (2001). High-frequency stimulation procludes a transient blockade of voltage-gated currents in subthalamic neurons. J Neurophysiol 85: 1351-1356.

Bland BH, Vanderwolf CH (1972). Diencephalic and hippocampal mechanisms of motor activity in the rat: effects of posterior hypothalamic stimulation on behavior and hippocampal slow wave activity. Brain Res 43: 67–88.

Blanton S, Wilsey H, Wolf SL (2008). Constraint-induced movement therapy in stroke reahabilitation: perspectives on future clinical applications. NeuroRehabilitation 23: 15-28.

Bloom FE, Algeri S, Groppetti A, Revuelta A, Costa E (1969). Lesions of central norepinephrine terminals with 6-OH-dopamine: biochemistry and fine structure. Science 166: 1284-1286.

Bonazzi L, Viaro R, Lodi E, Canto R, Bonifazzi C, Franchi G (2013). Complex movement topography and extrinsic space representation in the rat forelimb motor cortex as defined by long-duration intracortical microstimulation. J Neurosci 35: 2097-2107.

Boychuk JA, Adkins DL, Kleim JA (2011). Distributed versus focal cortical stimulation to enhance motor function and motor map plasticity in a rodent model of ischemia. Neurorehab. Neural Repair 25: 88-97.

Braak, H (1984). Architectonics as seen by lipofuscin stains. In: Cerebral Cortex - The Cellular Components of the Cerebral Cortex, Jones E. G., Peters A. (eds) New York, Plenum Press, pp. 59–104.

Branco DM, Coelho TM, Branco BM, Schmidt L, Calcagnotto ME, Portuguez M, Neto EP, Paglioli E, Palmini A, Lima JV, Da Costa JC (2003). Functional variability of the human cortical motor map: Electrical stimulation findings in perirolandic epilepsy surgery. Journal of Clinical Neurophysiology 20: 17-25.

Brown AR, Antle MC, HU B, Teskey GC (2011). High frequency stimulation of the subthalamic nucleus acutely rescues motor deficits and neocortical movement representations following 6-hydroxydopamine administration in rats. Exp Neurol 231: 82-90.

Brown AR, Hu B, Antle MC, Teskey, GC (2009). Neocortical movement representations are reduced and reorganized following bilateral intrastriatal 6-hydroxydopamine infusion and dopamine type-2 receptor antagonism. Exp Neurol 220: 162-170.

Brown P, Eusebio A (2008). Paradoxes of functional neurosurgery: clues from basal ganglia recordings. Mov Disord 23: 12-20.

Brus-Ramer M, Carmel JB, Martin JH (2009). Motor cortex bilateral motor representation depends on subcortical and interhemispheric interactions. J Neurosci 29: 6196-6206.

Buhmann C, Glauche V, Sturenburg HJ, Oechsner M, Weiller C, Buchel C (2003). Pharmacologically modulated fMRI cortical responsiveness to levodopa in drug-naive hemiparkinsonian patients. Brain 126: 451–461.

Campeau S, Davis M 1990. Reversible neural inactivation by cooling in anesthetized and freely behaving rats. J Neurosci Methods 32:25-35.

Canedo A (1997). Primary motor cortex influences on the descending and ascending systems. Prog Neurobiol 51: 287-335.

Carman LS, Gage FH, Shults CW (1991). Partial lesion of the substantia nigra: relation between extent of lesion and rotational behavior. Brain Res 553:275-283.

Castro-Alamancos MA, Borrel J (1995). Functional recovery of forelimb response capacity after forelimb primary motor cortex damage in the rat is due to the reorganization of adjacent areas of cortex. Neurosci 68: 793-805.

Castro-Alamancos MA, Donoghue JP, Connors BW. (1995). Different forms of synaptic plasticity in somatosensory and motor areas of the neocortex. J Neurosci 15: 5324-5333.

Ceballos-Baumann AO, Boecker H, Bartenstein P, von Falkenhayn I, Riescher H, Conrad B, Moringlane JP, Alexch, F (1999). A positron emission tomographic study of subthalamic nucleus stimulation in Parkinson disease. Enhanced movement-related activity of motor-association cortex and decreased motor cortex resting activity. Arch Neurol 56: 997-1003.

Cenci MA, Whishaw IQ, Schallert T (2002). Animal models of neurological deficits: how relevant is the rat? Nat Rev Neurosci 3:574-579.

Cheney PD, Fetz EE (1980). Functional classes of primate corticomotoneuronal cells and their relation to active force. J. Neurophysiol, 4: 773-791.

Cheney PD, Fetz EE (1985). Comparable patterns of muscle facilitation evoked by individual corticomotoneural (CM) cells and by single intracortical microstimuli in primates: evidence for functional groups of CM cells. J Neurophysiol 53: 786-804.

Cheney PD, Griffin DM, Van Acker GM 3rd (2013). Action of high-frequency electrical stimulation on cortical circuits. Neuroscientist 19: 434-441.

Choi-Lundberg DL, Lin Q, Schallert T, Crippens D, Davidson BL, Chang YN, Chiang YL, Qian J, Bardwaj L, Bohn MC (1998). Behavioral and cellular protection of rat dopamingergic neurons by an adenoviral vector encoding glial cell line-derived neurotrophic factor. Exp Neurol 154: 261-275.

Chomiak T, Hu B (2007). Axonal and somatic filtering of antidromically evoked cortical excitation by simulated deep brain stimulation in rat brain. J Physiol 579: 403-412.

Cohen G, Werner P (1994). Free radicals, oxidative stress, and neurodegeneration. In: Neurodegenerative diseases (Ed. Calne DB). Philadelphia, Saunders, pp. 139-161.

Colebatch JG, Gandevia SC (1989). The distribution of muscular weakness in upper motor neuron lesions affecting man. Brain 112: 749-763.

Collingridge G*,* Isaac JT, Wang YT *(*2004*).* Receptor trafficking and synaptic plasticity. Nat. Rev. Neurosci *5:* 952–962.

Conner JM, Culberson A, Packowski C, Chiba AA, Tuszynksi MH. (2003). Lesions of the basal forebrain cholinergic system impair task acquisition and abolish cortical plasticity associated with motor skill learning. Neuron 38: 819-829.

Coomber B, Edwards D, Jones SJ, Shackleton TM, Goldschmidt J, Wallace, MN, Palmer AR (2011). Cortical inactivation by cooling in small animals. Front Syst Neurosci 5: 53 (eCollection).

Dejean C, Hyland B, Arbuthnott G (2009). Cortical effects of subthalamic stimulation correlate with behavioural recovery from dopamine antagonist induced akinesia. Cereb Cortex 19: 1055-1.

DeLong MR, Wichmann T (1993). Basal ganglia-thalamocortical circuits in Parkinsonian signs. Clin Neurosci 1: 18-26.

Denenberg VH (1969). Open-field behavior in the rat: What does it mean? Ann of New York Acad Sci 159:852-859.

Deumens R, Blokland A, Prickaerts J (2002). Modeling Parkinson's disease in Rats: An Evaluation of 6-OHDA Lesions of the Nigrostriatal Pathway. Exp Neurol 175: 303-317.

Deuschl G, Schade-Brittinger C, Krack P, Volkmann J, Schäfer H, Bötzel K, Daniels C, Deutschländer A, Dillmann U, Eisner W, et al. (2006). A randomized trial of deep-brain stimulation for Parkinson's disease. N Eng J Med 355: 896-908.

Dombeck DA, Graziano MS, Tank DW (2009). Functional clustering of neurons in motor cortex determined by cellular resolution imaging in awake behaving mice. J Neurosci 29: 13751-13760.

Donoghue JP, Leibovic S, Sanes JN (1992). Organization of the forelimb area in squirrel monkey motor cortex: representation of digit, wrist, and elbow muscles. Exp Brain Res 89: 1-19.

Donoghue JP, Wise SP (1982). The motor cortex of the rat: cytoarchitecture and microstimulation mapping. J Comp Neurol 212: 76-88.

Dostrovsky JO, Lozano AM (2002). Mechanisms of deep brain stimulation. Mov Disord 17(S3): S63-S68.

Douglas RJ, Martin KAC (1990). Neocortex. In: The Synaptic Organization of the Brain. Sheperd GM (ed). New York: Oxford University Press. pp. 389-438.

Dum RP, Strick PL (2005). Frontal lobe inputs to the digit representations of the motor areas on the lateral surface of the hemisphere. J. Neurosci., 25: 1375-1386.

DvoráK K, Freit J (1977). Migration of neuroblasts through partial necrosis of the cerebral cortex in newborn rats: contribution to the problem of morphological development and developmental period of cerebral microgyria. Acta Neuropathol 38:203-212.

Evarts EV (1986). Relation of pyramidal tract activity to force exerted during voluntary movement. J Neurophysiol 31: 14-27.

Ferrier D (1874). Experiments on the brain of monkeys – No. 1. Pric R Soc Lond 409-430.

Fetz EE, Cheney PD, Mewes K, Palmer S (1989). Control of forelimb muscle activity by populations of corticomotoneuronal and rubromotoneuronal cells. Prog Brain Res 80: 437–49.

Flynn C, Young NA, Teskey GC (2010). Seizures, but not lowered seizure thresholds, results in larger neocortical motor maps and concomitant disruptions in skilled motor behaviour. Behav Brain Res 214: 60-65.

Freund P, Wannier T, Schmidlin E, Bloch J, Mir A, Schwab ME, Rouiller EM (2006). Nogo-A-specific antibody treatment enhances sprouting and functional recover after cervical lesion in adult primates. Nat Med 12: 790-792.

Friel KM, Heddings AA, Nudo RJ (2000). Effects of postlesion experience on behavioural recovery and neurophysiologic reorganization after cortical injury in primates. Neurorehabil Neural Repair 14: 187-198.

Fritsche G, Hitzig E (1870). Electric excitability of the excitability of the cerebrum (Uber die elektrische Erregbarkeit des Grosshirns). Epilepsy Behav 15: 123-130.

Frost SB, Barbay S, Friel KM, Plautz EJ, Nudo RJ. (2003). Reorganization of remote cortical regions after ischemic brain injury: a potential substrate for stroke recovery. J Neurophysiol 89: 3205-14.

Fuster JM, Alexander GE (1970). Delayed response deficit by cryogenic depression of frontal cortex. Brain Res 81:393-400.

Ganeshina O, Berry RW, Petralia RS, Nicholson DA, Geinisman Y (2004). Differences in the expression of AMPA and NMDA receptors between axospinous perforated and nonperforated synapses are related to the configuration and size of postsynaptic densities. J Comp Neurol, 468:86–95.

Gavrilovici C, D'Alfonso S, Dann M, Poulter MO (2006). Kindling-induced alterations in GABAA receptor-mediated inhibition and neurosteroid activity in the rat piriform cortex. Eur J Neurosci 24: 1373–1384.

Georgopoulos A, Kalaska J, Caminiti R, Masssey J (1982). On the relations between the direction of two-dimentional arm movements and cell discharge in primate motor cortex. J Neurosci 2:1527-1537.

Georgopoulos AP (1988). Spatial coding of visually guided arm movements in primate motor cortex. Can J Physiol Pharmacol 66**:** 518-526**.**

Gharbawie OA, Stepniewska I, Kaas JS (2011). Cortical connections of functional zones in posterior parietal cortex and frontal cortex motor regions in new world monkeys. Cereb Cortex 21: 1981–2002.

Gharbawie OA, Stepniewska I, Qi H, Kaas JK (2011). Multiple parietal-frontal pathways mediate grasping in macaque monkeys. J Neurosci 31: 11660-11677.

Gonzalez C, Kolb B (2003). A comparison of different models of stroke on behaviour and brain morphology. Eur J Neurosci 18:1950–1962.

Gradinaru V, Mogri M, Thompson KR, Henderson JM, Deisseroth K (2009). Optical deconstruction of parkinsonian neural circuitry. Science 324: 354-359.

Graziano MS (2009). The intelligent movement machine: An ethological perspective on the primate motor system. Oxford University Press: New York.

Graziano MS, Aflalo TN (2007). Mapping behavioral repertoire onto the cortex. Neuron 56: 239-251.

Graziano MS, Taylor CS, Moore T (2002). Complex movements evoked by microstimulation of precentral cortex. Neuron 34:841-851.

Graziano MS, Taylor CS, Moore T, Cooke DF (2002). the cortical control of movement revisited. Neuron 36: 349-362.

Graziano MSA, Aflalo TNS, Cooke DF (2005). Arm movements evoked by electrical stimulation in the motor cortex of monkeys. J Neurophysiol 94: 4209-4223.

Griffin DM, Hudson HM, Belhaj-Saif A, Cheney PD (2011) Hijacking cortical motor output with repetitive microstimulation. J Neurosci 31:13088-13096.

Gross CG (2007). The discovery of the motor cortex and its background. Journal of the History of the Neurosciences 16: 320-331.

Hagiwara S, Byerly L (1981). Calcium channel. Ann Rev Neurosci 4:69-125.

Haiss F, Schwarz C (2005). Spatial segregation of different modes of movement control in the whisker representation of rat primary motor cortex. J Neurosci 25: 1597-1587.

Hall CS (1934). Emotional behavior in the rat: defecation and urination as measures of individual differences in emotionality. J Comp Psych 18:385-403

Harrison NL, Simmonds MA (1985). Quantitative studies on some antagonists of N-methyl D-aspartate in slices of rat cerebral cortex. Br J Pharmacol 84: 381–391.

Harrison TC, Ayling OGS, Murphy TH (2012). Distinct cortical circuit mechanisms for complex forelimb movement and motor map topography. Neuron 74: 397-409.

Harrison TC, Murphy TH (2013). Towards a circuit mechanism for movement tuning in motor cortex. Front Neural Circuits 6: 127.

Haslinger B, Erhard P, Kampfe N, Boecker H, Rummeny E, Schwaiger M, et al. (2001). Event-related functional magnetic resonance imaging in Parkinson's disease before and after levodopa. Brain 124: 558-570.

Heffner R, Masterton RB (1975). Variation in form of the pyramidal tract and its relationship to digital dexterity. Brarin Behav Evol 23: 165-183.

Helmstaedter C, Kemper B, Elger CE (1996). Neuropsychological aspects of frontal lobe epilepsy. Neuropsychologia 34: 339-406.

Henderson AK, Galic MA, Fouad K, Dyck RH, Pittman QJ, Teskey GC (2011). Larger cortical motor maps after seizures. Eur J Neurosci 34: 615-621.

Henry L C, Goertzen C D, Lee A, Teskey GC (2008). Repeated seizures lead to altered skill

Hepp-Reymond MC, Wiesendanger M (1972). Unilateral pyramidotomy in monkeys: effects of force and speed of a conditioned precision grip. Brain 36: 117-31.

Hernandez MT, Sauerwein HC, Jambaque I, De Guise E, Lussier F, Lortie A, Dulac O, Lassonde M (2002). Deficits in executive functions and motor coordination in children with frontal lobe epilepsy. Neuropsychologia 40: 384-400.

Hess G (2004). Synaptic plasticity of local connections in rat motor cortex. Acta Neurobiol Exp (Wars) 64: 271-6.

Hess G, Donoghue JP (1994). Long-term potentiation of horizontal connections provides a mechanism to reorganize cortical motor maps. J Neurophysiol 71:2543-2547.

Hicks SP, D'Amato CJ (1970). Motor-sensory and visual behavior after hemispherectomy in newborn and mature rats. Exp Neurol 29: 416-438.

Hikosaka O, Wurtz RH (1985). Modification of saccadic eye movements by GABA-related substances: I. Effects of muscimol and bicuculine in monkey superior colliculus. J Neurophysiol 53: 266-291

Hiraba H, Sato T (2005). Cortical control of mastication in cats. 2. Deficits of masticatory movements following lesion in the motor cortex.Somatosens Mot Res 22:183-192.

Histed MH, Bonin V, Reid RC (2009). Direct activation of sparse, distributed populations of cortical neurons by electrical microstimulation. Neuron 63: 508-522.

Horel JA (1984). Cold lesions in inferotemperal cortex produce reversible deficits in learning and retention of visual discriminations. Physiol Psychol 12:259-270.

Horel JA (1991). Use of coldto reversibly suppress local brain function in behaving animals. In: Methods in Neurosciences: Lesions and Transplantation (Vol. 7, Ed. Conn PM). New York, Academic Press, pp. 97-110.

Horsley V, Clark RH (1908). The structure and functions of the cerebellum examined by a new method. Brain 31:45-124.

Hubsch C, Roze E, Popa T, Russo M, Balachandran A, Pradeep S, et al. (2013). Defective cerebellar control of cortical plasticity in writer's cramp. Brain 136: 2050-2062.

Isa T, Ohki Y, Alstermark B, Pettersson L, Sasaki S (2007). Direct and indirect cortico-motoneuronal pathways and control of hand/arm movements. Physiology 22:145-153

Ivinskis A (1968). The reliability of behavioural measures obtained in the open-field. Aus J Psych 20:173-177.

Iwaniuk AN, Whishaw IQ (2000). On the origin of skilled forelimb movments. Trends Neurosci 23: 372-376.

Jacobs KM, Donoghue JP (1991). Reshaping the cortical motor map by unmasking latent intracortical connections. Science 251: 944-946

Jankowska E, Padel Y, Tanaka R (1975). Projections of pyramidal tract cells to alpha-motoneurons innervating hind-limb muscles in the monkey. J Physiol 249: 637-667.

Jeannerod M (1981). Intersegmental coordination during reaching at natural visual objects. In: Long J, Badeley A (eds) Attention and performance IX. Lawrence Erlbaum Associates, Hillsdale, pp 153–169.

Jenkins IH, Fernandez W, Playford ED, Lees AJ, Frackowiak RS, Passingham RE, Brooks DJ (1992). Impaired activation of the supplementary motor areas in Parkinson's disease is reversed when akinesia is treated with apomorphine. Ann Neurol 32: 749–757.

Joosten EA, Bär DP (1999). Axon guidance of outgrowing corticospinal fibres in the rat. J Anat 194:15-32.

Kaas JH (1997). Topographic maps are fundamental to sensory processing. Brain Res Bull 44: 107-112.

Kaas JH, Gharbawie OA, Stepniewska I (2011). The organization and evolution of dorsal stream multisensory motor pathways in primates. Front Neuroanat 5: 1–7.

Kakei S, Hoffman DS, Strick PL (1999). Muscle and movement representations in the primary motor cortex. Science 285: 2136-2139.

Kargo WJ, Nitz DA (2003). Early skill learning is expressed through selection and tuning of cortically represented muscle synergies. J Neurosci 23: 11255-11269.

Karl JM, Whishaw IQ (2013). Different evolutionary origins for the Reach and Grasp: A potential explanation for dual sensorimotor channels in primate parietofrontal cortex. Neurosci Abstrs 43: 162.12.

Kartje-Tillotson G, Neafsey EJ, Castro AJ (1985). Electrophysiological analysis of motor cortical plasticity after cortical lesions in newborn rat. Brain Res 332: 103-111.

Kiernan, J.A., 2009. Barr's the human nervous system (9th ed.). Lippincott Williams and Wilkins, Philadelphia.

Kirik D, Rosenblad C, Bjorklund A (1998). Characterization of behavioural and neurodegenerative changes following partial lesions of the nigrostriatal dopamine system induced by intrastriatal 6-hydroxydopamine in the rat. Exp Neurol 152: 259-277.

Kleim JA, Barbay S, Cooper NR, Hogg TM, Reidel, Remple MS, Nudo RJ. (2002). Motor learning-dependent synaptogenesis is localized to functionally reorganizaed motor cortex. Neurobiol Learn Mem 77: 63-77.

Kleim JA, Barbay S, Nudo RJ (1998). Functional reorganization of the rat motor cortex following motor skill learning. J Neurophysiol 80: 3321-3325.

Kleim JA, Bruneau R, Calder K, Pocock D, VandenBerg PM, MacDonal E, Monfils MH, Sutherland RJ, Nader K (2003). Functional organization of adult motor cortex is dependent upon continued protein synthesis. Neuron 25: 167-176.

Kleim JA, Hogg TM, VandenBerg PM, Cooper NR, Bruneau R, Remple M (2004). Cortical synaptogenesis and motor map reorganization occur during late, but not early, phase of motor skill learning. J Neurosci 24: 628-633

Kolb B, Gorny G, Cote S, Ribeiro-da-Silva A, Cuello AC. (1996). Nerve growth factor stimulates growth of cortical pyramidal neurons in young adult rats. Brain Res 751: 289-294.

Krack P, Batir A, Van Blercom N, Chabardes S, Fraix V, Ardouin C, Koudsie A, Limousin PD, Benazzouz A, Lebas JF, Benabid AL, Pollack P (2003). Five-year follow-up of bilateral stimulation of the subthalamic nucleus in advanced Parkinson's disease. N Engl J Med 349: 1925-1934.

Kumar R, Lozano AM, Kim YJ, Hutchinson WD, Sime E, Halket E, Lang AE (1998). Double-blind evaluation of subthalamic nucleus deep brain stimulation in advanced Parkinson's disease. Neurology 51: 850-855.

Kuypers HGJM (1981). Anatomy of the descending pathways. In Brooks, V.B. (Ed.), Handbook of Physiology. Section 1: The Nervous System. Vol. II. Motor control, part 1. Bethesda: American Physiological Society.

Kwan HC, MacKay WA, Murphy JT, Wong YC (1978). Spatial organization of precentral cortex in awake primates. II. Motor outputs. J Neurophysiol 41: 1120–31.

Lamarre Y, Spidalieri G, Busby L, Lund JP (1980). Programming of initiation and execution of ballistic arm movements in the monkey. Prog Brain Res 54: 157-169.

Lashley KS (1950). In search of the engram. Society of experimental biology symposium No. 4: physiological mechanisms in animal behaviour. pp 454-482. Cambridge, Cambridge University Press, pp. 454-482.

Lawrence DG, Kuypers HG (1968). The functional organization of the motor system in the monkey. I: The effects of bilateral pyramidal lesions. Brain 91: 1-14.

Lemon RN (2008). Descending pathways in motor control. Annu Rev Neurosci 31: 195-218.

Lemon RN, Griffiths J (2005). Comparing the function of the corticospinal system in different species: organizational differences for motor specialization? Muscle Nerve 32: 261-279.

Lévesque M, Charara A, Gagnon S, Parent A, Deschênes M (1996). Corticostriatal projections from layer V cells in rat are collaterals of long-range corticofugal axons. Brain Res 709: 311-315.

Leyton SSF, Sherrington CS (1917*)*. Observations on the excitable cortex of the chimpanzee, orang-utan and gorilla. J Exp Physiol 11: 135–222.

Li S, Arbuthnott GW, Jutras MJ, Goldberg JA, Jaeger D (2007). Resonant antidromic cortical circuit activation as a consequence of high-frequency subthalamic deep-brain stimulation. J Neurophysiol 98: 3525-3537.

Li XG, Florence SL, Kass JH (1990). Areal distribution of cortical neurons projecting to different levels of the caudal brain stem and spinal cord in rats. Somatosens Mot Res 7: 315-335.

Liang F, Rouiller EM, Wiesendanger M (1993). Modulation of sustained electromyographic activity by single intracortical microstimuli: comparison of two forelimb motor cortical areas of the rat. Somatosens Mot Res 10:51-61

Limousin P, Pollak P, Benazzouz A, Hoffmann D, Broussolle E, Perret JE, Benabid AL (1995). Bilateral subthalamic nucleus stimulation for severe Parkinson's disease. Mov Disord 10: 672-674.

Liu Y, Kim D, Himes BT, Chow SY, Schallert T, Murray M, Tessler A, Fischer I (1999). Transplants of fibroblasts genetically modified to express BDNF promote regeneration of adult rat rubrospinal axons and recovery of forelimb function. J Neurosci 19: 4370-4387.

Lomber SG (1999). The advantages and limitations of permanent or reversible deactivation techniques in the assessment of neural function. J Neurosci Meths 86: 109-117.

Lomber SG, Cornwell P, Sun JS, MacNeil MA, Pyne BR (1994). Reversible inactivation of visual processing operations in middle suprasylvian cortex of the behaving cat. Proc Natl Acad Sci USA 91:2999-3003.

Lomber SG, Meredith MA, Kral A (2010) Cross-modal plasticity in specific auditory cortices underlies visual compensations in the deaf. Nat Neurosci 13: 1421-1427.

Lomber SG, Payne BR (1996). Removal of two halves restores the whole: reversal of visual hemineglect during bilateral cortical or collicular inactivation in the cat. Vis Neurosci 13: 1143-1156.

Lomber SG, Payne BR, Horel JA (1999). The cryoloop: an adaptable reversible cooling deactivation method for behavioral or electrophysiological assessment of neural function. J Neurosci Methods 86: 1790-195.

Luppino G, Matelli M, Camarda RM, Gallese V, Rizzolatti G (1991). Multiple representations of body movements in mesial area 6 and the adjacent cingulate cortex: an intracortical microstimulation study in the macaque monkey. J Comp Neurol 311: 463-482.

Malpeli JG (1999) Reversible inactivation of subcortical sites by drug injection. J Neurosci Methods 86:119-128.

Malpeli JG, Schiller PH, Colby CL (1981). Response properties of single cells in monkey striate cortex during reversible inactivation of individual lateral geniculate laminae. J Neurophysiol 46:1102-1119.

Mao YT, Pallas SL (2012) Compromise of auditory cortical tuning and topography after cross-modal invasion by visual inputs. J Neurosci 32: 10338-10351.

Martin JH, Ghez C (1988). Red nucleus and motor cortex: parallel motor systems for the initiation and control of skilled movement. Behav Brain Res 28**:** 217-223.

Martin JH. (2005). The corticospinal system: from development to motor control. Neuroscientist, 11, 161-173.

Maunsell JHR, Nealey TA, DePriest DD (1990). Magnocellular and parcocellular contributions to responses in the middle temporal visual area (MT) of the macaque monkey. J Neurosci 10:3323-3334.

Maurissen JP, Marable BR, Andrus AK, Stebbins KE (2003). Factors affecting grip strength testing. Neurotoxicol Teratol 25: 543-553.

McIntyre CC, Savasta M, Walter BL, Vitek JL (2004). How does deep brain stimulation work? Present understanding and future questions. *J Clin Neurophysiol 21*: *40*–50.

McKenna JT, Prusky GT, Whishaw IQ (2000). Cervical motoneuron topography reflects the proximodistal organization of muscles and movements of the rat forelimb: a retrograde carbocyanine dye analysis. J Comp Neurol 419: 286-296.

McKiernan BJ, Marcario JK, Karrer JH, Cheney PD (1998). Corticomotoneuronal postspike effects in shoulder, elbow, wrist, digit, and intrinsic hand muscles during a reach and prehension task. J Neurophysiol 80: 1961–80.

McNamara JO, Yeh G, Bonhaus DW, Okazaki M, Nadler JV (1990). NMDA receptor plasticity in the kindling model. Adv Exp Med Biol 268: 451–459.

Metz GA, Piecharka DM, Kleim JA, Whishaw IQ (2004). Preserved ipsilateral-to-lesion motor map organization in the unilateral 6-OHDA-treated rat model of Parkinson's disease. Brain Res 1026: 126-135.

Metz GA, Whishaw IQ (2002). Drug-induced rotation intensity in unilateral dopamine-depleted rats is not correlated with end point or qualitative measures of forelimb or hindlimb motor performance. Neuroscience 111: 325–336.

Miller MW (1987). The origin of corticospinal projection neurons in rat. Exp Bain Res 67: 339-351.

Molino A, McIntyre DC (1972). Another inexpensive headplug for the electrical recording and or stimulation of rats. Physiology and Behavior 9: 273-275.

Monfils MH, Teskey GC (2004). Skilled-learning-induced potentiation in rat sensorimotor cortex: a transient form of behavioural long-term potentiation. Neuroscience 125: 329–336.

Monfils MH, VandenBerg PM, Kleim JA, Teskey GC (2004). Long-term potentiation induces expanded movement representations and dendritic hypertrophy in layer V of rat sensorimotor neocortex. Cereb Cortex 14: 586-593.

Moon SK, Alaverdashvili M, Cross AR, Whishaw IQ (2009). Both compensation and recovery of skilled reaching following small photothrombotic stroke to motor cortex in the rat. Exp Neurol 218: 145-153.

Moran DW, Schwartz AB (1999). Motor cortical representation of speed and direction during reaching. J Neurophysiol 82: 2676-2692.

Narahanshi T (1972). Mechanism of action of tetrodotoxin and saxitoxin on excitable membranes. Fed Proc 31:1124-1132.

Neafsey EJ, Bold EL, Haas G, Hurley-Gius KM, Quirk G, Sievert CF, Terreberry RR (1986). The organization of the rat motor cortex: a microstimulation mapping study. Brain Res 396: 77–96.

Neafsey EJ, Sievert C (1982). A second forelimb motor area exists in the rat frontal cortex. Brain Res 232: 151-156.

Newsome WT, Paré EB (1988). A selective impairment of motion perception following lesions of the middle temporal visual area (MT). J Neurosci 8:2201-2211.

Nudo RJ, Frost SB (2006). The evolution of motor cortex and motor systems. In: Krubitzer, L.A., Kaas, J.H. (Eds), Evolution of Nervous Systems in Mammals. Elsevier, Oxford.

Nudo RJ (2006a). Mechanisms for recovery of motor function following cortical damage. Curr Opin Neurobiol 16: 638-644.

Nudo RJ (2006b). Plasticity. NeuroRx 3: 420-427.

Nudo RJ, Jenkins WM, Merzenich MM (1990). Repetitive microstimulation alters the cortical representation of movements in adult rats. Somatosen Mot Res 7: 463–483.

Nudo RJ, Jenkins WM, Merzenich MM, Prejean T, Grenda R. (1992). Neurophysiological correlates of hand preference in primary motor cortex of adult squirrel monkeys. J Neurosci 12: 2918–47.

Nudo RJ, Milliken GW, Jenkins WM, Merzenich MM (1996). Use-dependent alterations of movement representations in primary motor cortex of adult squirrel monkeys. J Neurosci 16: 785-807.

Nudo RJ, Plautz EJ, Milliken GW (1997). Adaptive plasticity in the primate motor cortex as a consequence of behavioural experience and neuronal injury. Semin Neurosci 9:13-23.

Nudo RJ, Wise BM, SiFuentes F, Milliken GW (1996). Neural substrates for the effects of rehavilitative training on motor recovery after ischemic infarct. Science 272: 1791-1794.

Orieux G, François C, Féger J, Hirsch EC (2002). Consequences of dopaminergic denervation on the metabolic activity of the cortical neurons projecting to the subthalamic nucleus in the rat. J Neurosci 22: 8762-8770.

Ozen LJ, Young NA, Koshimori Y, Teskey GC (2008). Low-frequency stimulation reverses kindling-induced neocortical motor map expansion. Neuroscience 153: 300-307.

Parent A, Hazrati LN (1995). Functional anatomy of the basal ganglia. I. The cortico-basal-ganglia-thalamo-cortical-loop. Brain Res Rev 20: 91–127.

Passingham RE, Perry VH, Wilkinson F (1983). The long-term effects of removal of sensorimotor cortex in infant and adult rhesus monkeys. Brain 106: 675-705.

Paxinos G, Watson C (2005). The Rat Brain in Stereotaxic Coordinates (5th ed). San Diego, CA: Elsevier Academic Press.

Penfield W, Boldrey E (1937). Somatic motor and sensory representation in the cerebral cortex of man as studied by electrical stimulation. Brain 60: 389-443.

Penfield W, Rasmussen T. (1950). The Cerebral Cortex of Man. New York: MacMillan

Perlmutter JS, Mink JW (2006). Deep brain stimulation. Annu Rev Neurosci 29: 229-257.

Peterson GM (1951). Reeducation of handedness in the rat following cerebral injuries. J Comp Physiol Psychol 44:191-196

Piecharka DM, Kleim JA, Whishaw IQ (2005). Limits on recovery in the corticospinal tract of the rat: partial lesions impair skilled reaching and the topographic representation of the forelimb in the motor cortex. Brain Res Bull 66: 203-211.

Playford ED, Jenkins IH, Passingham RE, Nutt J, Frackowiak RS, Brooks DJ (1992). Impaired mesial frontal and putamen activation in Parkinson's disease: a positron emission tomography study. Ann Neurol 32: 151–161.

Porter R, Lemon R (1993). Corticospinal function and voluntary movement. Oxford: Oxford University Press.

Prine EK, Maling N, Rivera B, Larson K, Thomas NJ, Fowler SC, Manfredsson FP, Shrivastav R, Kleim JA (2013). Differential sensitivity of cranial and limb motor function to nigrostriatal dopamine depletion. Behav Brain Res 237: 157-163.

Prine EP, Thomas NJ, Mailing N, Kleim JA (2010). Differential sensitivity of oral motor vs. Limb motor function in an animal model of Parkinson`s disease. Program No 52.2/L11.

San Diego, CA: Neuroscience Meeting Planner; 2010, Society for Neuroscience, Online.

Racine RJ (1972) Modification of seizure activity by electrical stimulation: II. motor seizure. Electroencephalogr Clin Neurophysiol 32:281-294.

Ramanathan D, Conner JM, Tuszynksi MH. (2006). A form of motor cortical plasticity that correlates with recovery of function after brain injury. Proc Natl Acad Sci U S A 103: 11370-11375.

Rascol O, Sabatini U, Chollet F, Celsis P, Montastruc JL, MarcVergnes JP, Rascol A (1992). Supplementary and primary sensory motor area activity in Parkinson's disease. Regional cerebral blood flow changes during finger movements and effects of apomorphine. Arch Neurol 49: 144–1448.

Rauch F, Schwabe K, Krauss JK (2010). Effect of deep brain stimulation in the pedunculopontine nucleus on motor function in the rat 6-hydroxydopamine Parkinson model. Behav Brain Res 210:46-53.

Rizzolatti G, Luppino G (2001). The cortical motor system. Neuron 31: 889-901.

Rolland AS, Herrero MT, Garcia-Martinez V, Ruberg M, Hirsch EC, François C (2007). Metabolic activity of cerebellar and basal ganglia-thalamic neurons is reduced in parkinsonism. Brain 130: 265-75.

Rothwell, J. C. (2012). Overview of neurophysiology of movement control. Clin Neurol Neurosurg, *114,* 432-435.

Rouiller EM, Moret V, Liang F (1993). Comparison of the connectional properties of the two forelimb areas of the rat sensorimotor cortex: support for the presence of a premotor or supplementary motor cortical area. Somatosens Mot Res 10: 269-289.

Rouiller EM, Yu XH, Moret V, Trempini A, Wiesendanger M, Liang F (1998). Dexterity in adult monkeys following early lesion of the motor cortical hand area: the role of cortex adjacent to the lesion. Eur J Neurosci 10: 729-740.

Russell WMS, Burch RL (1959). The principles of humane experimental technique. London: Methuen.

Sabatini U, Boulanouar K, Fabre N, Martin F, Carel C, Colonnese C, Bozzao L, Berry I, Montastruc JL, Chollet F, Rascol O (2000). Cortical motor reorganization in akinetic patients with Parkinson's disease. Brain 123: 394-403.

Sanes JN, Donoghue JP (1993). Oscillations in local field potentials of the primate motor cortex during voluntary movement. Proc Natl Acad Sci 90: 4470-4474.

Sanes JN, Donoghue JP (2000). Plasticity and primary motor cortex. Annu Rev Neurosci 23: 393-415.

Sanes JN, Suner S, Donoghue JP (1990) Dynamic organization of primary motor cortex output to target muscles in adult rats. I. Long-term patterns of reorganization following motor or mixed peripheral nerve lesions. Exp Brain Res 79: 479–491.

Sanes JN, Wang J, Donoghue JP. (1992). Immediate and delayed changes of rat motor cortical output representation with new forelimb configurations. Cereb Cortex 2: 141–52.

Schallert T, Fleming SM, Leasure JL, Tillerson JL, Bland ST (2000). CNS plasticity and assessment of forelimb sensorimotor outcome in unilateral rat models of stroke, cortical ablation, parkinsonism and spinal cord injury. Neuropharmacology 39: 777-787.

Schallert T, Tillerson JL (1999). Intervention strategies for degeneration of dopamine neurons in parkinsonism: optimizing behavioral assessment of outcome. In: Emerich DF, Dean RL,

Sanberg PR (Eds.) Central Nervous System Diseases. Totowa, Humana Press Inc, pp. 131–151.

Schallert T, Woodlee MT (2008). Orienting and Placing. In Whishaw IQ, Kolb B., Eds. The behaviour of the laboratory rat: A handbook with tests. New York: Oxford University Press.

Schieber MH (2001). Constraints on somatotopic organization in the primary motor cortex. J Neurophysiol 86: 2125-2143.

Schieber MH, Poliakov AV (1998). Partial inactivation of the primary motor cortex hand area: effects on individuated finger movements. J Neurosci 18: 9038–54.

Schiller PH, Malpeli JG (1977). The effect of striate cooling on area 18 cells in the monkey. Brain Res 126:366-369.

Schwarting RKW, Huston JP (1996). The unilateral 6-hydroxydopamine lesion model in behavioural brain research. Analysis of functional deficits, recovery and treatments. Progr Neurobiol 50:275-331.

Shepherd, GM (1974). *The Synaptic Organization of the Brain*. New York: Oxford University Press.

Sherrington CS (1939). On the motor area of the cerebral cortex. In: Selected writings of Sir Charles Sherrington. Denny-Brown, D (Ed.). London: Hamish Hamilton Medical Books, pp. 397-439.

Shi LH, Woodward DJ, Luo F, Anstrom K, Schallert T, Chang JY (2004). High-frequency stimulation of the subthalamic nucleus reverses limb-use asymmetry in rats with unilateral 6-hydroxydopammine lesions. Brain Res 1013: 98-106.

Shinoda Y, Yokota J, Futami T (1981). Divergent projection of individual corticospinal axons to motoneurons of multiple muscles in the monkey. Neurosci Lett 23: 7-12.

Steiner H, Kitai ST (2000). Regulation of the rat cortex function by D1 dopamine receptors in the striatum. J Neurosci 20: 5449-5460.

Stepniewska I, Fang PC, Kaas JH. (2005). Microstimulation reveals specialized subregions for different complex movements in posterior parietal cortex of prosimian galagos. Prpc Natl Acad Sci USA 102: 4878-4883.

Stojic AS, Lane RD, Killackey HP, Rhoades RW (2000). Suppression of hindlimb inputs to S-I forelimb-stump representation of rats with neonatal forelimb removal: GABA receptor blockade and single-cell responses. J Neurophysiol 83: 3377-3387.

Stoney SD Jr, Thompson WD, Asanuma H (1968). Excitation of pyramidal tract cells by intracortical microstimulation: effective extend of stimulating current. J Neurophysiol 31: 659-669.

Sullivan RM, Gratton A (2002). Behavioral effects of excitotoxic lesions of ventral medial prefrontal cortex in the rat are hemisphere-dependent. Brain Res 927:69-79.

Tandon S, Kambi N, Jain N (2008). Overlapping representations of the neck and whiskers in the rat motor cortex revealed by mapping at different anaesthetic depths. Eur J Neurosci 27: 228–237.

Taylor CSR, Gross CG (2003). Twitches versus movements: a story of the motor cortex. History of Neuroscience 9: 332-342.

Tehovnik EJ (1996). Electrical stimulation of neural tissue to evoke behavioral responses. J Neurosci Meth 65: 1-17

Terashima,T. (1995). Anatomy, development and lesion-induced plasticity of rodent corticospinal tract. Neuroscience Research, 22, 139-161.

Teskey GC, Flynn C, Monfils MH, Goertzen CD, Henry LC, Valentine PA (2005). From ultrastructure to networks: Kindling-induced changes in neocortex. In: M.E. Corcoran, S.L. Moshe (Eds.), Kindling. New York: Plenum Press (pp. 125–133).

Teskey GC, Monfils MH, Flynn C, Young NA, van Rooyen F, Henry LC, Ozen LJ, Henderson, AK, Reid AY, Brown AR (2008). Motor maps, seizures, and behaviour. Can J Exp Psychol 62: 132-139.

Teskey GC, Monfils MH, VandenBerg PM, Kleim JA (2002). Motor map expansion following repeated cortical and limbic seizures is related to synaptic potentiation. Cereb Cortex 12: 98-105.

Teskey GC, Young NA, van Rooyen F, Larson SEM, Flynn C, Monfils MH, Kleim JA, Henry LC, Goertzen CD (2007). Induction of neocortical long-term depression results in smaller movement representations, fewer excitatory perforated synapses and more inhibitory synapses. Cereb. Cortex 17: 434-442.

Thickbroom GW, Byrnes ML, Walters S, Stell R, Mastaglia FL (2006). Motor cortex reorganization in Parkinson's disease J Clin Neurosci 13: 639-642.

Tillerson JL, Castro SL, Zigmond MJ, Schallert T (1998). Motor rehabilitation of forelimb use in a unilateral 6-hydroxydopamine (6-OHDA) rat model of Parkinson's disease. Soc Neurosci Absts, 25, p. 672.18.

Tilson HA, Mitchell CL, Cabe PA (1979). Screening for neurobehavioral toxicity: The need for and examples of validation of testing procedures. Neurobehav Toxicol 1:137-148.

Tolias AS, Sultan F, Augath M, Oeltermann A, Tehovnik EJ, Schiller PH, Logothetis NK (2005). Mapping cortical activity elicited with electrical microstimulation using FMRI in the macaque. Neuron 48: 901-911.

Towe AL (1973). Relative numbers of pyramidal tract neurons in mammals of different sizes. Brain Behav. Evol., 7: 1-17**.**

Tracey D (2004). Ascending and decending pathways in the spinal cord. In: Paxinos, G. (Ed.), The rat nervous system (3rd Ed). Academic Press, New York.

Tyc F, Boyadjian A, Devanne H (2005). Motor cortex plasticity induced by extensive training revealed by transcranial magnetic stimulation in human. Eur J Neurosci 21:259-266.

Uematsu S, Lesser R, Risher RS, Gordon B, Hara K, Krauss GI, Vining EP, Webber RW (1992). Motor and sensory cortex in humans: topography studied with chronic subdural stimulation. Neurosurgery 31: 59-72.

Ungerstedt U (1968). 6-hydroxy-dopamine induced degeneration of central monoamine neurons. Eur J Pharmacol 5:107-110.

Upton D, Thompson PJ (1997). Age at onset and neuropsychological function in frontal lobe epilepsy. Epilepsia 38: 1103-1113.

van Rooyen F*,* Young NA*,* Larson SE, Teskey, GC (2006). Hippocampal kindling leads to motor map expansion. Epilepsia 47*:* 1383–1391.

Viaro R, Morari M, Franchi G (2011). Progressive motor cortex function reorganization following 6-hydroxydopamine lesioning in rats. J Neurosci 31: 4544-4554.

Walsh RN, Cummins RA (1976). The open-feild test: ac critical review. Psych Bull 83:482-504.

Wang L, Conner JM, Rickert J, Tuszynski MH (2011). Structural plasticity within highly specific neuronal populations identifies a unique parcellation of motor learning in the adult brain. Proc Natl Acad Sci USA 108: 2545-2550.

Weiskrantz L (1956). Behavioral changes associated with ablation of the amygdaloid complex in monkeys. J Comp Physiol Psychol 49*:* 381–391.

Welker C (1971). Microelectrode delineation of fine grain somatotopic organization in SmI cerebral neocortex in albino rat. Brain Res 26: 259-275.

Whishaw IQ, Dringenberg HC, Pellis SM (1992) Spontaneous forelimb grasping in free feeding by rats: motor cortex aids limb and digit positioning. Behav Brain Res 48: 113-125.

Whishaw IQ, Gorny B, Foroud A, Kelim J (2003). Long-Evans and Sprague Dawley rats have similar skilled reaching success and limb representations in motor cortex but different movements: some cautionary insights into the selection of rat strains for neurobiological motor research. Behav Brain Res 145: 221-232

Whishaw IQ, Pellis SM (1990). The structure of skilled forelimb reaching in the rat: a proximally driven movement with a single distal rotatory component. Behav Brain Res 41: 49-59.

Whishaw IQ, Pellis SM, Gorny BP (1992). Skilled reaching in rats and humans: evidence of parallel development or homology. Behav Brain Res 47: 59-70

Whishaw IQ, Pellis SM, Gorny BP, Pellis VC (1991). The impairments in reaching and the movements of compensation in rats with motor cortex lesions: an endpoint, videorecording, and movement notation analysis. Behav Brain Res 42: 77-91.

Whishaw IQ, Suchowersky O, Davis L, Sarna J, Metz G, Pellis S (2002). Impairment of pronation, supination, and body co-ordination in reach-to-grasp tasks in human

Parkinson's disease (PD) reveals homology to deficits in animal models. Behav Brain Res 133:165–176.

Whishaw IQ, Tomie J (1989). Olfaction directs skilled forelimb reaching in the rat. Behav Brain Res 32: 11–21.

Whishaw, IQ, Sarna, JR, Pellis, SM (1998). Evidence for rodent-common and species-typical limb and digit use in eating, derived from a comparative analysis of ten rodent species. Behav Brain Res 96: 79–91.

Wise SP, Murray EA, Coulter JD (1979). Somatotopic organization of corticospinal and corticotrigeminal neurons in the rat. Neuroscience 4: 65-78

Wolpert DM, Ghahramani Z, Flanagan JR (2001). Perspectives and problems in motor learning. Trends Cogn Sci 5: 487-494.

Woolsey CN, Settlage PH, Meyer DR, Sencer W, Hamuy TP, Travis AM (1952). Pattern of localization in precentral and "supplementary" motor areas and their relation to the concept of a premotor area. In association for research in nervous and mental desease (Vol 30), pp. 238-264. New York: Raven Press.

Xerri C, Merzenich MM, Peterson BE, Jenkins W. (1998). Plasticity of primary somatosensory cortex paralleling sensorimotor skill recovery from stroke in adult monkeys. J Neurophysiol 79: 2119-2148.

Yang XF, Kennedy BR, Lomber SG, Schmidt RE, Rothman SM (2006). Cooling produces minimal neuropathology in neocortex and hippocampus. Neurobiol Dis 23: 637-643.

Young CK, Brown AR, Robinson JHB, Tuor UI, Dunn JF, Bland BH, Teskey GC (2011). Functional MRI response and correlated electrophysiological changes during posterior hypothalamic nucleus deep brain stimulation. NeuroImage 56: 35-44.

Young NA, Vuong J, Flynn C, Teskey GC (2011). Optimal parameters for microstimulation derived forelimb movement thresholds and motor maps in rats and mice. J Neurosci Methods 196: 60-69.

Young NA, Vuong J, Ozen LJ, Flynn C, Teskey GC (2009). Motor map expansion in the pilocarpine model of temporal lobe epilepsy is dependent on seizure severity and rat strain. Exp Neurol 217: 421-428.

Young NA, Vuong J, Teskey GC (2012). Development of motor maps in rats and their modulation by experience. J Neurophysiol 108: 1309-1317.

Zhang J, Ni H, Harper RM (1986). A miniaturized cryoprobe for functional neuronal blockade in freely moving animals. J Neurosci Methods 16:79-87.

Zhou Q, Zhang Q, Zhao X, Duan YY, Lu Y, Li C, Li T (2010). Cortical electrical stimulation alone enhances functional recovery and dendritic structures after focal cerebral ischemia in rats. Brain Res 1311: 148-157.

Zhuravin IA, Bures J (1991). Extent of tetrodotoxin induced blockage examined by papillary paralysis elicited by intracerebral injection of drug. Exp Brain Res 83: 687-690.